2016

Examining the Effects of Anti-Nogo a Immunotherapy on Post-Stroke Neurogenesis in the Adult Rat

Daniel Shepherd
Loyola University Chicago

LOYOLA UNIVERSITY CHICAGO

EXAMINING THE EFFECTS OF ANTI-NOGO-A IMMUNOTHERAPY ON POST-STROKE NEUROGENESIS IN THE ADULT RAT

A DISSERTATION SUBMITTED TO

THE FACULTY OF THE GRADUATE SCHOOL

IN CANDIDACY FOR THE DEGREE OF

DOCTOR OF PHILOSOPHY

PROGRAM IN NEUROSCIENCE

BY

DANIEL SHEPHERD

MAYWOOD, IL

DECEMBER, 2016

ACKNOWLEDGEMENTS

I would first like to thank Dr. Wendy Kartje for her constant support and guidance that was instrumental in crafting, revising, and completing this project. Thank you to the members of the Kartje laboratory who have all in some way helped out during my time in the lab. In partcular, I would like to acknowledge the contributions of those whose work directly contributed this dissertation, including Robert Farrer, PhD, Stefanie Cappucci, Ian Vaagenes, PhD, Vicki Husak, and Shih-Yen Tsai, MD, PhD. Thank you to the members of my dissertation committee, whose guidance and constructive critiques helped hone and strengthen this project. I am grateful for the financial support of American Heart Association predoctoral fellowship 15PRE24470136 that helped fund these studies, and for the provision of reagents by Novartis International AG. Lastly, thank you to my family and my wife, Elise, for their continuing love and support

TABLE OF CONTENTS

LIST OF TABLES

LIST OF FIGURES

LIST OF ABBREVIATIONS

3T3 .....3T3 fibroblast cell line
Ab .....Antibody
ATP .....Adenosine triphosphate
BrdU .....5-bromo-2'-deoxyuridine
CC .....Corpus callosum
CCA.....Common carotid artery
CNS.....Central nervous system
CNS.....Central nervous system
CREB .....Cyclic-AMP response element binding protein
CRMP2 .....Collapsin response mediator protein 2
CSF.....Cerebrospinal fluid
DAB.....Diaminobenzidene
DCX .....Doublecortin
DG.....Dentate gyrus
dMCAO.....Distal middle cerebral artery occlusion
DRG.....Dorsal root ganglion
ER .....Endoplasmic reticulum
GABA.....Gamma-aminobutyric acid
GCL.....Granule cell layer
GFAP .....Glial fibrillary acidic protein
GPCR.....G protein-coupled receptor
GTPase.....Guanosine triphosphatase
IgG.....Immunoglobulin G
IN-1 .....Monoclonal antibody IN-1
KO.....Knockout
LARG.....Leukemia-associated RhoGEF
LIMK.....LIMkinase
LINGO1 .....Leucine-rich repeat and Ig domain-containing Nogo receptor interacting protein
LTD.....Long term depression
LTP .....Long term potentiation
LV.....Lateral ventricle
MCA.....Middle cerebral artery
MCAO.....Middle cerebral artery occlusion
MLC2 .....Myosin light chain 2
NeuN.....Neuronal nuclei (marker)
NSPC.....Neural stem and/or progenitor cell

OB .....Olfactory bulb
PC12.....Pheochromocytoma-12 neuron-like cell line
PNS .....Peripheral nervous system
RMS .....Rostral migratory stream
ROCK.....Rho kinase
RTN .....Reticulon
S1P Sphingosine-1-phosphate
S1PR1, 2, etc .....Sphingosine-1-phosphate receptor 1, 2…
SDS-PAGE.....Sodium dodecyl sulfate - polyacrylamide gel electrophoresis
SGZ.....Subgranular zone
SVZ .....Subventricular zone
tMCAO .....Transient middle cerebral artery occlusion
tPA .....Tissue plasminogen activator
TROY.....Tumor necrosis factor α receptor superfamily member 19
WT .....Wild type
Δ20 .....Nogo-A Δ20 domain

ABSTRACT

Stroke is a leading cause of adult disability with no pharmacological treatments to restore lost function. Our laboratory has shown that treatment with neutralizing antibodies against the neurite growth-inhibitory protein Nogo-A improves sensorimotor and cognitive recovery after stroke in adult and aged rats. This recovery is paralleled by increased dendritic and axonal plasticity in anti-Nogo-A-treated rats. Neurogenesis, an alternate form of plasticity involving the *de novo* production of new neurons, may contribute to post-stroke neural repair. While previous studies have found roles for Nogo-A in adult neurogenesis, neurogenesis has not been investigated after stroke and anti-Nogo-A treatment.

The goal of these studies was to examine whether anti-Nogo-A antibody treatment potentiated post-stroke neurogenesis in the brain's two main neurogenic niches, the subventricular zone (SVZ) and dentate gyrus (DG). We first identified that immature neurons, but not stem cells, in the SVZ expressed Nogo-A. However, Nogo-A was not found at the surface of SVZ-derived neuroblasts and accordingly, the motility of SVZ-derived neuroblasts was not altered by anti-Nogo-A antibody treatment *in vitro*. However, these cells were still susceptible to Nogo-A signaling, as treatment with recombinant Δ20 peptide, one of the inhibitory domains of Nogo-A, led to a modest reduction in neuroblast

maximum velocity. After stroke, anti-Nogo-A treatment had no effect on the number of proliferating cells in the SVZ, or on the density of doublecortin-positive neuroblasts, suggesting that anti-Nogo-A treatment does not stimulate neurogenesis in the SVZ after stroke. In the DG, Nogo-A was again found to be expressed by immature neurons, but not neural stem cells. However, as in the SVZ, anti-Nogo-A treatment did not affect the number of proliferating neural precursors or the number of new neurons produced after stroke.

These results suggest that neurogenesis contributes little to the sensorimotor and cognitive recovery observed after stroke and anti-Nogo-A treatment. Due to its stage-specific expression in immature neurons, Nogo-A is likely to play a role in adult neurogenesis in both the SVZ and DG, but is not targeted by anti-Nogo-A antibody treatment.

CHAPTER ONE

GENERAL OVERVIEW AND HYPOTHESIS

Stroke is a leading cause of adult disability worldwide. While thrombolytic or mechanical endovascular therapy can improve outcomes, the majority of stroke patients presenting to emergency rooms are ineligible for these treatments. Furthermore, there are currently millions of people living with permanent stroke-related disabilities. Despite the personal and public health burdens imposed by stroke-related disability, there are no drugs on the market that can improve recovery of function after stroke. Clearly, there is a desperate need for effective therapies to relieve this burden.

Injuries to the adult brain, such as stroke, are particularly devastating because the adult central nervous system has only a limited capacity for repair. This limited capacity is due to failure or inadequacy of several adaptive processes, including the regeneration of damaged axons, compensatory plasticity from intact circuits, and cell replacement.

However, the identification of barriers to neural repair has led to the development of targeted pharmaceuticals with promising preclinical results. Our laboratory has pioneered the use of neutralizing antibodies against the neurite outgrowth inhibitor Nogo-A as a way to improve recovery after stroke in adult and aged rats (reviewed in Kumar and

Moon, 2013). This recovery is paralleled by increases in dendritic complexity and compensatory axonal sprouting from the contralesional, intact hemisphere. While most of the work done in the Kartje laboratory has focused on improving *sensorimotor* recovery after stroke, other studies in the laboratory have also shown that anti-Nogo-A treatment is effective in promoting *cognitive* recovery after brain lesions (including stroke) (Brenneman et al., 2008; Gillani et al., 2010). These results show that targeting Nogo-A is a promising approach for improving recovery from a variety of clinically relevant stroke deficits.

Intriguingly, recent studies have suggested a role for Nogo-A and its signaling mediators in adult neurogenesis, the process by which new neurons are created (Rolando et al., 2012; Tong et al., 2013; Turnley et al., 2014; Vadodaria and Jessberger, 2013). Endogenous neurogenesis has been implicated in neuroprotection and recovery after stroke (Marlier et al., 2015). However, whether anti-Nogo-A antibody treatment affects the neurogenic response to stroke has not been investigated. Research into this area is necessary to fully understand the mechanisms of recovery after stroke and anti-Nogo-A treatment. Furthermore, as anti-Nogo-A antibodies have been used in clinical trials for spinal cord injury and a trial for stroke is in the planning stages, it is critical to be aware of the full scope and limitations of anti-Nogo-A's effects on the brain. The goal of this study was to determine whether anti-Nogo-A treatment influenced neurogenesis after stroke in the adult brain's two major neurogenic niches, the subventricular zone and dentate gyrus.

HYPOTHESIS: Anti-Nogo-A immunotherapy potentiates the neurogenic response to stroke in the adult brain's two main neurogenic niches, the subventricular zone (SVZ) and the dentate gyrus (DG).

Aim 1: Identify potential direct cellular treatment targets within the SVZ and DG by characterizing the expression pattern of Nogo-A within these two areas.

Aim 2: Determine whether the motility of SVZ-derived neuroblasts is influenced by the Δ20 domain of Nogo-A.

Aim 3: Determine whether anti-Nogo-A immunotherapy affects post-stroke neurogenesis by quantifying, after stroke and anti-Nogo-A treatment:

- Cellular proliferation in the SVZ,
- The density of immature neurons in the SVZ,
- Cellular proliferation in the SGZ/DG, and
- Neuronal differentiation and survival in the SGZ/DG

CHAPTER TWO

LITERATURE REVIEW

ISCHEMIC STROKE: A MAJOR CAUSE OF ADULT DISABILITY

Stroke results when brain tissue becomes critically deprived of blood flow, leading to cell death and associated neurological deficits. While stroke can be fatal, most stroke patients survive, making stroke one of the leading causes of adult disability (Feigin et al., 2014; Mozaffarian et al., 2016). Most strokes are ischemic (Mozaffarian et al., 2016), in which the occlusion of a blood vessel robs that vessel's territory of oxygen and nutrients. Within minutes, neuronal ATP levels in the ischemic territory fall to levels no longer able to sustain the ion pumps that maintain membrane potential. Neuronal depolarization triggers the massive release of glutamate, which binds glutamate receptors and induces calcium influx. This large increase in intracellular calcium leads to indiscriminant activation of enzymes such as proteases, phospholipases, and enzymes that contribute to oxidant production, which degrade vital cellular molecules (Lo et al., 2003). Glutamate receptor activation also increases rampant sodium influx into neurons, leading to cell swelling (Moskowitz et al., 2010). Thus, *excitotoxicity* is a major mechanism contributing to cell death after ischemia. While neuroprotective treatments designed to stave off acute

stroke damage have been successful in animal models, the complexity of cell death mechanisms after stroke may contribute to the failure of the more than 100 clinical trials that have investigated neuroprotective therapy in humans (Gladstone et al., 2002).

While cell death in the infarct core is rapid, the tissue surrounding the core may be hypoperfused but viable, sustained by collateral arteries. The penumbra may be salvaged if blood flow is restored in a timely manner, but will otherwise become infarcted in time. Salvaging the penumbra is the goal of treatment with tissue plasminogen activator (tPA), the only approved pharmacological treatment for acute ischemic stroke. Intravenous tPA works by converting plasminogen to plasmin, which degrades cross-linked fibrin clots, thereby restoring blood flow distal to the occlusion (Yaghi et al., 2014). While tPA can improve stroke outcomes, current research supports a therapeutic window for treatment of within only 4.5 hours of stroke onset, after which time tPA is no more effective than control treatment and the risk of intracranial hemorrhage increases (Emberson et al., 2014; Mazya et al., 2012). With other exclusion criteria factored in, it is estimated that less than 10% of ischemic stroke patients actually receive tPA treatment (Moskowitz et al., 2010). Recent trials of endovascular thrombectomy as a standalone intervention or as an adjunct therapy to tPA have shown promising results (Mokin et al., 2016). The therapeutic window for thrombectomy may be larger than that for tPA, but relatively little data exist from patients treated beyond 6 hours (Mokin et al., 2016). Therefore, we may still anticipate a substantial number of patients with new stroke-related disabilities even with advances in acute stroke care.

Stroke patients often recover some degree of function in the weeks to months after stroke (Cramer, 2008). However, many patients are still left with long-lasting disabilities, including hemiparesis, cognitive deficits, aphasia, and visual and other sensory deficits (Kelly-Hayes et al., 2003), in large part because of the limited ability of the brain to repair itself after injury, as discussed in the next sections.

NOGO-A: A BARRIER TO GROWTH AND PLASTICITY IN THE ADULT CENTRAL NERVOUS SYSTEM

The growth-inhibitory environment of the adult central nervous system

The failure of regeneration in the damaged central nervous system (CNS) has been long recognized. Landmark studies from Albert Aguayo's laboratory in the early 1980's provided the first evidence that CNS axons could regenerate into PNS nerve grafts (David and Aguayo, 1981; Richardson et al., 1980), showing that adult CNS neurons were intrinsically capable of growth given a favorable or permissive environment. These results helped provide direction for research into growth-promoting therapies. Using dorsal root ganglion neurons cultured in an optimal growth media containing nerve growth factor, Martin Schwab and Hans Thoenen showed that the substrate itself, and not differential trophic support in the two environments, was responsible for the differences in growth potential (Schwab and Thoenen, 1985). Furthermore, even dead optic nerve sections (ie., a CNS-derived tissue) were inhibitory, suggesting that a tissue-bound, non-soluble factor mediated this inhibitory activity.

Three studies published by Martin Schwab's laboratory in 1988 rapidly moved the regeneration field forward. First, oligodendrocytes, along with their product, myelin, were identified as the cells and substance responsible for the growth-inhibitory environment of the adult CNS (Schwab and Caroni, 1988). Protease treatment of CNS myelin abolished its inhibitory activity, suggesting that this inhibitory activity was protein-mediated. This inhibitory factor was found specifically in two distinct protein fractions that resolved to 250 and 35 kDa on SDS-PAGE gels, and were necessary and sufficient for the inhibition of neurite outgrowth and fibroblast adhesion and spreading (Caroni and Schwab, 1988b). Lastly, an antibody (termed "IN-1") raised against these inhibitory fractions was able to promote axon growth on CNS myelin (Caroni and Schwab, 1988a). *In vitro* time lapse microscopy later demonstrated that the growth cones of growing axons collapsed upon contact with oligodendrocytes (Bandtlow et al., 1990).

Function blocking antibodies against myelin proteins promote growth and recovery after injury

These proof-of-principle experiments laid the groundwork for the first study showing *in vivo* efficacy of IN-1 application after a CNS injury (Schnell and Schwab, 1990). Here, rats implanted with IN-1-secreting hybridoma cells prior to transection of the corticospinal tract at the level of the mid-thoracic spinal cord exhibited longer axon regrowth compared to controls. A follow-up study showed that not only did post-transection IN-1 treatment improve the regrowth of corticospinal, raphespinal (serotonergic), and coeruleospinal (noradrenergic) axons, but also improved behavioral

recovery (Bregman et al., 1995). Subsequent studies likewise reported IN-1-mediated enhancement of growth and plasticity of cholinergic fibers after fimbria/fornix lesions (Cadelli and Schwab, 1991), and optic nerve after freeze-crush injury (Weibel et al., 1994).

Though long suspected, the inhibitory nature of myelin in the *human* CNS was experimentally confirmed in 1997 (Spillmann et al., 1997). As was the case for CNS myelin derived from other mammals (including rats, mice, opposums, and cattle), the inhibitory nature of human CNS myelin toward PC12 neurite outgrowth and 3T3 fibroblast spreading could be neutralized with IN-1 antibody, providing further evidence for phylogenetic conservation of the (as yet unidentified) inhibitory IN-1 antigen among higher mammals.

Until the late 1990's, much of the research surrounding post-injury treatment with IN-1 had focused on its ability to disinhibit *regeneration*, the bona fide regrowth of severed axons. However, other forms of neuroplasticity besides regeneration can promote functional recovery after CNS injury. For example, brain injury in neonatal mammals stimulates *compensatory* plasticity, whereby intact brain areas make new connections to re-innervate areas of the brain deafferented by the injury (Castro, 1975). The potential for plasticity in the early postnatal CNS is greatest before myelination ensues. In adult rats, application of IN-1 after unilateral pyramidotomy to disrupt the corticospinal tract promoted not only CST regeneration (Raineteau et al., 1999), but also compensatory axon sprouting from intact corticofugal pathways, crossing the midline to project into the deafferented spinal cord, red nucleus, and basilar pontine nuclei (Thallmair et al., 1998;

Z'Graggen et al., 1998). Importantly, treatment also promoted functional recovery in sensorimotor behavioral tasks. After cortical aspiration lesions, IN-1 treatment promoted topographically accurate axonal sprouting from the spared hemisphere into the deafferented striatum (Kartje et al., 1999) and pons (Wenk et al., 1999). These studies showed that IN-1 treatment could promote compensatory plasticity from uninjured pathways in addition to the regeneration of damaged axons, which is especially important for injuries involving significant loss of neuronal cell bodies, precluding axon regeneration.

In subsequent years, anti-Nogo-A antibody treatment was shown to promote corticofugal fiber plasticity, dendritic remodeling, and sensorimotor recovery after cortical stroke (eg., (Markus et al., 2005; Papadopoulos et al., 2002; 2006; Tsai et al., 2007; Wahl et al., 2014; Wiessner et al., 2003), and reviewed in (Kumar and Moon, 2013)). The importance of these newly sprouted fibers for recovery was confirmed by silencing crossing corticospinal fibers, which resulted in the loss of regained sensorimotor function (Wahl et al., 2014). In stroke, therefore, anti-Nogo-A treatment appears to work by disinhibiting plasticity from intact, spared projections.

While much of the work on Nogo-A blockade has focused on sensorimotor recovery, studies have shown that anti-Nogo-A treatment is also effective in promoting cognitive recovery in several injury models. For example, anti-Nogo-A treatment after traumatic brain injury improved spatial learning in the Morris water maze (Lenzlinger et al., 2005), and anti-Nogo-A treatment after medial agranular cortex aspiration lesion promoted recovery from hemispatial neglect, one of the most common cognitive

impairments after ischemic stroke (Brenneman et al., 2008; Gottesman and Hillis, 2010). After stroke in aged rats, anti-Nogo-A treatment significantly improved the rate of acquisition of the hidden platform location in the Morris water maze, however this did not correlate with dendritic plasticity in the hippocampus, suggesting a different mechanism of efficacy (Gillani et al., 2010).

Cloning of the *nogo* gene and biochemical features of Nogo-A

Until 2000, the identity of the protein antigen for IN-1 was unknown. However, a milestone study published that year reported the cloning of the gene designated '*nogo*' (Chen et al., 2000). The *nogo* gene was shown to give rise to three protein products—Nogo-A, -B, and –C—based on differential promoter usage (Nogo-C) and alternative splicing (Nogo-A and –B). The largest of the three, Nogo-A (1,163 amino acids), contained all of the sequence fragments derived from the bovine equivalent of the 250 kDa inhibitory fraction ("bNI-220") first identified in rat CNS myelin. Therefore, it was believed that specifically the 'A' isoform of Nogo contained the growth inhibitory activity. All three isoforms share a region of homology at the C-terminus, the so-called reticulon homology domain (see below). Recombinant Nogo-A expressed and purified from CHO cells was inhibitory toward fibroblast spreading and neurite outgrowth, and antibodies generated against recombinant Nogo-A recapitulated the growth promotion into CNS myelin seen with IN-1 treatment.

In the same issue of *Nature*, two additional studies confirmed the identity of the inhibitory protein. Stephen Strittmatter's laboratory reported that Nogo is a member of

the reticulon protein family and proposed both the first membrane topology model and the first inhibitory domain for this protein (GrandPré et al., 2000). In COS-7 cells overexpressing full length Nogo-A cDNA, a 66-amino acid loop found between the two hydrophobic regions ("Nogo-66") was found to be exposed at the cell surface, whereas N- or C-terminal Myc epitope tags were not labeled under nonpermeabilizing conditions. Oligodendrocytes derived from spinal cord explants also showed Nogo-66 surface staining. Recombinant Nogo-66 was able to collapse E12 chick DRG growth cones with an EC_{50} in the low nanomolar range, identifying Nogo-66 as an inhibitory domain within the Nogo-A protein (GrandPré et al., 2000). Lastly, Prinjha and colleagues identified human Nogo-A and confirmed that the human protein could indeed potently inhibit neurite growth (Prinjha et al., 2000).

Extensive screening of peptide sequences derived from full-length Nogo-A led to the identification of additional domains inhibitory toward fibroblast spreading and neurite outgrowth, and/or capable of collapsing neuronal growth cones (Oertle et al., 2003). Peptides comprising amino acids 59-172 ("NiR-Δ2") and 544-725 ("NiG-Δ20"), when pre-adsorbed to tissue culture plates, were both sufficient to inhibit 3T3 fibroblast spreading at low concentrations, and adhesion at high concentrations. (The designation "NiG" refers to the region of Nogo-A that is not shared by either Nogo-B or Nogo-C, ie. amino acids 174-979.) However, of the two domains, only Δ20 was found to inhibit neurite outgrowth. Monomeric Nogo-66 was capable of inducing growth cone collapse, though this activity was potentiated by peptide dimerization. Dimeric but not monomeric

Δ20 was likewise capable of growth cone collapse. The results of this study are summarized in table 2.1.

	Effect (by cell type)					
Nogo-A domain	**3T3 cells**	**PC12 cells**	**E7-9 chicken RGCs**	**P7 rat cerebellar granule cells**	**E13-E15 chicken DRG neurons**	**P6 rat DRG neurons**
NiR-Δ2	Spreading ↓ Adhesion ↓ (at high conc.)	Minor effect on neurite outgrowth	Marginal effects on axon growth in stripe assay	NT	NT	NT
NiG-Δ20	Spreading ↓ Adhesion ↓ (at high conc.)	Neurite outgrowth ↓	Nonpermissive to axon growth in stripe assay	NT	Growth cone collapse when dimeric No growth cone collapse when monomeric	Growth cone collapse when dimeric
Nogo-66	No effect on spreading	No effect on neurite outgrowth	NT	Neurite outgrowth ↓ (Niederöst et al., 2002)	Growth cone collapse (more potent when dimeric)	Growth cone collapse when dimeric
NiG	NT	NT	NT	Neurite outgrowth ↓ (& confirmed in (Niederöst et al., 2002))	No growth cone collapse when monomeric	NT

Table 2.1 ▲ Summary of (Oertle et al., 2003) and supplemented with additional studies where indicated. RGC: retinal ganglion cells; DRG: dorsal root ganglion. NT not tested.

Subcellular trafficking and localization of Nogo-A

The exact membrane topology of Nogo-A has been intensely scrutinized, because presumably, the inhibitory domains must be exposed at the cell surface of oligodendrocytes to exert an effect on neighboring cells. The presence of two 35 and 36 aa hydrophobic stretches suggests sites of membrane insertion. These sequences are longer than typical single-pass membrane insertion domains, suggesting the formation of a hairpin whereby the protein dips into the membrane and exits again on the same side (Kempf and Schwab,

2013). The membrane topology or surface fraction may be cell type-specific: primary oligodendrocytes express both Nogo-66 and N-terminal Nogo-A domains at the cell surface, whereas in CHO cells transfected with Nogo-A, the 11C7 epitope (and possibly, all of Nogo-A) is exclusively intracellular (Oertle et al., 2003). Antibodies against N-terminal, Nogo-A-specific epitopes also revealed surface localization in 3T3 fibroblasts, neonatal rat DRG neurons, and C2C12 myoblast cells (Dodd et al., 2005). Regardless, the intracellular fraction of Nogo-A predominates in oligodendrocytes and most cell types, estimated to comprise approximately 99% of the total cellular Nogo-A content (Oertle et al., 2003). Intracellularly, Nogo-A has been found to colocalize with markers of the endoplasmic reticulum and Golgi in oligodendrocytes (Oertle et al., 2003). The function of ER-associated Nogo-A is largely unknown, but may be involved in maintaining ER membrane curvature (Voeltz et al., 2006). However, this function is likely subserved by other proteins outside of the CNS, where Nogo-A expression is minimal.

Nogo-A contains a di-lysine ER retention motif, but lacks a conventional N-terminal ER signal sequence (Schwab, 2010). Why Nogo-A, which contains an ER retention sequence, is transported to the cell surface is unclear, but not unprecedented. For example, other myelin proteins, AMPA and NMDA glutamate receptors, GABA-B receptors, and even the ER markers calnexin and calreticulin contain ER retention sequences but can be found to varying degrees at the cell surface (Dodd et al., 2005). It has been hypothesized that Nogo-A may be transported to the cell surface independently of

the Golgi apparatus through either direct ER-plasma membrane fusion or ER vesicle budding (Kempf and Schwab, 2013).

Nogo-A receptors and intracellular mediators

In 2001, the first neuronal receptor for Nogo-A was reported (Fournier et al., 2001). The receptor, named NgR1, could bind with high affinity to soluble Nogo-66 and cause growth cone collapse. Because NgR1 is anchored to the plasma membrane by a glycophosphatidylinositol (GPI) linkage, rather than possessing an intracellular domain, it was hypothesized that NgR1 signals through complexing with other proteins. The first co-receptor for NgR1 was identified as the low affinity neurotrophin receptor p75 (Wang et al., 2002). However, due to the limited expression of p75—including a lack of expression in some Nogo-A-responsive neurons—other components of the NgR signaling complex were theorized. This led to the identification of TROY (aka TAJ) as an NgR co-receptor, which is more abundantly expressed in the adult brain than p75 (Shao et al., 2005). A third major component of the signaling complex, LINGO-1, was identified after the observation that NgR1 and p75 co-transfection was not sufficient to activate downstream signaling in COS7 (non-neuronal) cells (Mi et al., 2004). Notably, NgR1 can also be activated by other neurite growth inhibitors, such as myelin-associated glycoprotein (MAG), oligodendrocyte myelin glycoprotein (OMgp), and chondroitin sulfate proteoglycans (Schwab and Strittmatter, 2014). More recently, paired immunoglobulin receptor B (PirB) was identified as an additional receptor for Nogo-66, MAG, and OMgp (Atwal et al., 2008).

The identity of the receptor for the Δ20 domain of Nogo-A, located within amino-Nogo, proved to be more elusive. One study found that amino-Nogo antagonized the activity of certain integrins (Hu and Strittmatter, 2008), thereby inhibiting adhesion to extracellular matrix components. The orphan GPCR GPR50 was found to bind Nogo-A partially through an interaction site within amino-Nogo and influence neurite outgrowth, though it appears no follow-up studies have been performed regarding the role of GPR50 in Nogo-A signaling (Grünewald et al., 2009). A comprehensive study published in 2014 provided the most compelling evidence for an amino-Nogo receptor responsible for its multiple effects on restricting anatomical and synaptic plasticity, the previously characterized sphingosine-1-phosphate (S1P) receptor sphingosine-1-phosphate receptor 2 (S1PR2) (Kempf et al., 2014). S1PR2 is expressed by several neuron populations in the adult brain, as well as by Δ20-responsive 3T3 and cerebellar granule cells *in vitro*. S1P and Nogo-A-Δ20 bind to different parts of the receptor, and Δ20 binding affinity is not affected by the presence of S1P. However, the presence of S1P can potentiate the cell spreading inhibition induced by Δ20, suggesting modulation by S1P (Kempf et al., 2014).

Both Nogo-66 and amino-Nogo-A are believed to exert their inhibitory effects by activating the small GTPase RhoA (Niederöst et al., 2002) (Fig. 2.1). Therefore, signaling from both S1PR2 and NgR1 converges on the activation of RhoA. RhoA then activates the Rho-associated protein kinase ROCK, whose downstream phosphorylation targets include LIM kinase, myosin light chain 2 (MLC2), and collapsin response mediator protein 2 (CRMP2) (Schmandke et al., 2014). Interestingly, while RhoA or ROCK

inhibition completely restored neurite outgrowth on a myelin-associated glycoprotein (MAG) substrate, RhoA or ROCK inhibition could restore only around 60 and 70% of neurite outgrowth on Nogo-66 and amino-Nogo substrates, respectively, suggesting an alternate, Rho/ROCK independent mechanism of Nogo-A signaling (Niederöst et al., 2002). In this same study, treatment of cerebellar granule cells with Nogo-66 or Nogo-A-Δ20 peptides *in vitro* also led to a decrease in the activation of Rac1, another Rho family GTPase.

To transduce Δ20 signals, S1PR2 couples to the G protein G_{13}, which activates the Rho guanine nucleotide exchange factor LARG and subsequently RhoA (Kempf et al., 2014). Once bound to Δ20, S1PR2 dimerizes with tetraspanin 3 follwed by internalization of this complex (Thiede-Stan et al., 2015). Internalization of Δ20 in ligand-receptor complex "signalosomes" is required for the inhibitory activity of this domain (Joset et al., 2010). This suggests the existence of a protease that can cleave the extracellular domain for Nogo-A to free it for endocytosis. Alternatively, after brain injury, fragments of myelin debris containing Nogo-A could potentially be endocytosed since they are no longer associated with an intact plasma membrane. Soluble Δ20 has also been found to reduce CREB phosphorylation in cultured DRG cells (Joset et al., 2010). Much of the work on Δ20 intracellular signaling mediators was performed before S1PR2 was identified as a Δ20 receptor. Therefore, it is likely that these signaling mediators are downstream of S1PR2, but in most cases this has not been shown experimentally.

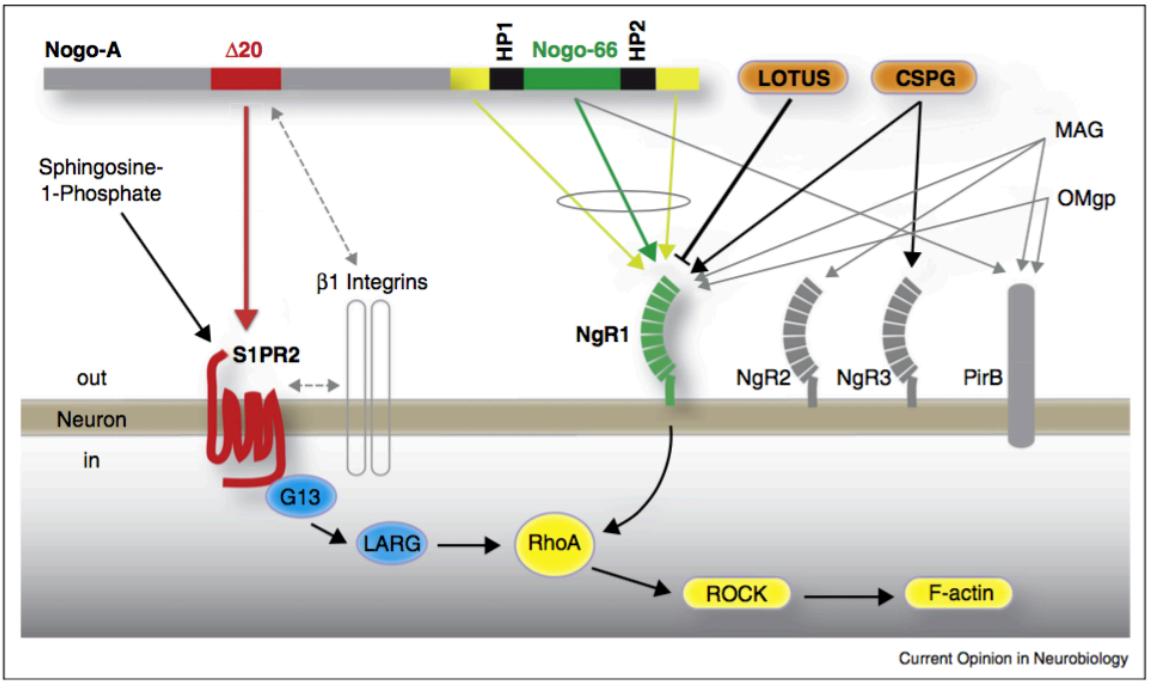

Figure 2.1 ▲ Nogo-A signal transduction pathway. Nogo-A-Δ20 interacts with two receptors, S1PR2 and integrins, while Nogo-66 activates NgR1 and PirB. S1PR2 and NgR1 signaling both converge on activation of the small GTPase RhoA, which modulates cytoskeletal contractility. HP1, HP2: hydrophobic segments; LOTUS: Cartilage Acidic Protein 1B; CSPG: chondroitin sulfate proteoglycans. (Schwab and Strittmatter, 2014).

Not just a neurite outgrowth inhibitor: Roles of Nogo-A in the normal brain

The role of Nogo-A in embryonic neural development

Expression patterns

Nogo-A has been detected in the embryonic brains of several species, including chickens, rodents, and humans (Caltharp et al., 2007; Haybaeck et al., 2012; Huber et al., 2002; Josephson et al., 2001; Mathis et al., 2010; Mingorance-Le Meur et al., 2007). In mice, Nogo-A expression is present from as early as embryonic day 12.5 (E12.5) in the

olfactory bulb, cerebellum, cortex, thalamus, and hippocampus (Mingorance-Le Meur et al., 2007). Radial glia, the neural stem cells of the embryonic brain, also express Nogo-A (Mathis et al., 2010; Mingorance-Le Meur et al., 2007). At E15.5 and E17.5, Nogo-A expression is evident throughout the cortical anlage, including the marginal zone, cortical plate, subplate, intermediate zone, and subventricular zone in both radially- and tangentially-migrating neural precursors (Mathis et al., 2010). While Nogo-A expression is most appreciable in the cell bodies of radially migrating neurons, tangentially migrating neurons strongly express Nogo-A in both the cell body and especially in the leading process (Mathis et al., 2010; Mingorance-Le Meur et al., 2007). Post-migratory neurons in the cortical plate were also noted to express Nogo-A (Mathis et al., 2010). At 15.5, Nogo-A expression localizes to the growing axons of developing corticofugal projections. Nogo-A expression precedes NgR1 expression (Mingorance et al., 2004), suggesting an NgR1-independent function in the earliest stages of neural development. Nogo-A expression in oligodendrocytes is concomitant with myelination, occurring during early postnatal development (~P5-P9) (Huber et al., 2002).

Transcripts for the Nogo receptor components NgR1, Lingo-1, TROY, and p75 were found in E15.5 mouse brain-derived neurospheres. Migrating cells expressing nestin or βIII-tubulin were positive for NgR1, Lingo-1, and p75 by immunocytochemistry, while TROY expression was found only in nestin-positive cells, showing that these neural precursors expressed the components of the Nogo-66 receptor complex (Mathis et al., 2010). Importantly, Nogo-A was found to be expressed at the surface of embryonic

neurosphere-derived cells by immunocytochemistry (Mathis et al., 2010). *In vivo*, Nogo-66 receptors NgR1 and PirB were found to be expressed in nestin-positive neural stem cells in E14.5 mouse brain (Ramasamy et al., 2014).

Roles in proliferation, migration, and maturation/morphogenesis

Many studies involving Nogo-A in embryonic neural development have focused on its roles in migration and morphogenesis. Mathis *et al.* reported no effect of Nogo-A knockout on the number of BrdU+ cells in the cortex of E17.5 mice, consistent with a lack of an effect on cellular proliferation (Mathis et al., 2010). However, Nogo-66 peptide treatment of embryonic forebrain cortex-derived neural stem/progenitor cells was found to stimulate survival and proliferation in an NgR1- and PirB-dependent manner (Ramasamy et al., 2014). Therefore, a compensatory mechanism may counteract the effect of Nogo KO to maintain normal progenitor cell numbers *in vivo*.

A study in Nogo-A/B/C knockout mice revealed no changes in the radial migraton of neural precursor cells and normal development of cortical tracts (Mingorance-Le Meur et al., 2007), while a subsequent study did note subtle disturbances in radial migration in Nogo-A-specific KO mice (Mathis et al., 2010). Nogo-A-specific knockout did not affect the development or morphology of radial glia (Mathis et al., 2010). The migration of *early* cortical interneurons (labeled at E12.5) is delayed in Nogo knockout mice, while interneurons born at E15.5 are unaffected, suggesting differential roles of Nogo-A in these two populations (Mingorance-Le Meur et al., 2007). In both Mingorance-Le Meur's and Mathis's studies, these migration deficits in Nogo-A KO mice were not permanent, as

cortical neuron quantity was normal when examined in adulthood. This lack of gross defects is consistent with the viable and behaviorally mild phenotype observed in Nogo-A KO mice.

In vitro, the motility of E15.5 mouse brain-derived neural precursors was affected by various manipulations of Nogo-A signaling. The distance traveled by both neural precursors from Nogo-A KO mice and neural precursors treated with anti-Nogo-A antibody 11C7 was increased versus controls, due in part to fewer pauses made during their migratory cycles. The maximum speed attained by Nogo-A knockout cells did not significantly differ from wildtype controls, though anti-Nogo-A antibody treatment led to an increase in maximum speed. Interestingly, these results (distance covered, maximum speed, and number of pauses) could be recapitulated by neutralizing antibodies to NgR1 or LINGO-1, even though 11C7 targets Δ20, the Nogo-A domain that is not believed to bind to NgR1 (Mathis et al., 2010). The authors speculated that the antibody may interfere with NgR1 directly by steric hindrance, or indirectly by inducing internalization of surface Nogo-A (Mathis et al., 2010; Weinmann et al., 2006). The adhesion and spreading of neural precursors from both WT and Nogo-A KO mouse brains was inhibited by Δ20 peptide, and to a similar degree in both genotypes, suggesting that adhesion/spreading inhibition is mediated in a non-cell autonomous manner. However, the effect of exogenous Δ20 peptide—either presented as a substrate or applied to the media—on the migration of embryonic neural precursors was not investigated in this study (Mathis et al., 2010).

Neurons cultured from E15.5 Nogo-A/B/C knockout mice become polarized (ie., extend a single, major neurite) more quickly than wildtype neurons and display increased neurite branching (Mingorance-Le Meur et al., 2007). Consistent with this result, cerebellar purkinje cells in Nogo-A KO mice display larger, more complex dendritic trees *in vivo*(Petrinovic et al., 2013b). However, ventral mesencephalic dopaminergic neurons from E13.5 Nogo-A knockout mice exhibited lower average neurite length and branching, an effect that is likely cell autonomous given the lack of an effect of Nogo-A neutralizing antibody (Kurowska et al., 2014). These results suggest that Nogo-A is involved in the morphogenesis of populations of neurons in the embryonic brain, but its role may differ depending on the specific cell type.

Neurospheres—aggregates of neural progenitors that develop when neural stem cells are grown in suspension culture—from E15.5 Nogo-A knockout mouse brain, or wildtype neurospheres differentiated in the presence of anti-Nogo-A antibody 11C7, did not differ in the proportions of neurons, astrocytes, or oligodendrocytes generated upon differentiation, suggesting that Nogo-A does not regulate lineage commitment of multipotent progenitors in the embryonic brain (Mathis et al., 2010). However, a separate study found that treatment of neonatal rat telencephalic neural stem/progenitor cells *in vitro* with recombinant Nogo-66 peptide skewed the differentiation of these cells toward an astroglial fate at the expense of neuronal differentiation (Wang et al., 2008). As this effect was dependent on NgR1, the availability of other NgR1 ligands (eg., MAG) may explain the lack of an effect of Nogo-A KO on lineage commitment *in vivo*.

The role of Nogo-A in the migration of non-neuronal cells

Several studies have implicated Nogo-A in the migration of non-neuronal CNS cells. Nogo-A has been found to inhibit the migration of microglia, malignant glioma cells, brain vascular endothelial cells, and olfactory ensheathing cells as measured in transwell Boyden chamber assays (summarized in table 2.2). While migration of these cell types is inhibited by Nogo-A signaling, the influence of Nogo-A on cell adhesion appears to depend on cell type, as microglia, glioma, and endothelial cells adhere poorly to substrate bound Nogo-66, while olfactory ensheathing cells adhere more avidly.

Reference	Cell type	Manipulation	Effect
(Yan et al., 2012)	Microglia	Nogo-66 peptide substrate coating	↓ microglia adhesion to recombinant Nogo-66 spotted on tissue culture plates. ↓ microglia migration on substrate-bound recombinant Nogo-66.
(Liao et al., 2004)	Glioma cells	Nogo-66 peptide substrate coating	↓ adhesion and migration of U87MG human glioma cells on substrate-bound recombinant Nogo-66
(Nocentini et al., 2012; Reginensi et al., 2015; Su et al., 2007)	Olfactory ensheathing cells (OECs)	Nogo-66 peptide substrate coating	↑ adhesion and ↓ migration of OECs
(Wälchli et al., 2013)	Vascular endothelial cells	Δ20 peptide substrate coating	↓ adhesion and migration of primary mouse brain-derived microvascular endothelial cells

Table 2.2 ▲ Summary of the effects of Nogo-A on the motility of various cell types found in the CNS.

The roles of Nogo-A in the hippocampus

Due to the high hippocampal expression of Nogo-A, especially in neurons, the function of Nogo-A in hippocampal function and synaptic plasticity has been attracted particular attention. In the hippocampus, both Nogo-A and NgR1 are localized pre- and post-synaptically, though NgR1 is more enriched post-synaptically (Lee et al., 2008). The induction of long-term depression (LTD) at CA3-CA1 synapses is impaired in NgR1-knockout mice, while these mice display enhanced CA3-CA1 LTP in the presence of fibroblast growth factor (Lee et al., 2008). In accordance, Nogo-66 peptide application significantly suppressed the induction of LTP at CA3-CA1 synapses. (Raiker et al., 2010). Δ20-S1PR2 signaling appears to play a similar role in restricting synaptic plasticity as Nogo-66-NgR1. LTP at CA3-CA1 synapses is enhanced in transgenic Nogo-A knockdown rats and after acute application of anti-Nogo-A antibody 11C7 or the S1PR2 antagonist JTE-013 (Delekate et al., 2011; Kempf et al., 2014; Tews et al., 2013). Therefore, Nogo-A plays a role in restricting synaptic plasticity.

Despite these effects of Nogo-A on synaptic plasticity, cognitive manifestations of Nogo-A knockout are typically mild. The performance of transgenic Nogo-A knockdown rats in Carousel maze place avoidance, but not Morris water maze delayed-matching-to-place, is impaired (Petrasek et al., 2014a). Both are tests of spatial memory, but the Carousel maze requires dissociating reference cues within the testing room from those of the maze itself, which can be rotated during testing. These findings suggest that the proper

balance of Nogo-A signaling, including during the development of behaviorally relevant circuits, is necessary for optimal learning and memory.

ADULT NEUROGENESIS

History of adult neurogenesis

It is now widely accepted that new neurons continue to be added to the adult brain, including in humans. The presence of proliferative zones in the adult rodent brain has been noted for over 100 years, including in the walls of the lateral ventricles (Allen, 1912). Beginning in the 1960's, several studies by Joseph Altman renewed the study of postnatal mammalian neurogenesis, using tritiated thymidine autoradiography (which required a film exposure time of 2-4 months) to demonstrate cellular proliferation in the walls of the lateral ventricles and the production of dentate granule neurons in the hippocampus of the adult rat (Altman, 1962; 1963; Altman and Das, 1965). In the 1980's, Fernando Nottebohm's laboratory demonstrated substantial addition of new neurons to songbird vocal centers (eg., (Goldman and Nottebohm, 1983)). Beginning the next decade, much of the work on postnatal neurogenesis continued focusing on two areas: the walls of the lateral ventricles, termed the subventricular zone (SVZ), and the dentate gyrus (DG) of the hippocampus.

The SVZ and DG: Two major neurogenic niches in the adult brain

While cellular proliferation in the SVZ and the appearance of new neurons in the olfactory bulb (OB) had been appreciated for decades, as late as the early 1990's, the connection between the two was unclear. One prominent study concluded that the adult

rodent SVZ was essentially vestigial and generated only cells destined for cell death, based on the lack of retention of newly generated cells in the SVZ or surrounding tissue (Morshead and van der Kooy, 1992). However, a seminal study in 1994 by Arturo Alvarez-Buylla's laboratory showed that, while labeled cells typically are not retained in the SVZ, rather than dying they instead migrate long distances into the OB and mature into neurons (Lois and Alvarez-Buylla, 1994).

Subsequent work continued to generate a coherent picture of SVZ-OB neurogenesis (Fig. 2.2). Quiescent, astrocyte-like neural stem cells (aka type B cells) can become activated and divide asymmetrically to generate another stem cell and a transit-amplifying progenitor (type C cell). Type C cells then divide rapidly and give rise to neuroblasts (type A cells), which are neuronally-committed. Neuroblasts migrate tangentially from the SVZ to the OB through the rostral migratory stream (RMS) in a distinctive migratory mode called "chain migration," in which chains of neuroblasts in close contact slide past one another on their way to the OB. Once these chains of neuroblasts reach the olfactory bulb core, they separate and migrate radially as single cells into the olfactory bulb parenchyma. They then complete their maturation and integrate into local circuitry as GABAergic granule (about 95% of newborn cells) and periglomerular (less than 3%) interneurons, or glutamatergic juxtaglomerular cells (an even smaller percentage) (Lazarini and Lledo, 2011; Lim and Alvarez-Buylla, 2016).

SVZ neural stem cells can also generate oligodendrocytes that migrate dorsally into the corpus callosum (Menn et al., 2006) and astrocytes that can migrate toward sites of

injury (Benner et al., 2013). Intriguingly, a recent study showed that SVZ neural stem cells, normally thought to be sessile, can migrate toward a cortical infarction and generate reactive astrocytes, which can give rise to neurospheres *in vitro*, suggesting the potential for local neuronal replacement under the right circumstances (Faiz et al., 2015)

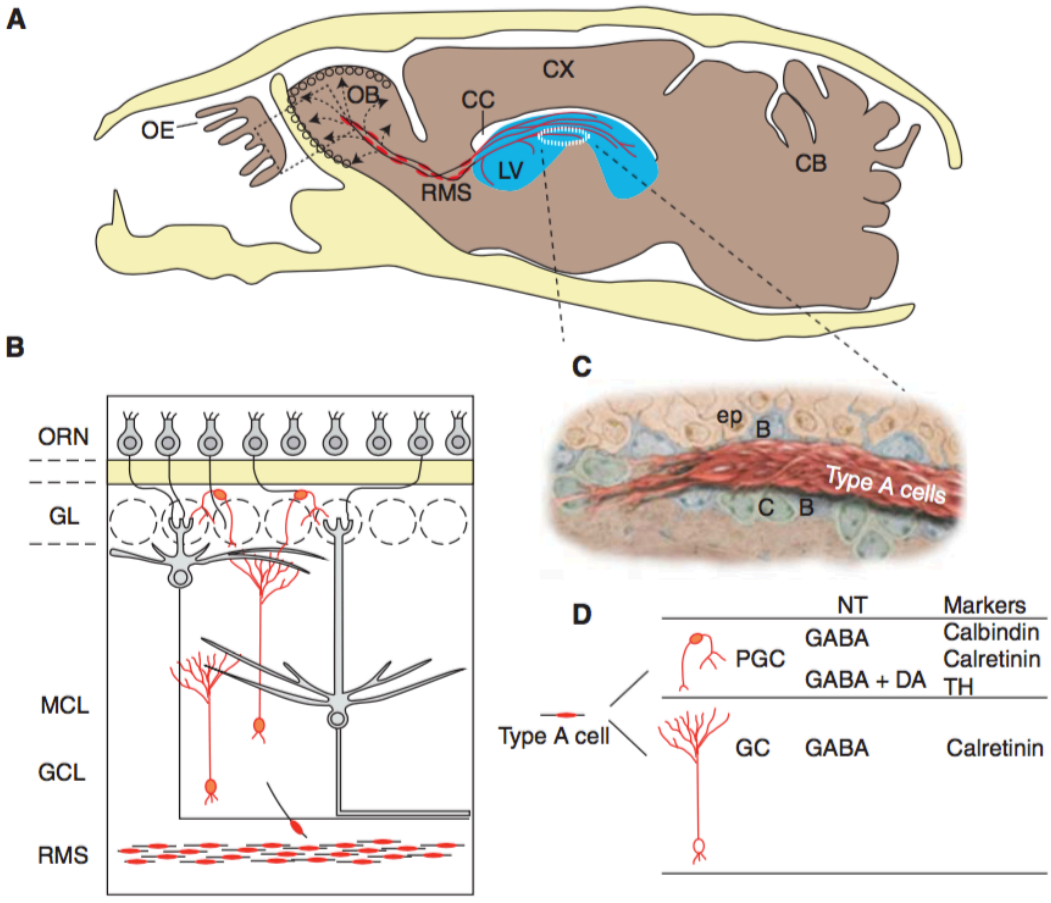

Figure 2.2 ▲ Overview of SVZ-OB neurogenesis. From (Lim and Alvarez-Buylla, 2016). (A) Sagittal view demonstrating the anatomical relationships between the lateral ventricle (LV), rostral migratory stream (RMS), olfactory bulb (OB), and olfactory epithelium (OE). CC: corpus callosum; CX: cortex; LV: lateral ventricle; CB: cerebellum. (B) Enlargement of boxed area in 'A.' Olfactory receptor neurons (ORNs) project axons into the glomerular layer (GL), where they synapse with mitral and tufted cells. New neurons detach from the RMS and migrate radially, maturing mainly into granule cells (GCL: granule cell layer), or periglomerular cells. MCL: mitral cell layer. (C) Depiction of chain migrating neuroblasts

(type A cells). (D) Mature neuron types generated in SVZ/OB neurogenesis. PGC: periglomerular cell; GC: granule cell; NT: neurotransmitter.

In the hippocampus, neural stem cells reside in the subgranular zone (SGZ) of the dentate gyrus, located at the interface of the hilus and granule cell layer. The naming convention is different in the DG than in the SVZ: stem cells (type 1 cells) give rise to progenitors (type 2a and 2b cells), which generate neuroblasts that develop into glutamatergic dentate granule cells (Fig. 2.3). Most newborn cells in the DG die by apoptosis within the first few days of birth (at the early progenitor stage), or 1-3 weeks after birth (at the immature neuron stage). A fundamental property of newborn DG neurons is their hyperexcitability. During a critical period between 3-6 weeks after birth, young neurons, like their mature counterparts, receive excitatory, glutamatergic input from the entorhinal cortex. However, unlike mature granule cells, young neurons lack strong inhibitory GABAergic input, contributing to a lower threshold for the induction of long-term potentiation (LTP). Importantly, functional input from the entorhinal cortex means that the activity of newborn neurons can be regulated by behavioral experience (Christian et al., 2014).

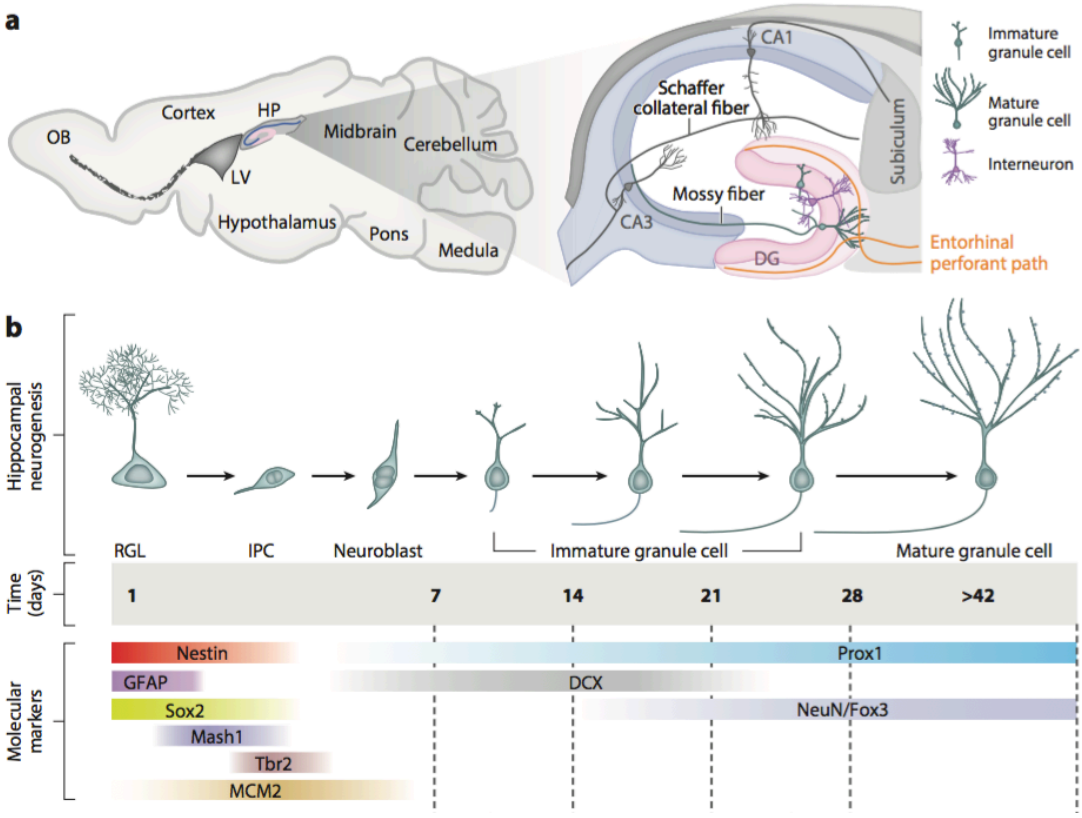

Figure 2.3 ▲ Overview of adult neurogenesis in the dentate gyrus. (A) Representation of a sagittal rodent brain section (left), with the hippocampus enlarged (right) to show details. Right: the classical hippocampal trisynaptic circuit. Inputs from the entorhinal cortex synapse on the dendrites of dentate granule cells (the cell type generated in adult hippocampal neurogenesis) via the perforant path. Granule cell axons (mossy fibers) then synapse onto CA3 pyramidal cells, which in turn project Schaffer collaterals to CA1. (B) Overview of lineage progression from radial glia-like (RGL) neural stem cells, to intermediate progenitor cells (IPCs), to neuroblasts, immature, and finally mature granule cells. From (Christian et al., 2014)

The functions of adult SVZ-OB and DG neurogenesis

The functions of adult neurogenesis in the normal brain are continuing to be elucidated. Adult neurogenesis is not necessary for survival, and typically, phenotypes after ablating neurogenesis are evident only under strict experimental circumstances.

The role of SVZ-OB neurogenesis is still poorly understood, but as in the DG, new OB neurons integrate into and influence the activity of existing circuits. The olfactory system processes chemosensory signals from the outside world. Odorant molecules enter the nose and partition into the olfactory mucosa where they bind to olfactory receptors expressed by olfactory sensory neurons (OSNs). These OSNs in turn project axons through the cribriform plate into the OB, where they synapse on the main projection neurons of the olfactory bulb, mitral and tufted cells. Notably, each OSN expresses just a single olfactory receptor gene, and axon terminals of OSNs expressing the same gene converge on only a few OB glomeruli, discrete bundles of synaptic contacts between OSNs and mitral and tufted cells (Munger et al., 2009). The cell types generated in SVZ-OB neurogenesis—periglomerular and granule cells—are inhibitory neurons that refine the sensory input relayed by OSNs to the OB. Periglomerular cells can modulate incoming information by interacting with OSN axon terminals and mitral and tufted cell dendrites. Granule cells, which lack traditional axons and are located in deeper layers of the OB, release GABA onto mitral cell dendrites at dendro-dendritic synapses (Lazarini and Lledo, 2011). After processing, odor information is then relayed to higher-order brain centers. New neurons are not required for olfactory detection or discrimination, but appear to be

involved in cognitive processing of odorant context. For example, new neurons are critical in *learning* to discriminate two similar odors (ie., olfactory perceptual learning) (Moreno et al., 2009). Irradiation of the SVZ, which reduces cellular proliferation, had no effect on odorant detection or discrimination, but impaired olfactory fear conditioning and the long-term memory of particular odorants that were associated with a reward (Lazarini et al., 2009; Valley et al., 2009).

New neurons in the hippocampus are most commonly implicated in *pattern separation*, the means by which similar inputs are processed as distinct (Clelland et al., 2009). Therefore, ablation or stimulation of adult hippocampal neurogenesis manifests as deficits or improvements, respectively, in discriminating subtle differerences in spatial patterns (Lacar et al., 2014; Sahay et al., 2011). Younger neurons receive the same entorhinal cortical input as their mature counterparts, but are transiently more excitable, segregating immature and mature dentate granule cells into electrophysiologically distinct groups. Certain studies have found that ablating hippocampal neurogenesis manifests as deficits in spatial memory tasks in the Morris water maze, in which animals must use visual cues from the environment to find the location of a hidden platform in a pool of water (reviewed in (Garthe and Kempermann, 2013)). Most consistently, neurogenesis is important for acquisition of the platform location, probe trial performance (in which the platform is removed and the amount of time spent in the goal quadrant is measured), and reversal (where the platform is moved to a new location and the animal must re-learn a navigation strategy) (Garthe and Kempermann, 2013).

Adult neurogenesis in humans

The human SVZ and DG are both capable of generating new neurons into adulthood. Neurospheres can be cultured from the adult human SVZ and differentiate into both neurons and astrocytes (Sanai et al., 2004), and cells expressing doublecortin and PSA-NCAM, markers of immature neurons, can be found in the walls of the lateral ventricle (Bergmann et al., 2015). The existence of the human RMS was once a matter of debate, which played out in the editorial pages of *Science* (Curtis et al., 2007a; 2007b; Sanai et al., 2007), but now consensus seems to support the dissolution of the RMS shortly after birth (Bergmann et al., 2015; Sanai et al., 2011). Another difference between the rodent and human SVZ is the cytoarchitecture of this area—the human SVZ lacks chain migrating neuroblasts, but contains a unique "astrocyte ribbon" at the lateral SVZ (Quiñones-Hinojosa et al., 2006; Sanai et al., 2004). The number of neurons produced in the human olfactory bulb is thought to be extremely small (if it happens at all), which is not entirely surprising given the relative small size of the olfactory bulbs, and relative lack of evolutionary importance of olfaction in humans compared to other mammals (Bergmann et al., 2015; Lim and Alvarez-Buylla, 2016). A recent study found evidence of new striatal neurons in humans and suggested that these may derive from the SVZ (Ernst et al., 2014), though these results were not subsequently replicated using either human or rhesus macaque samples (Wang et al., 2014).

The literature regarding neurogenesis in the human DG is somewhat less contentious. A seminal study by Fred Gage's laboratory was the first to report hippocampal neurogenesis in humans, using samples from patients that had received BrdU for diagnostic purposes (Eriksson et al., 1998). As in the human SVZ, DCX-positive cells can be found in the human DG throughout adulthood, though the number of cells declines with age (Knoth et al., 2010). It has been estimated that roughly 700 new neurons are added to the human hippocampus each day (Spalding et al., 2013). Beyond its role in cognition, hippocampal neurogenesis, or disturbances thereof, has been implicated in the pathophysiology of a diverse array of conditions, including epilepsy, depression, and age-related cognitive decline. However, many of these relationships are purely correlative as neurogenesis cannot be easily experimentally manipulated in humans and confirmed with histological studies (Bowers and Jessberger, 2016).

Neurogenesis after stroke

A comprehensive review of all post-stroke neurogenesis studies is daunting (as of May, 2016, more than 1,700 publications were returned when searching PubMed for the key words stroke/ischemia and neurogenesis/subventricular). Many different strategies have been developed to model ischemic stroke in animals. Combined with species and even strain differences in the effects of these models on the brain (Carmichael, 2005), it is difficult to make a unifying statement about the degree to which ectopic neurogenesis occurs after stroke. Variables that may contribute to differences in measurements in neurogenesis after injury are found in table 2.3.

Species and *strains*	Ischemia models	Infarct sizes (% of intact hemisphere)	Areas of ischemia	Post-surgical methodology
Rat *Sprague-Dawley* *Wistar* *Fischer 344* *Long-Evans* Mouse *C57BL/6* *BALBc* *Sv129* *CD-1* Gerbil	Global Focal Transient MCAO Permanent MCAO Photothrombotic Endothelin-1 Pial vessel disruption Cardio-embolic	6-50+%	Cortex Striatum Thalamus Hypothalamus Hippocampus	Definition of neurogenesis (BrdU, BrdU/DCX, BrdU/NeuN) BrdU injection schedule Sampling rigor (# of tissue sections, # of cells examined, confocal vs widefield microscopy)

Table 2.3 ▲ Selected variables in preclinical rodent models that can influence how neurogenesis is induced and measured after stroke.

The majority of studies investigating post-stroke neurogenesis employ the transient middle cerebral artery occlusion (tMCAO) model, in which a suture is threaded into the internal carotid artery to the origin of the middle cerebral artery and transiently (30-120 min) left in place before withdrawal (Carmichael, 2005). This produces an infarction core in the ipsilateral striatum, while the overlying cortex is hypoperfused and vulnerable (ie., the ischemic penumbra). However, other regions, including the thalamus, hypothalamus, and substantia nigra may be damaged with prolonged vessel occlusion. A critical factor that may complicate the extrapolation of post-tMCAO neurogenesis studies to post-stroke neurogenesis in general is the proximity of the infarcted area to the SVZ. Occasionally, the infarcted region can even abut the SVZ (eg., (Jin et al., 2010; Thored et al., 2007)).

Effects of focal ischemia on the SVZ could possibly be distance-dependent. Additionally, counting proliferating cells in the SVZ after injury involving the medial striatum could lead to an overestimate of the number of *bona fide* proliferating neural precursor cells due to inadvertent counting of microglia or macrophages, which proliferate robustly after injury (see Fig. 2.4 for a comparison of infarct territory in tMCAO versus smaller cortical stroke).

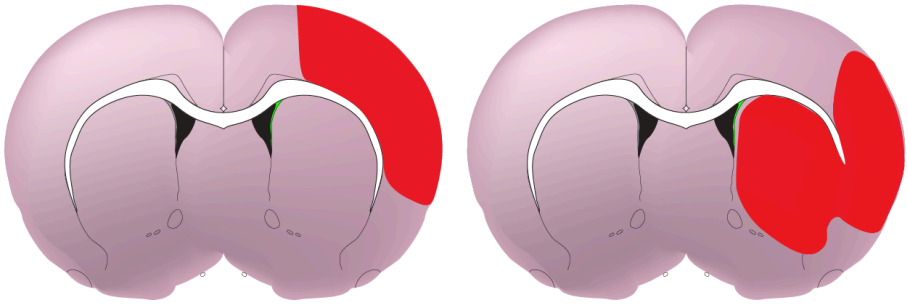

Figure 2.4 ▲ Representative lesion (red) locations for distal versus severe transient MCAO and proximity to the SVZ (green). In tMCAO, involvement of the medial striatum, as depicted here, is more prominent with prolonged occlusion.

There have been numerous reports of subventricular zone-derived neurogenesis after tMCAO. The first study to investigate this phenomenon found that a 90 minute tMCAO in rats increased cellular proliferation in the ipsilesional and contralesional SVZ, peaking at 2 weeks post-ischemia before decreasing back to baseline (Jin et al., 2001). The following year, two prominent studies—one published while the other was in press—provided evidence for the production of new mature striatal neurons after stroke (Arvidsson

et al., 2002; Parent et al., 2002). Arvidsson and colleagues reported that stroke stimulated proliferation within the SVZ—however these results need to be interpreted cautiously because their BrdU injection schedule (twice daily injections for 14 days after stroke) was not specific for cellular proliferation. Over the course of 14 days, newly proliferated, BrdU+ cells would be expected to migrate out of the SVZ toward the olfactory bulbs, a process that may be disrupted by the presence of injury (Ohab et al., 2006). The survival of newborn cells could also be affected. In this study, DCX+ neuroblasts were seen apparently migrating from the SVZ toward the damaged striatum, but were not found in the vicinity of the infarcted parietal cortex. The DCX+ cells in the striatum expressed Meis2, a transcription factor associated with medium spiny neurons, the predominant type of mature neuron in the striatum. At 6 weeks after stroke, following twice daily BrdU injections at days 1-14 post-stroke, an average of 750 BrdU+/NeuN+ new neurons per mm^3 were found in the ipsilesional striatum, whereas only 78 new neurons per mm^3 were found at 2 weeks post-stroke (Arvidsson et al., 2002). Importantly, the increase in BrdU+/NeuN+ cells over a time frame consistent with the maturation of new neurons argues against significant BrdU incorporation by mature neurons undergoing DNA repair or abortive cell cycle re-entry, which are always caveats when using thymidine analogs as markers of proliferation (Taupin, 2007). The SVZ origin of these newborn striatal neurons was confirmed by pre-labeling SVZ cells and finding that these labeled cells, but not pre-labeled striatal cells, had matured into striatal neurons after stroke (Yamashita et al., 2006).

Post-ischemic neurogenesis in the cortex is not as well established. The early studies of post-stroke striatal neurogenesis found no evidence of new cortical neurons (Lindvall and Kokaia, 2015). Two studies from the same lab reported new cortical neurons in adult rats subject to either cortical photothrombotic stroke or tMCAO (Gu et al., 2000; Jiang et al., 2001). Later studies by different laboratories found cortical neurogenesis induced by distal MCAO in spontaneously hypertensive rats and by photothrombotic stroke in mice (Leker et al., 2007; Ohab et al., 2006). The number of new neurons produced in the cortex after ischemia is likely very low, and determining the factors that limit cortical neurogenesis could help design interventions to promote cortical repair.

Generally, current dogma holds that brain injury increases the number of proliferating cells in the SVZ. However, reports of *decreased* proliferation are not unprecedented. For example, the SVZ responds to cortical aspiration lesion in mice in a biphasic manner, with an early transient decrease in proliferation (between 6 hours and 3 days after injury), followed by a return to baseline, and then a longer-term decrease once again (after day 25 post-injury) (Goings et al., 2002). After distal MCAO in spontaneously hypertensive rats, the number of SVZ cells positive for the proliferation marker Ki67 was reduced at 5 weeks post-stroke versus control (a longer term time point than most post-stroke proliferation studies) (Komitova et al., 2005).

Ectopic, post-stroke neurogenesis in humans is not well established. Some studies have reported stroke-induced increases in proliferating cells and immature neurons in the SVZ and ischemic cortex (Jin et al., 2006; Macas et al., 2006; Martí-Fàbregas et al., 2010).

However, a subsequent study found no evidence that any mature neurons in the ischemic cortex were adult-born, and suggested that upregulation of doublecortin by mature neurons had been misinterpreted as a neurogenic response (Huttner et al., 2014).

The relevance of post-stroke neurogenesis in neuroprotection or longer-term behavioral recovery is not fully understood. Ablation of doublecortin-expressing cells prior to tMCAO exacerbates behavioral deficits and increases lesion size at 24 hours post-stroke in young and middle aged mice, suggesting a role of neurogenesis in mitigating the severity of ischemic injury (Jin et al., 2010; Sun et al., 2012). This group later performed behavioral testing out to 8 weeks after ablation of all neural stem cells and distal MCAO, and found minor but sustained sensorimotor deficits in mice with ablated versus intact neurogenesis (Wang et al., 2012). However, in this study the reduction in neurogenesis was only transient, with neurogenesis substantially restored by 8 weeks post-stroke. The effect of an absolute ablation of neurogenesis on long-term sensorimotor recovery is therefore unknown. Furthermore, none of these studies provide evidence that newborn mature neurons play any role in recovery. Rather, they suggest that the presence of neural stem cells and neuroblasts is beneficial after injury, whether by maturing into neurons or by other mechanisms. Future studies measuring the behavioral effects of selectively and reversibly silencing newborn neurons (eg., pharmacogenetically or optogenetically) would provide strong evidence for or against the importance of new neurons in behavioral recovery after stroke.

In general, neurogenesis in the DG is also upregulated by ischemia. Early studies using a transient global ischemia model in gerbils showed increased cellular proliferation in the SGZ peaking at 11 days post-ischemia and a total increase in new neurons in the dentate granule cell layer at longer time points (Liu et al., 1998). Transient MCAO, distal permanent MCAO, and photothrombotic cortical strokes, which produce focal rather than global ischemia, likewise induce increased cellular proliferation and new neuron production in the SGZ/GCL (Jin et al., 2001; Kluska et al., 2005; Matsumori et al., 2006). Increased neurogenesis *per se* is not sufficient to stave off the cognitive deficits that follow stroke, but cranial irradiation to ablate neurogenesis exacerbates post-stroke spatial memory deficits (Raber et al., 2004). Conversely, interventions that increase hippocampal neurogenesis correlate with improved spatial memory performance after stroke (Wurm et al., 2007).

The role of Nogo-A in adult neurogenesis

There is very little published work on the role of Nogo-A in adult neurogenesis. NgR1 decoy protein treatment decreased the astrocytic differentiation of transplanted adult rat SVZ-derived neural stem/progenitor cells (NSPCs) after spinal cord transection, suggesting a role for NgR1 in NSPC differentiation (Guo et al., 2012). However, whether this was a direct effect on NSPCs, or occurred through modulation of the tissue microenvironment is unknown.

A study from Annalisa Buffo's laboratory, published in 2012, established much of what is known about the role of Nogo-A in the adult SVZ (Rolando et al., 2012). First, the expression pattern of Nogo-A and NgR1 was described. The expression of these two

proteins was found to be mutually exclusive: among neural precursor cells in the SVZ (ie., stem cells, progenitors, and neuroblasts), Nogo-A was expressed only by DCX+ neuroblasts and NgR1 was expressed only by neural stem cells. NgR1 antagonism led to increases in neural stem cell proliferation both *in vitro* and *in vivo*, while antibody-mediated neutralization of Nogo-A-Δ20 inhibited the migration of SVZ neuroblasts, possibly by causing neuroblasts to be too strongly adhesive to their substrate. The authors proposed a model whereby neuroblasts, expressing Nogo-A at their surface, could activate NgR1 on neural stem cells to inhibit their proliferation. This would serve as a negative feedback loop to maintain appropriate numbers of neural precursors in the SVZ. Additionally, the Δ20 domain of Nogo-A, acting through its receptor, would signal to neighboring neuroblasts to promote migration to the olfactory bulbs (Rolando et al., 2012). However, several issues were not addressed in this study. First, surface localization of Nogo-A was not experimentally demonstrated, but rather assumed given the effects of anti-Nogo-A antibody on migration. Second, demonstration of the anti-adhesive effects of Δ20 on SVZ-derived neuroblasts was performed by comparing adhesion on polylysine-coated coverslips to coverslips coated with polylysine plus Δ20. The predicted isoelectric point of Δ20 is approximately 4 (web.expasy.org), meaning that Δ20 would be mainly negatively charged at typical cell culture media pH and potentially neutralize the adhesion-promoting charge of the polylysine. Without using a control peptide with similar properties, it is difficult to determine whether Δ20 inhibits adhesion through receptor activation, or simply neutralizes the charge of the polylysine and makes the substrate less

favorable for attachment. Third, explants for *in vitro* migration analysis were taken from P5 mice, a stage that precedes most myelin development (and therefore, before myelin-associated Nogo-A is abundant) (Foran and Peterson, 1992; Huber et al., 2002). Therefore it is possible that the effects of Nogo-A signaling in P5 cells cannot be extrapolated to adult neuroblasts. Lastly, it was not known at the time of publication that S1PR2 was a receptor for Δ20. Therefore, the expression of this receptor by SVZ neuroblasts was hypothesized by the authors, but not experimentally shown.

No published studies have investigated a role of Nogo-A in normal hippocampal neurogenesis. After traumatic brain injury, however, $NgR1^{-/-}$ mice exhibited increased proliferation in the dentate gyrus SGZ and increased numbers of new neurons compared to wild-type controls, suggesting involvement of this receptor in new neuron production (Tong et al., 2013).

Nogo-A signaling mediators in adult neurogenesis

Effects of intracellular Nogo-A signaling mediators (eg., RhoA, ROCK, CREB) on adult neurogenesis have been more extensively studied, as these molecules are also targets of other non-Nogo-based signaling pathways.

In the hippocampus, RhoA/ROCK activation generally exerts a suppressive influence on adult neurogenesis in the form of decreased neuronal differentiation and survival (Christie et al., 2013; Keung et al., 2011). CREB activation (phosphorylation), which can be inhibited by Nogo-A-Δ20 signaling in dorsal root ganglion neurons (Joset et al., 2010), is particularly important for adult-born dentate granule cell development. Most

DCX+ immature neurons, but not mature granule cells, are positive for phospho-CREB, and CREB activation maintains proper neuronal polarity and stimulates dendritogenesis and neuronal survival (Jagasia et al., 2009). After tMCAO, phospho-CREB levels in the ipsilateral DG increased and peaked at 4 days post-stroke before returning back to baseline at day 15, and CREB phosphorylation was found to be important for the survival of neural prescursors (Zhu et al., 2004).

Inhibition of RhoA/ROCK in neonatal SVZ-derived neural stem/progenitor cells increases neurite outgrowth *in vitro*, including on a myelin substrate (Gu et al., 2013). The migration distance of cells from the adult mouse SVZ was increased by ROCK inhibition, but decreased by Rac1 inhibition (Leong et al., 2011). Furthermore, ROCK inhibition dissociated neuroblast chains, suggesting that ROCK is important for chain formation. *In vivo*, ROCK inhibition decreased the number of newborn neurons in the olfactory bulb, likely due to ectopic migration away from the rostral migratory stream (Leong et al., 2011).

The function of S1PR2 in SVZ neurogenesis has been investigated in the context of sphingosine-1-phosphate (S1P) biology. S1P, acting through S1PR1, is a potent chemoattractant for embryonic neural stem/progenitor cells (NSPCs) *in vitro*, and S1P upregulation after spinal cord contusion contributes to the recruitment of transplanted NSPCs (Kimura et al., 2007). After photothrombotic cortical stroke in adult mice, intracerebroventricular infusion of an S1PR2 small molecule antagonist enhanced neuroblast migration toward the infarct (Kimura et al., 2008). Interestingly, based on their

representative images, the dorsolateral striatum is also infarcted, and it appears that the vast majority of neuroblast migration occurs ventral to the corpus callosum toward the infarcted striatum. Furthermore, while Kimura and colleagues showed S1PR2 mRNA in cultured embryonic NSPCs, expression of S1PR2 at either the transcript or protein level has never been shown in the adult SVZ. Notably, chemotaxis toward S1P is reduced in Chinese hamster ovary cells transfected with S1PR2, and S1PR2 antagonism enhances the migration of human umbilical vein endothelial cells and coronary artery smooth muscle cells, suggesting a common feature of S1PR2 signaling in the inhibition of cell migration (Okamoto et al., 2000; Osada et al., 2002).

Lastly, CREB activation plays a number of roles in SVZ-OB neurogenesis. Similar to the DG, interfering with CREB activation impairs the normal morphogenesis and survival of new OB neurons (Giachino et al., 2005; Herold et al., 2011). Therefore, the general trend gleaned from these studies is that the molecular mediators of Nogo-A signaling (ie., its receptors NgR1 and S1PR2, and intracellular signaling molecules RhoA, ROCK, and CREB inhibition) negatively regulate neurogenesis—though in these contexts, Nogo-A was not investigated as the initiating ligand.

CHAPTER THREE

METHODOLOGY AND EXPERIMENTAL DESIGN

In this section, general experimental design, methodology, and rationale pertaining to studies of both SVZ and DG neurogenesis after stroke and anti-Nogo-A immunotherapy are discussed.

DISTAL PERMANENT MIDDLE CEREBRAL ARTERY OCCLUSION (dMCAO) MODEL OF ISCHEMIC STROKE

Our stroke model is adapted from a study by Chen and colleagues (Chen et al., 1986). This procedure occludes the middle cerebral artery (MCA), the most commonly occluded artery in human ischemic stroke (Ng et al., 2007), and produces a highly replicable, low mortality infarct involving the ipsilateral frontal and parietal cortices. After induction in 5% isoflurane inhalant anesthesia in oxygen, rats were maintained at 2% isoflurane in oxygen during surgery. The middle cerebral artery (MCA) was accessed through a craniotomy in the lateral skull after dissection through the temporalis muscle, occluded with 10-0 suture, and transected. The occlusion is distal to the lenticulostriate branches of the MCA, and therefore avoids direct ischemia of the striatum (Bacigaluppi et al., 2010). However, MCA occlusion is not sufficient to generate an infarct due to

extensive collateral blood supply in the rat brain. Therefore, the ipsilateral common carotid artery (CCA) was permanently occluded, and the contralateral CCA was transiently occluded for 60 minutes, as described by Chen *et al.* (Chen et al., 1986). Temperature was maintained at approximately 37° C with a heating pad connected to a circulating water heater.

Sham surgeries were conducted by anesthetizing animals for an equivalent duration of time and making neck and scalp incisions. Craniotomy and manipulation of the MCA during sham surgery was noted by Chen *et al*. to produce a small lesion, and therefore we did not proceed beyond scalp incision in our sham procedure (Chen et al., 1986).

INTRACEREBROVENTRICULAR ANTIBODY TREATMENT

Previous studies performed in the Kartje laboratory have shown that anti-Nogo-A antibody treatment given 1 week after stroke promotes neuroplasticity and sensorimotor and cognitive recovery (Gillani et al., 2010; Markus et al., 2005; Seymour et al., 2005; Tsai et al., 2007). Therefore, antibody treatment began one week after stroke in all studies described in this dissertation.

Antibody 11C7, a monoclonal mouse IgG1 targeting amino acids 623-640 within the Nogo-A-specific Δ20 domain (Oertle et al., 2003), was produced from a hybridoma cell line provided by Prof. Martin Schwab (Brain Research Institute, University of Zurich). Purification was performed by Protein-G column chromatography, and Coomassie-stained denaturing SDS-PAGE gels routinely revealed only two bands corresponding to heavy and light chains of the antibody. An isotype and subclass-matched antibody against the fungal

product cyclosporine A was obtained from Novartis Pharmaceuticals and used to control for potential nonspecific effects of IgG infusion (Craveiro et al., 2013; Zhao et al., 2013).

At one week post-stroke, rats were anesthetized with isoflurane and implanted subcutaneously with osmotic minipumps (Alzet 2ML2, Durect Corporation) containing either mAb 11C7 or anti-cyclosporine (2.5 mg/mL in phosphate-buffered saline). A cannula was inserted into the ipsilesional lateral ventricle through a burr hole in the skull, fixed to the skull via a spacer and cyanoacrylate glue, and connected to the pump. Antibodies were delivered at 5 μL/hour (12.5 μg/hr) for 14 days, followed by pump removal under isoflurane anesthesia.

BROMODEOXYURIDINE (BrdU) INJECTION

Bromodeoxyuridine (BrdU) is an analog of the nucleoside thymidine that can be incorporated into DNA during DNA synthesis. As extensive DNA synthesis occurs in genome replication prior to cell division, incorporation of BrdU is used as a stable marker of proliferation (Taupin, 2007). Commonly, BrdU is administered through intraperitoneal (i.p.) injection, and it is estimated that BrdU is available for labeling proliferating cells in the brain for approximately 2 hours after administration (Taupin, 2007). BrdU can be detected histologically using monoclonal antibodies and combined with labeling various cell phenotype markers, allowing birthdating and phenotype determination of newborn cells.

There is a dose-dependent effect of BrdU administration on the number of labeled cells in proliferative brain regions, with saturation occurring at approximately 200 mg/kg. This dose has been found to maximally label proliferating cells in the dentate gyrus even

after stimulating proliferation through exercise (Cameron and McKay, 2001; Eadie et al., 2005). Therefore, a single injection of 200 mg/kg BrdU followed by rapid (1-3 hour) post-injection sacrifice is sufficient for quantifying the number of proliferating cells (Taupin, 2007). However, cells that proliferate several times may dilute out incorporated BrdU below the limit of detection. For long-term assessment of newborn cell phenotypes, therefore, it is beneficial to administer multiple doses of BrdU spaced further apart to mitigate the effects of BrdU dilution over successive cell divisions.

In the studies described in this dissertation, two separate BrdU injection strategies were used (Fig 3.1). In each case, BrdU was prepared at 20 mg/mL in sterile saline plus 0.007 N NaOH. The solution was warmed in a water bath and repeatedly vortex-mixed until dissolved and then sterile-filtered through a 0.22 μm syringe filter. To measure cellular proliferation, a single injection of BrdU at 200 mg/kg body weight i.p. was injected followed by sacrifice 2 hours thereafter. For long-term determination of newborn cell phenotypes, BrdU was injected at 50 mg/kg i.p. beginning on day 7 post-stroke, twice per day (6 hours apart), for 5 consecutive days.

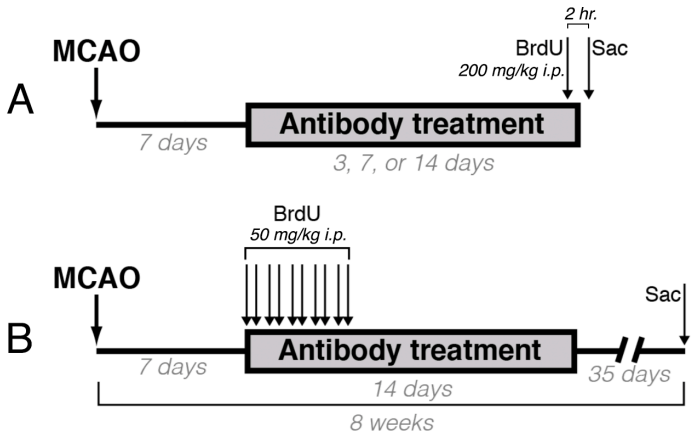

Figure 3.1 ▲ BrdU injection schedules. (A) For measuring proliferation, a single BrdU injection (200 mg/kg) is given 2 hours prior to sacrifice. (B) For long term phenotype analysis of newborn cells, BrdU (50 mg/kg) is injected multiple times, followed by sacrifice approximately 6 weeks later.

PERFUSION, TISSUE PROCESSING, AND HISTOLOGY

At various time points, rats were overdosed with Euthasol (phenytoin/pentobarbital; 390 mg/kg i.p.) and transcardially perfused with cold heparinized saline followed by 4% paraformaldehyde (PFA). Brains were extracted and post-fixed overnight at 4˚ C in 4% PFA, then cryoprotected in 30% sucrose in phosphate buffer pH 7.4 until sinking. 40 µm sections were cut on a cryostat and stored in ethylene glycol-based antifreeze cryoprotectant at -20˚ C until use.

BrdU requires an antigen retrieval procedure to be identified immunohistochemically. Our method was adapted from (Tang et al., 2007), where tissue sections are subjected to high heat (99-100˚ C) sodium citrate solution for 10-15 min. This method was preferable to hydrochloric acid-based procedures since this severely weakens subsequent DNA staining, such as with DAPI or Hoechst, which were to be used

in subsequent steps for identifying regions for cell counting. However, incubation of free-floating sections in boiling sodium citrate leads to excessive wrinkling of the tissue that impairs downstream processing steps. Therefore, we adapted a staining method where the tissue sections were extensively washed in phosphate buffer pH 7.4, mounted on plus-charged slides, and then allowed to dry overnight at room temperature. The following day, the slides were incubated in 99-100° 10 mM sodium citrate pH 6, which had been placed in a container in a boiling vegetable steamer water basin, for 10 minutes. The slides were then removed and immediately immersed in room temperature phosphate buffer pH 7.4 From there, the tissue sections were carefully removed from the slides using a razor blade and rinsed in phosphate buffer. We found that using this strategy, tissue wrinkling was nearly eliminated, while still allowing us to perform free-floating tissue staining (which allows for better antibody penetration) on thick tissue sections (which are required for the optical fractionator stereology probe).

This procedure led to bright BrdU staining that was compatible with general DNA labeling using DAPI, as described by Tang and colleagues (Tang et al., 2007). However, we experienced very high white matter nonspecific fluorescence, as if the white matter had become extremely "sticky" to antibodies. This was traced to the use of high concentrations of the detergent Triton X100 in the incubation buffers. Switching to Tween-20 greatly reduced the background fluorescence and was therefore used in all steps after high heat antigen retrieval.

Immunostaining was performed by diluting primary antibodies in phosphate-buffered saline (PBS) pH 7.4 plus 0.2% Tween-20 (when high heat antigen retrieval was used) or 0.3% Triton-X100 (when no antigen retrieval was used). Tissue sections were then incubated in primary antibody solution overnight at 4° C with gentle agitation. The following day, the tissue sections were extensively washed in PBS/0.2% Tween 20 (for high heat antigen retrieval) or phosphate buffer pH 7.4 (when antigen retrieval was not performed). The sections were then incubated in fluorophore- or biotin-conjugated secondary antibodies in the same dilution buffers listed above for 2 hours at room temperature with shaking, and then washed. For fluorescent imaging, nuclei were counterstained with DAPI, then mounted on gelatin-subbed slides and coverslipped with Fluoromount G anti-fade mounting media. For signal detection with the chromogenic substrate diaminobenzidine (DAB), tissue sections were incubated in avidin-biotin-peroxidase complex (Vector Laboratories, 1 drop component A plus 1 drop component B per 5 mL dilution buffer, as above) for 1 hour at room temperature. Lastly, sections were reacted in nickel-enhanced DAB in the presence of hydrogen peroxide to visualize the target antigens.

A list of antigens, antibodies, and dilutions used in this disseration appears in table 3.1.

Marker/ antigen	Abbreviation	Class or function	Associated cell type	Antibody source; host; concentration
Glial fibrillary acidic protein	GFAP	Intermediate filament	Astrocytes; neural stem cells in SVZ and DG	DAKO Z0334; Rabbit; 1:1,000
Sex determining region-box 2	Sox2	Transcription factor	Astrocytes; neural stem and progenitor cells in SVZ and DG	Abcam Ab97959; Rabbit; 1:1,000
Doublecortin	DCX	Microtubule-associated protein	Immature neurons in SVZ and DG; mature neurons in piriform cortex	CellSignaling; Rabbit; 1:500 (IF), 1:5000 (IHC)
βIII-tubulin (Tuj1)	Tuj1	Microtubule monomer	Immature and mature neurons	Covance MMS-435P; Mouse IgG2a; 1:1,000
Ionized binding adapter molecule 1	Iba1 (aka AIF1)	EF-hand containing calcium binding protein	Microglia, macrophages	Wako 019-19741; Rabbit; 1:5,000
5-bromo-2'-deoxyuridine	BrdU	Thymidine analog	Incorporated into cells during DNA synthesis, a marker of proliferation	Thermo MA3-071; IgG2a; 1:500 (IF); 1:5,000 (IHC)
Myelin basic protein	MBP	Structural component of myelin	Myelinating oligodendrocytes	Abcam Ab7349; Rat; 1:1,000
Neuronal nuclei	NeuN (aka Fox3)	RNA splicing factor	Mature neurons	Millipore MAB377(Ms IgG1); ABN78 (rabbit); 1:1,000
Nogo-A		Reticulon protein	Oligodendrocytes, certain immature and mature neurons	mAb 11C7; mouse IgG1; 1:10,000
Ki67		Ribosomal RNA synthesis	Proliferating cells (expressed in all cell cycle phases except G0)	Abcam Ab16667; Rb; 1:5,000
2',3'-cyclic nucleotide 3'-phosphodiesterase	CNPase	Enzyme	Oligodendrocytes	Sigma C5922; Ms IgG1; 1:1,000

Table 3.1 ▲ Summary of cell-type markers and antibodies used in this dissertation. IF: immunofluorescence; IHC: immunohistochemistry (with avidin-peroxidase complex and DAB detection).

UNBIASED STEREOLOGY

Unbiased stereology is a method of estimating properties (number, length, volume, etc.) of three-dimensional structures from tissue sections without making assumptions about the size, shape, or orientation of the objects of interest (Peterson, 1999; West, 2013). Various stereology "probes" can be applied to tissue sections to estimate these quantities. One of these probes, the optical fractionator, is designed to quantify the number of features (for example, cells) within a region of interest. The software-based optical fractionator probe superimposes a grid with counting boxes at systematically-spaced intervals, and features within the box are counted with specific counting rules after excluding "guard zones" at the tissue surfaces. An estimate of the total number of features within the brain structure of interest is calculated by:

$$N = \sum Q^{-} \cdot \frac{1}{ssf} \cdot \frac{1}{asf} \cdot \frac{1}{tsf}$$

where 'N' is an estimate of the total number of features, ΣQ- is the the sum of the counted features, *ssf* is the section sampling fraction (for example, 1/6 if 1 of every 6 sections is examined), *asf* is the area sampling fraction (the proportion of the initially defined area that is sampled), and *tsf* is the thickness sampling fraction (the fraction of the tissue section thickness that is sampled).

Use of the optical fractionator is warranted in studying cellular proliferation in the subventricular zone, as the number of proliferating cells is high and generally evenly distributed, especially in the dorsolateral SVZ. However, the optical fractionator is less useful for studies of neural precursor proliferation in the dentate gyrus, where proliferating cells are often found in discrete clusters with large spaces in between (Noori and Fornal, 2011). For this reason, and because of the the lower level of cellular proliferation in the DG versus the SVZ, absolute counting has been advised (Noori and Fornal, 2011).

LESION ANALYSIS

A 1 in 24 tissue section series throughout each brain (excluding olfactory bulbs and cerebellum) was mounted on gelatin-subbed slides and stained with toluidine blue. Slides were then scanned at high resolution using a flatbed scanner and imported into Adobe Photoshop CS3, where the number of pixels in the intact and lesioned hemispheres was measured. To compute a lesion size as a percentage of the intact hemisphere, the total number of pixels in the lesioned hemisphere was subtracted from the total number of pixels in the intact hemisphere, and divided by the total intact hemisphere pixel number.

CHAPTER FOUR

EXPRESSION PATTERN OF NOGO-A IN THE ADULT SUBVENTRICULAR ZONE & THE ROLE OF NOGO-A IN THE MIGRATION OF SVZ-DERIVED NEUROBLASTS

ABSTRACT

The mechanisms that regulate the motility of subventricular zone-derived neuroblasts are not fully understood. In this study, we investigated the expression pattern of Nogo-A in SVZ neural precursor cells, and used an *in vitro* migration assay to quantify effects of Nogo-A signaling on SVZ-derived cell motility. We found that Nogo-A was expressed by SVZ neuroblasts, but not neural stem cells, *in vivo* and *in vitro*. The Nogo-A Δ20 receptor S1PR2 was also found in SVZ neuroblasts, but no clear evidence of NgR1 expression was found in the SVZ. Nogo-A colocalized with an endoplasmic reticulum marker in SVZ neuroblasts *in vitro*, but was not found at the cell surface. However, we characterized a potential source of Nogo-A in the form of a myelin-rich zone just adjacent to the lateral edge of the SVZ, which could play a role in the regulation of the SVZ niche. Lastly, we found that Δ20 peptide treatment reduced the maximum speed of SVZ-derived neuroblasts *in vitro*. These results suggest that due to the lack of cell surface expression,

neuroblast-expressed Nogo-A likely does not signal to other cells in *trans*, but the motility of SVZ neuroblasts can still be modulated by exogenous Nogo-A.

INTRODUCTION

In the adult brain, neuroblasts from the subventricular zone (SVZ) migrate long distances via the rostral migratory stream (RMS) to the olfactory bulb, where they mature into neurons. Migration in the subventricular zone is regulated by both diffusible and contact-dependent factors, ensuring the regulation of the complex dynamics of new neuron production and long distance migration (Capilla-Gonzalez et al., 2015). Netrins and sonic hedgehog mediate chemoattraction toward the OB by activating receptors on neuroblasts (Capilla-Gonzalez et al., 2015). Meanwhile, chemorepulsive Slit ligands released from the septum and choroid plexus activate Robo receptors on neuroblasts to direct migration rostrally (Nguyen-Ba-Charvet et al., 2004). Structural features of the SVZ/OB system important for homeostasis include extracellular matrix molecules such as laminin-rich "fractones" that concentrate growth factors and stimulate proliferation (Kerever et al., 2007; Mercier et al., 2002), and tenascin-C, which supports the development of the SVZ (Garcion et al., 2004). Beyond normal physiological migration into the olfactory bulb, brain injuries such as stroke can recruit SVZ neuroblasts to ectopic sites under the guidance of soluble factors such as SDF1α, MCP1, and VEGF (Capilla-Gonzalez et al., 2015).

Cellular features such as astrocytic process tubes (Peretto et al., 1997) and radially-oriented vasculature guide tangential and radial migration into the olfactory bulb parenchyma, respectively (Bovetti et al., 2007). In humans, a myelin layer in the

transitional zone between the SVZ and striatum has been described (Quiñones-Hinojosa and Chaichana, 2007); (Quiñones-Hinojosa et al., 2006) but has not been characterized in the rodent brain. While the presence of myelin contacts in the subventricular zone has been noted previously (Doetsch et al., 1997), the existence of a distinct myelin band in the rodent SVZ has been disputed (Quiñones-Hinojosa and Chaichana, 2007). Myelin-associated proteins, including Nogo-A (Rolando et al., 2012), oligodendrocyte myelin glycoprotein (OMGP) (Martin et al., 2009), and myelin associated glycoprotein (Li et al., 2009), may play distinct roles in regulating neurogenesis (reviewed recently in (Xu et al., 2015)), so it is important to consider the expression of these molecules not only in the SVZ itself but also in boundary areas that may impact the organization and function of the niche. Given the critical importance of rodent models of neurological disorders, it is necessary to fully understand the unique cytoarchitecture of the SVZ in these models to better interpret preclinical studies and reveal new avenues for treatment.

In this study, we undertook two main objectives: 1) define the expression pattern of Nogo-A within and around the SVZ, and 2) examine the impact of Nogo-A on the motility of SVZ-derived neuroblasts. We found that Nogo-A is expressed by immature neurons throughout the SVZ-RMS-OB axis. Nogo-A colocalizes with an endoplasmic reticulum marker intracellularly, whereas no evidence was found for Nogo-A expression at the surface of immature neurons. Expression of the Nogo-A-Δ20 receptor S1PR2 was also found in immature neurons in the SVZ, whereas clear evidence for Nogo-66 receptor NgR1 expression in the SVZ was not found. We characterized a myelin-rich zone just

lateral to the SVZ that appears well-positioned to play a role in SVZ function. Lastly, using an *in vitro* migration assay, we found that chronic treatment with Nogo-A-Δ20 peptide reduced the maximum speed of SVZ-derived neuroblasts, but found no effect of anti-Nogo-A antibody on various properties of neuroblast motility. These results suggest that Nogo-A likely plays a cell-autonomous role in SVZ neuroblasts, due to its lack of cell surface expression, and that neuroblast-expressed Nogo-A likely does not signal to other cells in *trans*. However, neuroblast motility can still be influenced by exogenous sources of Nogo-A.

EXPERIMENTAL DESIGN

SVZ explant collection and culture

The method for SVZ explant culture is adapted from (Wichterle et al., 1997). 3-4 month old male Long-Evans black hooded rats were deeply anesthetized with inhalant isoflurane and decapitated. The brains were then rapidly extracted and placed in cold phosphate-buffered saline on ice. 300 μm coronal sections were then cut on a vibratome and stored in sterile HEPES-buffered artificial CSF with glucose on ice. Under a dissecting microscope, 500 μm diameter tissue punches were taken from the SVZ and transferred onto tissue culture dishes that had been pre-coated with a 3:1 mixture of growth factor-reduced Matrigel:Neurobasal medium. Explants were isolated as matched pairs, so that a treated explant was paired with a control explant from the same position within the SVZ on the contralateral side (see Fig. 4.1). Once all explants were collected, the plates were placed in a 37° C incubator for 5-10 minutes to allow the Matrigel to

congeal. Afterwards, the explants were overlaid with media composed of Neurobasal-A, 2% B27 without vitamin A, Glutamax, and penicillin-streptomycin, plus either anti-Nogo-A or anti-cyclosporine-A control antibodies (50 μg/mL) or Δ20 or scrambled Δ20 recombinant peptides (500 nM). Plates were stored in a 37° C cell culture incubator supplemented with 5% CO_2. Half media changes were performed on day 4 with re-supplementation of antibodies or peptides.

Quantification of total cell dispersion from explants

Low magnification (2.5x) phase contrast images of explants were acquired daily for 7 days after plating. These images were imported into ImageJ and the distance from the edge of the explant to the farthest rim of migrating cells was measured at approximately the same position of each explant per day.

Live cell imaging

Between 3-5 days *in vitro*, time lapse videos of migrating cells were acquired. To facilitate tracking, cells were labeled with Hoechst 33342 DNA dye (25 nM) the night before imaging. The following day, images were acquired every 5 minutes for 6 hours using a Zeiss Axiovert microscope with 10x objective in a humidified chamber maintained at 37° C with 5% CO_2. To mitigate phototoxicity, the cells were imaged using the lowest lamp power possible. In our hands, this combination of Hoechst concentration, lamp power, and imaging frequency resulted in minimal toxicity as measured by qualitative assessment of the long-term health of the cultures and low level of apoptosis observed

during live cell imaging. Cells undergoing apoptosis were easily visualized due to nuclear condensation and/or fragmentation and were excluded from analysis.

Cell videos were imported into ImageJ and manually tracked by an investigator blinded to treatment group using the TrackMate or mTrackJ plugins. In TrackMate, cell tracking can be semi-automated based on automatic detection of cell nuclei in successive video frames. In all cases, cells were tracked one at a time to ensure accuracy. Neuroblast nuclei (small, bright, round to oblong in shape) were visually distinct from the nuclei of astrocytes that had migrated out of the explant (larger, less bright). Due to the difficulty of distinguishing cells in chains, especially closer to the explant, only singly-migrating cells were tracked. These cells were typically located on the periphery of the halo of migrating cells and displayed the typical unipolar to bipolar morphology of migrating neuroblasts. As phase contrast images were also acquired at each time point, nuclei could be referenced against cell morphology if the identity of the cell (neuroblast vs. astrocyte) was not clear. Maximum and average migration speeds for each cell were computed by the software based on the change of cell position over time. Since neuroblasts migrate in a saltatory manner, information about pause and movement phases and directional persistence (straightness of migration path) were also computed using a custom script written in the statistical software R. To define a pause, the nuclei of 16 cells that were visibly stationary were first automatically tracked. The computed average velocity of these cells, representing the small, random-appearing motions of the nucleus, was then multiplied by the frame interval (300 seconds) to obtain the minimum distance traveled beween frames that could be

considered actual cell migration. Any change in position less than or equal to this value was therefore considered a pause. For calculations regarding pauses, the first and last phases of an individual cell's movement were excluded because these phases are cut off by the beginning and end of the time lapse video, and are therefore inaccurate. Therefore, cells consisting of just 1 or 2 distinct movement phases over the course of the time lapse video were excluded from analysis, leading to the reporting of lower total cell numbers for pause properties (Fig 4.2).

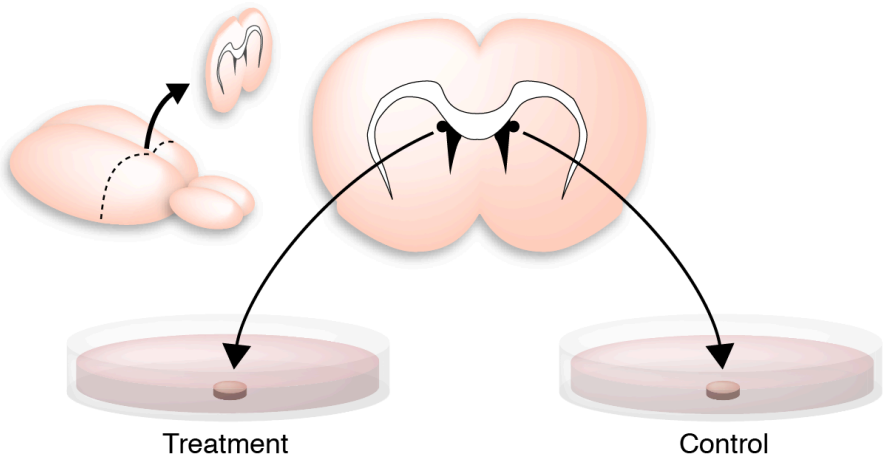

Figure 4.1 ▲ Diagram of explant collection as matched pairs.

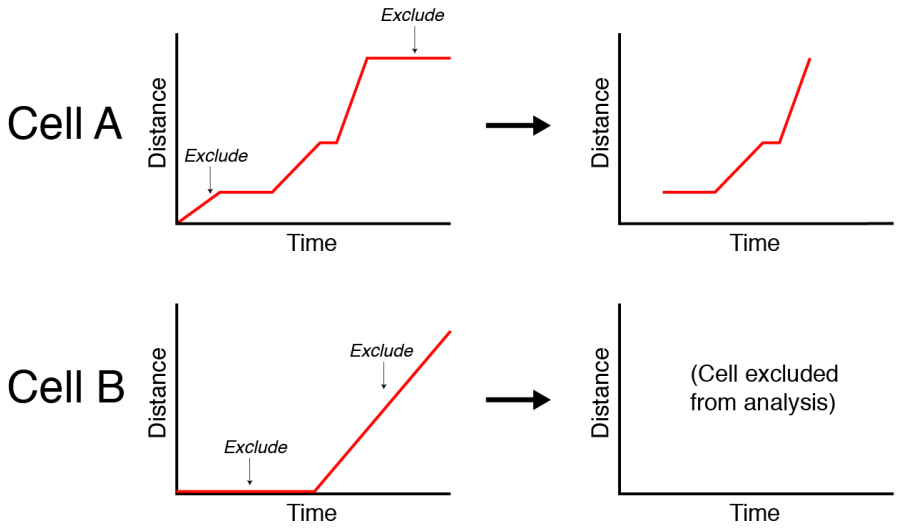

Figure 4.2 ▲ Exclusion of first and last movement or pause phases for pause analysis. For Cell A, 4 distinct phases (2 pause phases, 2 movement phases) will still remain for analysis. In contrast, Cell B only had two phases to begin with, and therefore cannot be analyzed.

Immunocytochemistry and imaging

Explants in Matrigel were fixed with 2% paraformaldehyde in PBS for 15 min at room temperature, and then washed in PBS. The explants were then incubated in primary antibodies diluted in PBS plus 0.2% Tween 20 overnight at 4° C. The following day, explants were washed in PBS and incubated in secondary antibodies in PBS/0.2% Tween 20 for 2 hours at room temperature. After washing in PBS, explants were coverslipped in Fluoromount G.

For surface staining, explants were plated on laminin-coated coverlsips. Once cells began migrating out, the coverslips were rinsed once with room temperature PBS, then once with cold PBS and placed on ice. Primary antibodies (anti-Nogo-A antibodies 11C7 or 7B12) were applied at a concentration of 25 µg/mL in PBS plus 5% fetal bovine serum

on ice for 30 min. The coverslips were then washed 3 times in cold PBS and fixed in 4% paraformaldehyde on ice for 30 min. Cells were then incubated in rabbit anti-doublecortin antibody under membrane-permeabilizing conditions (1:500 in PBS plus 5% normal goat serum and 0.1% Triton-X100) overnight at 4° C. The following day, the converslips were washed, incubated in fluorescent secondary antibodies against rabbit (doublecortin) and mouse (11C7 or 7B12) IgG, washed again, and mounted on slides in Fluoromount G.

Images were acquired on a Leica SPE confocal microscope. For demonstration of colocalization, cells were imaged using a 63x/1.3 NA oil objective with pinhole size 1 Airy unit. After acquisition, images were imported into Adobe Photoshop CS6 for preparation of figures. All levels adjustments were applied equally to the entire image within each channel. Gamma adjustment was not performed. Occasionally, levels adjustments required to show fine details resulted in signal saturation of brighter parts of the image.

RESULTS

Expression pattern of Nogo-A in the adult rat subventricular zone

To determine potential direct targets of anti-Nogo-A antibody treatment, we performed double immunofluorescent staining for Nogo-A or its receptors, NgR1 and S1PR2, and markers of neural stem cells and neuroblasts. In agreement with a previous report in adult mice (Rolando et al., 2012), DCX+ neuroblasts, but not GFAP+ astrocytes and stem cells, were positive for Nogo-A (Figs. 4.3, 4.4). After stroke, Nogo-A continued to be expressed by neuroblasts, including those presumably migrating toward the

lesion. In these singly-migrating neuroblasts, Nogo-A expression was especially evident in the leading process.

We found evidence for S1PR2 expression in DCX+ neuroblasts, though this required high antibody concentration and enzymatic signal amplification, so expression is likely low in this cell type. In contrast, no clear evidence of specific NgR1 expression was found in the SVZ, even with signal amplification. NgR1-positive cells were seen in the adjacent striatum and cortex, confirming the adequacy of the staining procedure.

In examining Nogo-A expression in SVZ neural precursors, we noted the presence of a prominent myelin-rich (MBP-positive, CNPase-positive) zone at the lateral edge of the SVZ (Fig. 4.6). The myelin band appears to also extend dorsolaterally in association with the DCX-rich dorsolateral extension of the SVZ. This band is most prominent at the levels of the rostral-most appearance of the lateral ventricles and where, in coronal section, the SVZ (as visualized by DCX staining) extends prominently in the dorso-ventral axis. The myelin band is no longer apparent at the level of the caudal emergence of the hippocampus.

Conspicuous CNPase/Nogo-A+ cells can be found ~50 μm from the lateral ventricle wall, extending processes toward the SVZ and terminating in processes oriented dorso-ventrally. In the dorsal and dorsolateral part of the SVZ, where most DCX staining is found, the myelin fibers appear to course dorso-ventrally, whereas this organization is not as apparent in more ventral parts of the SVZ. However, myelin is still observed in these regions in close contact with the SVZ. The band is not continuous—it does not extend

without interruption from the dorsal-most to ventral-most parts of the lateral ventricle. Especially ventrally, there are often individual, discontinuous bands of myelin that also contact the SVZ.

This myelin band appears to "contain" the SVZ, as if preventing the lateral spread of neuroblasts into the adjacent striatum. However, this is just correlative and myelin could just be a marker or proxy of another structural feature that constrains the lateral border of the SVZ. The great majority of DCX+ neuroblasts lie medial to the myelin band, in the "SVZ proper" where there is a high density of DAPI+ cell nuclei. However, on occasion, some neuroblasts (either in chains or individually) appear to be located *within* individual myelin bundles. As seen in sagittal section, myelin fibers are oriented parallel to the migrating neuroblasts at the origin of the RMS. In the rostral RMS, as seen in coronal section, there is a dense cluster of DCX+ neuroblasts found in a region devoid of MBP staining. However, lateral to this dense neuroblast cluster, neuroblasts in smaller clusters are found in smaller MBP-negative spaces. The significance of this organization is unknown; potentially it could represent the segregation of multiple subpopulations of neuroblasts. Both populations of neuroblasts are DCX+/Tuj1+, suggesting that they are all immature neurons. Within the olfactory bulb, neuroblasts do not appear to interact with myelin (MBP+) fibers. However, they do appear to make extensive contacts with Nogo-A+ fibers (cell type unknown).

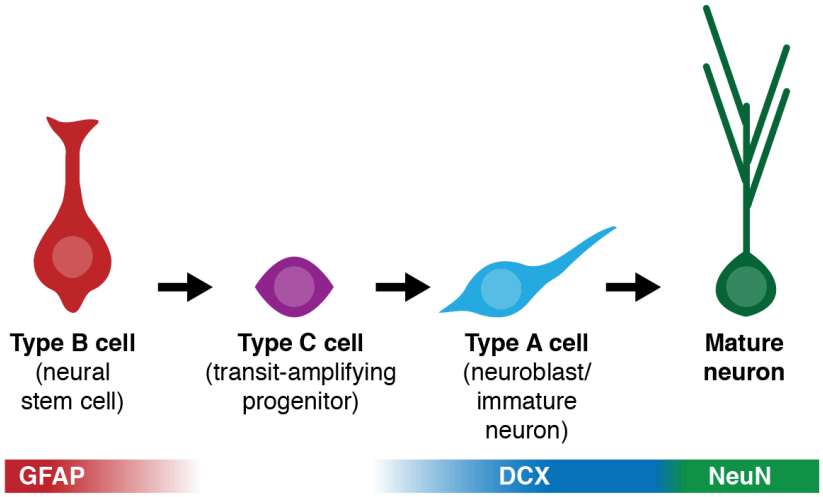

Figure 4.3 ▲ Overview of lineage progression and key marker expression in SVZ-OB neurogenesis.

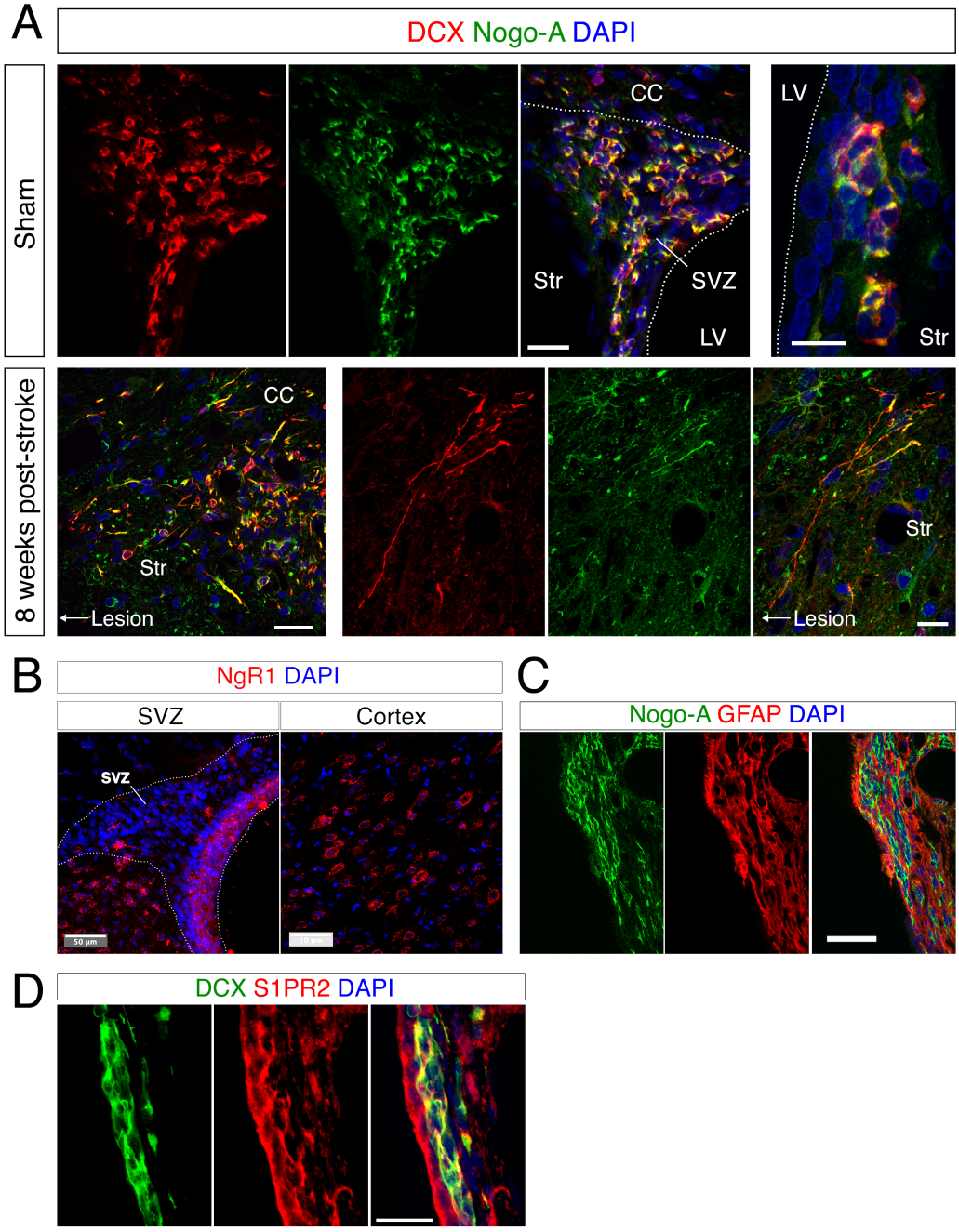

Figure 4.4 ▲ Evidence for expression of Nogo-A and S1PR2, but not NgR1, in the adult rat SVZ. (A) Nogo-A (green) is expressed by DCX-positive neuroblasts in the SVZ. CC: corpus callosum; Str: striatum; LV: lateral ventricle. Top panel: SVZ from a sham surgery rat. Scale bars: 25 μm (left); 10 μm (right). Bottom panel: The ipsilesional tip of the SVZ and striatum of a rat at 8 weeks post-stroke, with Nogo-A visible in the processes of DCX+

neuroblasts. (B) NgR1 immunostaining in the SVZ appears nonspecific, with indistinct staining along the ependymal cell layer. Scale bar: 50 µm. (C) Nogo-A is not expressed by GFAP+ astrocytes and neural stem cells within the SVZ. Scale bar: 50 µm. (D) Expression of S1PR2 in DCX+ neuroblasts. Scale bar: 20 µm.

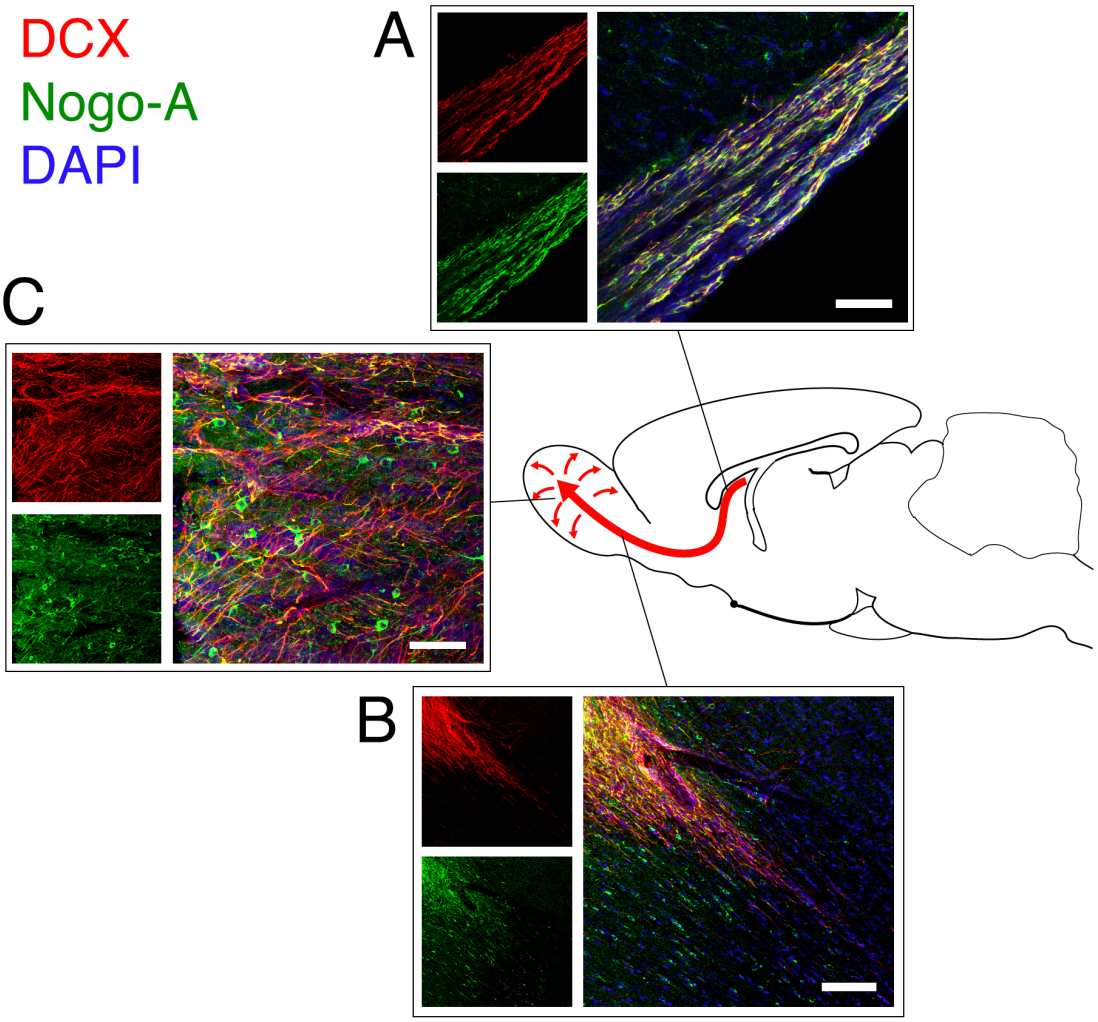

Figure 4.5 ▲ Nogo-A is expressed by neuroblasts throughout the SVZ-RMS-OB axis. Depicted are representative sagittal sections of Nogo-A (green)/doublecortin (red) staining. (A) Proximal rostral migratory stream. Scale bar: 50 µm. (B) Rostral migratory stream transitioning into the olfactory bulb. Scale bar: 100 µm. (C) Olfactory bulb. Nogo-A expression appears to be expressed in both tangentially and radially migrating neuroblasts. Radially migrating neuroblasts also occasionally appear to associate with Nogo-A positive fibers in the olfactory bulb. Scale bar: 50 µm.

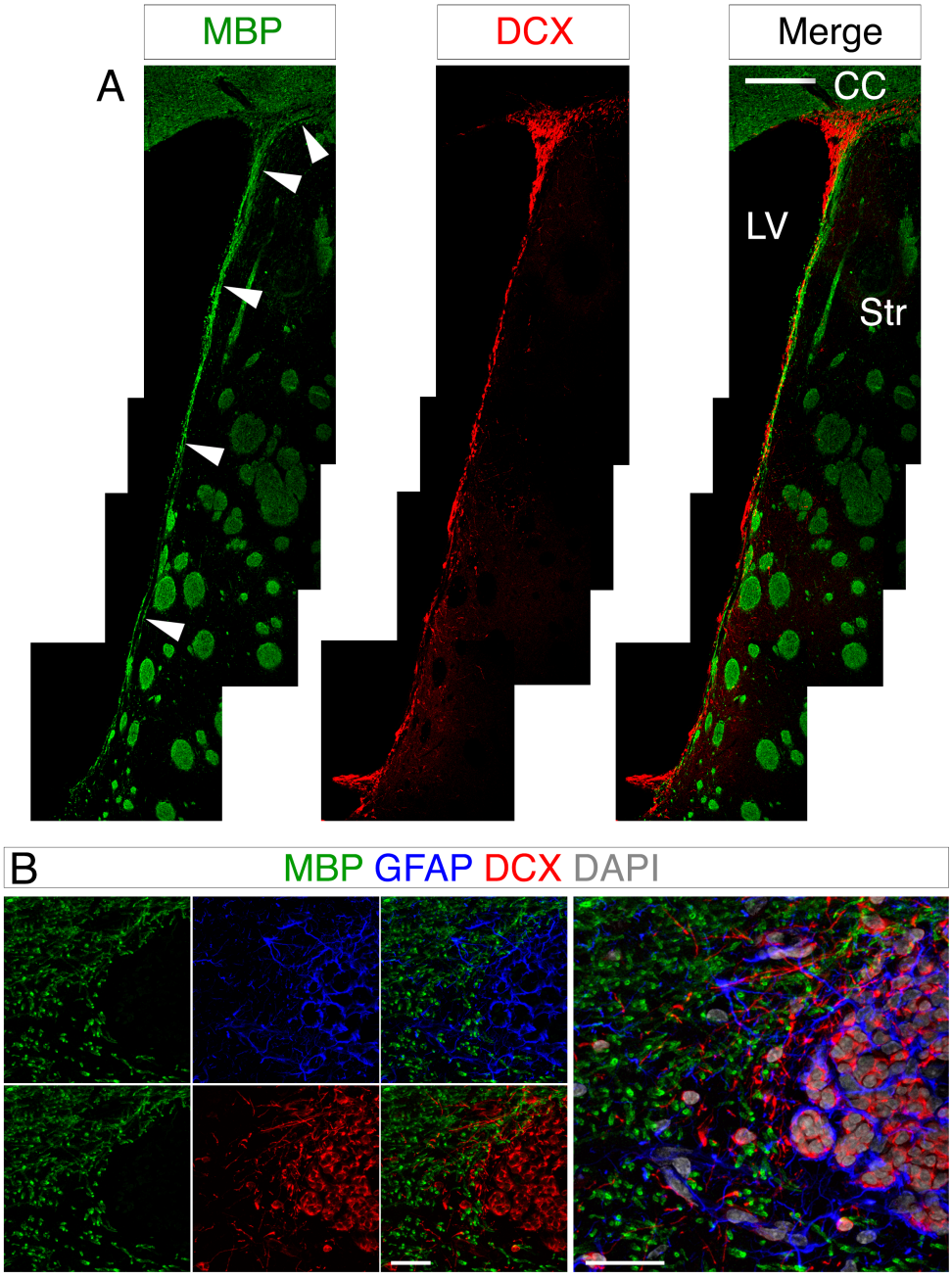

Figure 4.6 ▲ Myelin anatomy at the boundaries of the SVZ/RMS. (A) Low magnification image of myelin basic protein (MBP; green) and doublecortin (DCX; red) immunostaining along the lateral ventricle wall. Scale bar: 200 μm. (B) Coronal section through the rostral migratory stream showing the relationship between myelin (MBP+), neuroblasts (DCX+), and astrocyte "glial tubes" (GFAP+). Scale bar: 25 μm.

Subcellular localization of Nogo-A in SVZ-derived neuroblasts

Nogo-A contains two long hydrophobic stretches that serve as sites of membrane insertion. As a reticulon protein, Nogo-A is primarily localized to the endoplasmic reticulum in various cell types, but can also be found at the surface, embedded in the plasma membrane. Since a protein's subcellular localization can provide clues as to potential functions, we investigated the subcellular localization of Nogo-A in SVZ-derived neuroblasts in vitro. We observed colocalization between Nogo-A and βIII tubulin throughout the leading processes, with the exception of the very distal tips of the growth cone and finer processes emanating from the main leading process, where βIII tubulin, but not Nogo-A, was expressed (Fig. 4.7). This result suggests co-occurrence of Nogo-A and microtubules in the same subcellular compartments. Triple labeling for βIII-tubulin, Nogo-A, and calnexin, an endoplasmic reticulum (ER) marker, showed extensive colocalization throughout the leading process, suggesting that the ER extends far toward the distal tip of this structure and contains Nogo-A (Fig 4.8).

To investigate whether Nogo-A is expressed at the surface of SVZ neuroblasts, SVZ explants were plated on laminin-coated coverslips. After cells migrated out from the explants, they were then stained live on ice with one of two different anti-Nogo-A antibodies directed against epitopes in the Nogo-A-specific N-terminal domain (mAbs 11C7 and 7B12). Numerous DCX-negative cells demonstrated positive, mostly punctate surface staining. In contrast, no obvious Nogo-A surface staining was seen in DCX-positive cells (Fig. 4.9).

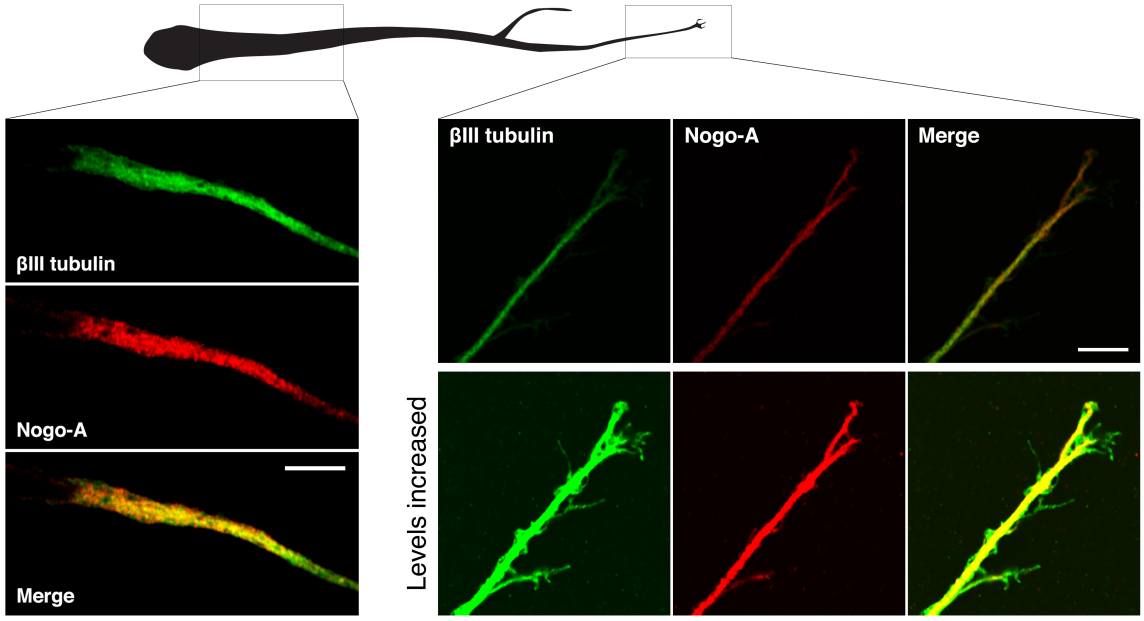

Figure 4.7 ▲ Colocalization of Nogo-A with βIII-tubulin in SVZ-derived neuroblasts. Nogo-A is found throughout the leading process. However, it appears to be excluded from the very distal tips of the growth cone and the fine, filamentous processes emanating from the leading process, which are βIII tubulin positive. The black neuroblast silhouette at the top is for schematic purposes only and was not traced from an actual cell. Scale bars: 5 μm.

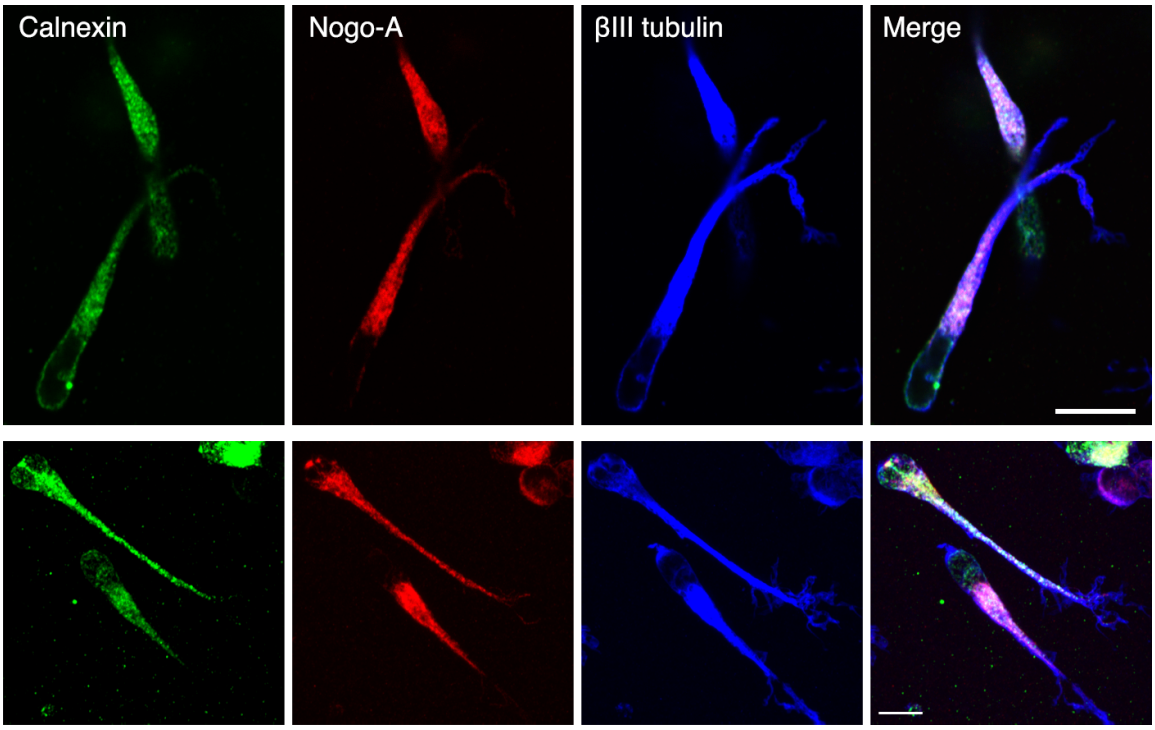

Figure 4.8 ▲ Colocalization of Nogo-A and calnexin in throughout the leading process of SVZ explant-derived neuroblasts after 2 days in vitro. Nogo-A (red) and calnexin (green) labeling are not seen in the most distal tips of the βIII tubulin-positive (blue) growth cone. Scale bars: 10 μm.

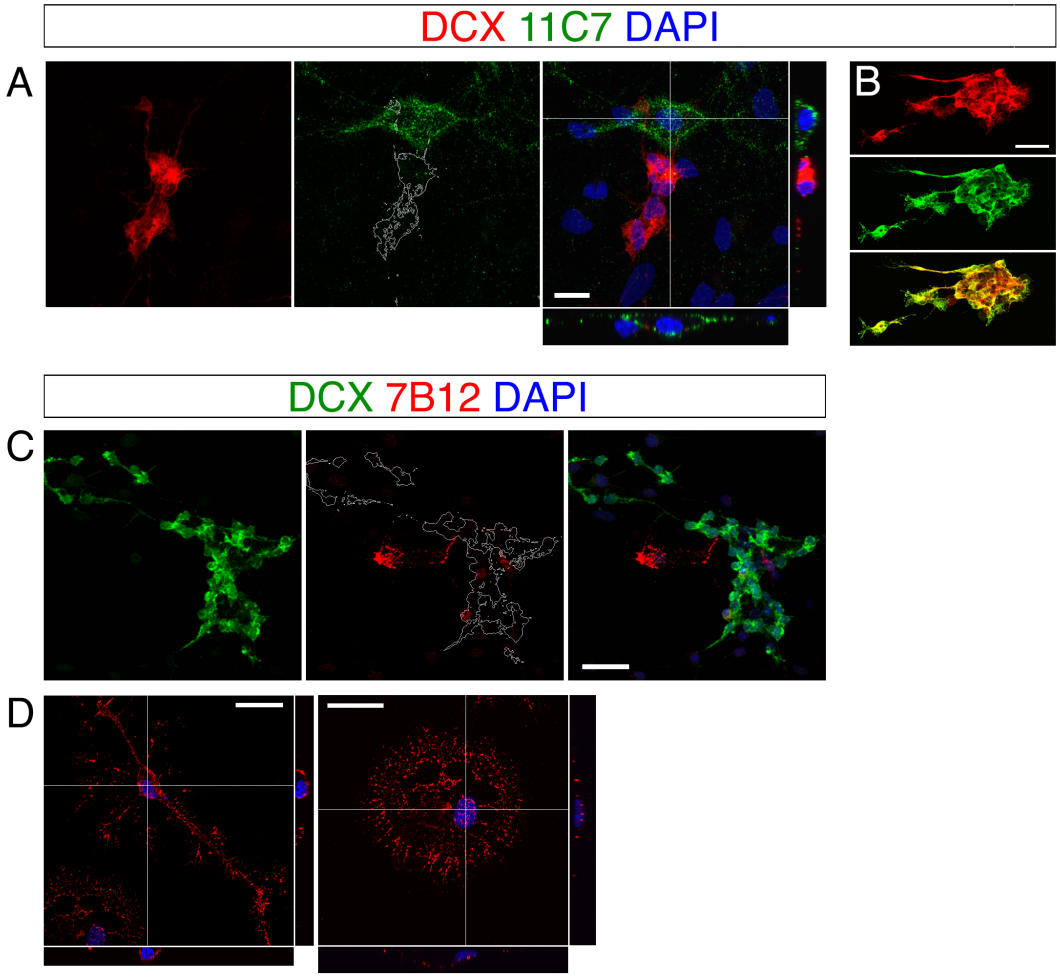

Figure 4.9 ▲ Lack of evidence for surface localization of Nogo-A in SVZ-derived neuroblasts. (A) Live-cell surface staining with anti-Nogo-A antibody 11C7. Note DCX-negative, 11C7-positive cell at the top of the frame, while DCX-positive cells are devoid of surface staining. Scale bar: 10 µm. (B) Positive 11C7 Nogo-A staining in neuroblasts fixed and permeabilized before antibody addition, showing expressing of all Nogo-A regardless of subcellular localization. Scale bar: 20 µm. (C), (D) Live-cell surface staining with anti-Nogo-A antibody 7B12 corroborates the lack of surface staining seen with 11C7. Scale bar in C: 25 µm. (D) DCX-negative cells from the same conditions demonstrating punctate surface staining for 7B12 that is especially appreciable in orthogonal views. Scale bars: 20 µm. Outlines of DCX+ cells have been superimposed on Nogo-A staining (middle panels) in (A) and (C) to demonstrate lack of appreciable Nogo-A surface staining in these cells.

Effects of Nogo-A signaling perturbation on SVZ-derived neuroblast motility

SVZ explants were treated with recombinant Nogo-A-Δ20 peptide (500 nM) or mAb 11C7 (50 ug/mL), and singly-migrating cells were tracked in time lapse videos to quantify changes in motility. Additionally, explants were imaged daily and the cell dispersal distance was measured over time.

Treatment with Δ20 peptide did not significantly alter the cell dispersal distance. 11C7 treatment led to a small but statistically significant reduction in cell dispersal distance only on the final day that explants were imaged (day 7 *in vitro*) (Fig. 4.10).

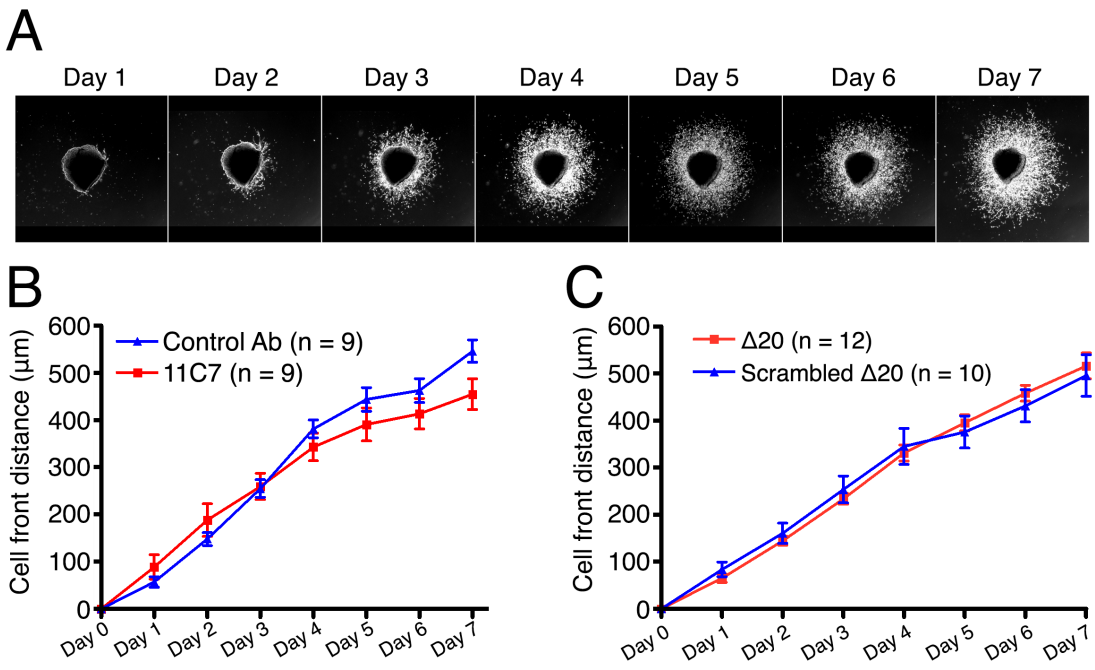

Figure 4.10 ▲ Neither anti-Nogo-A antibody 11C7 nor Δ20 peptide significantly alter total dispersal distance over a 7-day time course. (A) Representative images of cell dispersal from a single explant over the course of 7 days. (B) Total cell dispersal distance in mAb 11C7- versus control antibody-treated explants. (C) Total cell dispersal distance in recombinant Δ20 peptide- versus control (scrambled Δ20)-treated explants.

Individual cells were tracked in time lapse videos to analyze their motion in the presence of anti-Nogo-A antibodies or exogenous Δ20 peptide (Fig. 4.11). The addition of Δ20 peptide to the media did not lead to any acute changes in the maximum speed of SVZ-derived neuroblasts (Fig. 4.12). In constrast, chronic treatment with Δ20 peptide led to a modest but statistically significant reduction in the maximum speed attained by these cells, and a non-significant trend toward a reduction in average speed (Fig. 4.13). Treatment with anti-Nogo-A antibody did not significantly alter either the average or maximum speeds of SVZ neuroblasts (Fig. 4.14).

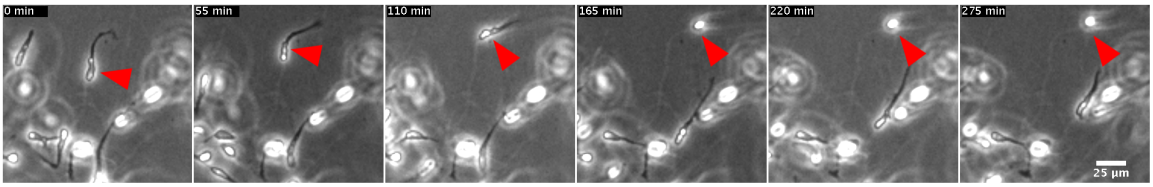

Figure 4.11 ▲ Example of neuroblast locomotion in time-lapse videography. A cell with the typical morphology of a migrating neuroblast (red arrowhead), with phase-bright cell body and phase-dark leading process, can be seen migrating and resting over the course of 275 minutes.

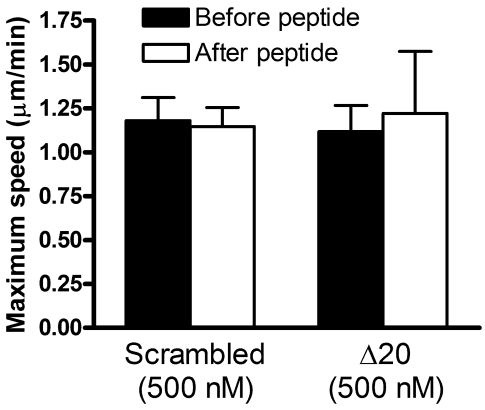

Figure 4.12 ▲ Acute Δ20 peptide addition does not immediately alter neuroblast maximum speed.

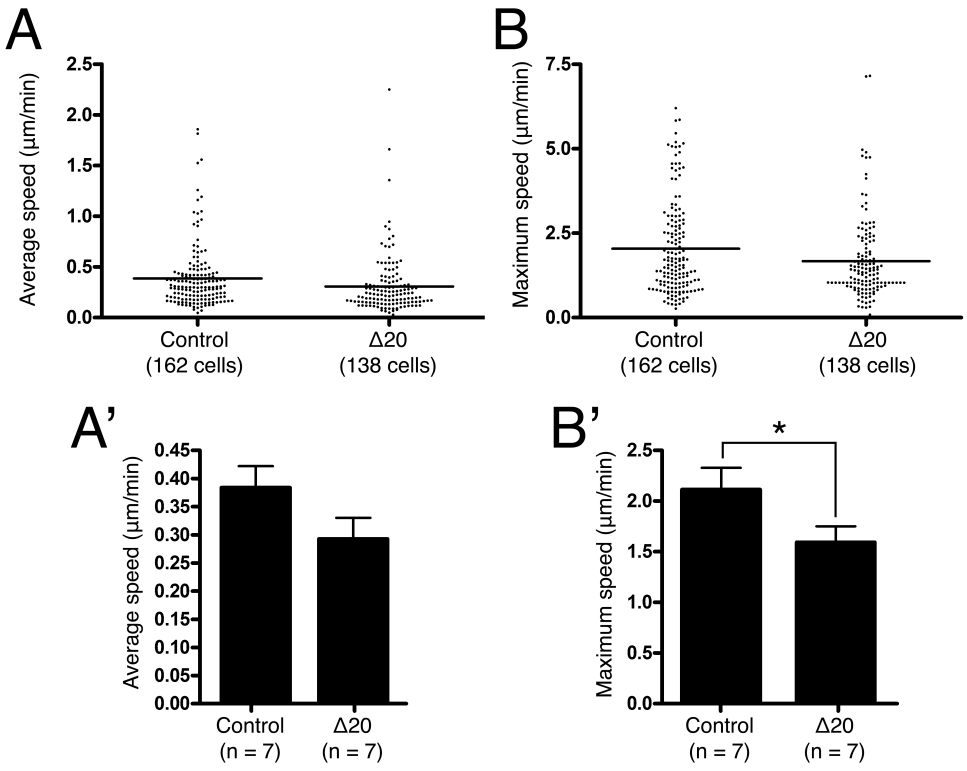

Figure 4.13 ▲ Chronic treatment with Δ20 peptide modestly reduces neuroblast maximum speed. (A), (A') Average neuroblast speed. (B), (B') Maximum speed. (A), (B) All tracked cells, combined across explants. (A'), (B') Means ± SEM with each explant treated as an independent sample. * $p < 0.05$ (two-tailed paired t test).

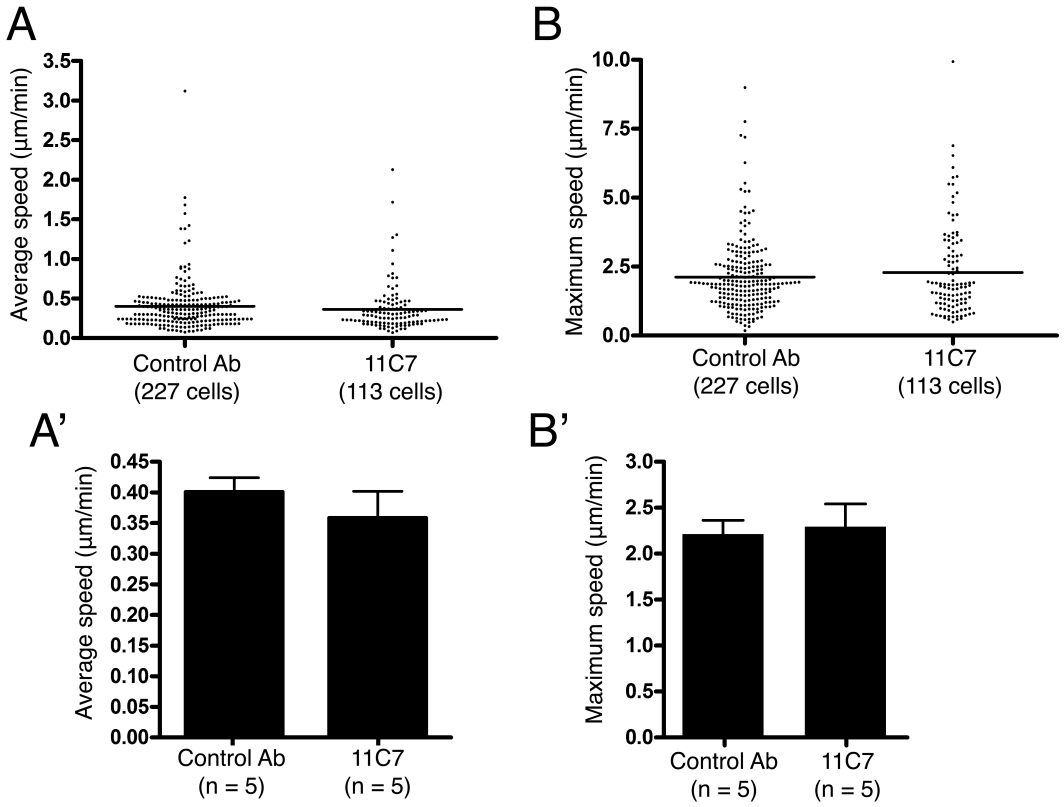

Figure 4.14 ▲ Chronic treatment with anti-Nogo-A antibody 11C7 does not significantly alter average or maximum speed. (A), (A') Average speed. (B), (B') Maximum speed. (A), (B) All tracked cells, combined across explants. (A'), (B') Means ± SEM with each explant treated as an independent sample.

Neuroblasts migrate in a saltatory manner, alternating between movement and pause phases (James et al., 2011; Marín et al., 2010). Therefore, we also investigated whether these distinct phases were individually altered by anti-Nogo-A antibody or exogenous Δ20 peptide. However, we found no evidence that that either pause frequency or pause duration were altered by antibody or peptide treatment (Figs 4.15 and 4.16).

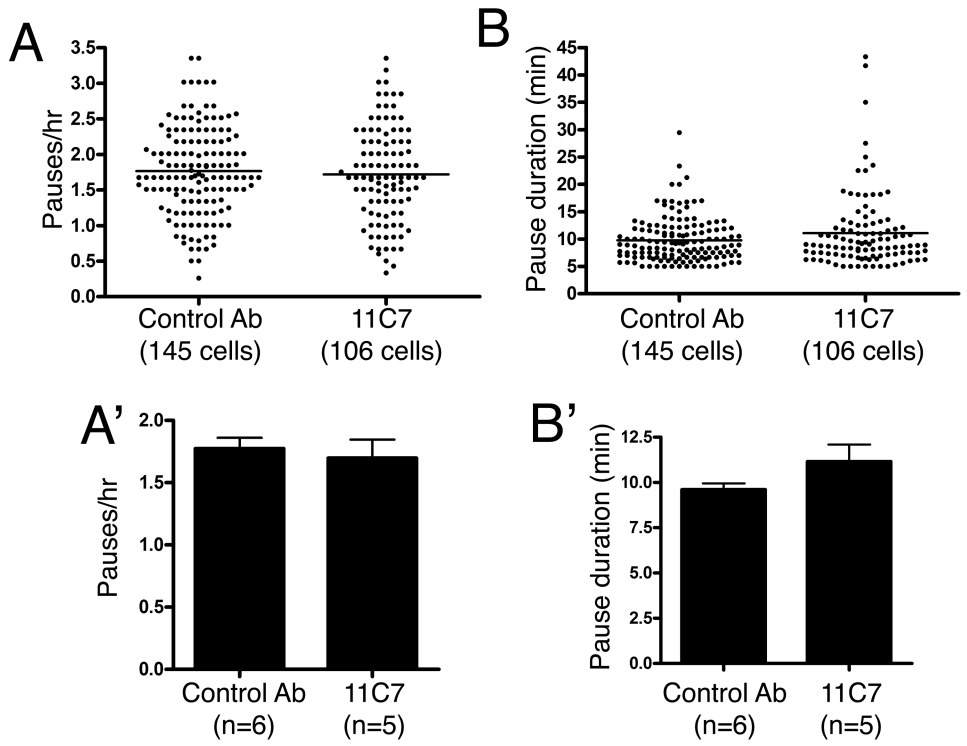

Figure 4.15 ▲ Anti-Nogo-A antibody 11C7 does not alter pause frequency or duration in SVZ neuroblasts. (A), (A') Frequency of pauses (pauses per hour). (B), (B') Pause duration. (A), (B) All tracked cells, combined across explants. (A'), (B') Means ± SEM with each explant treated as an independent sample.

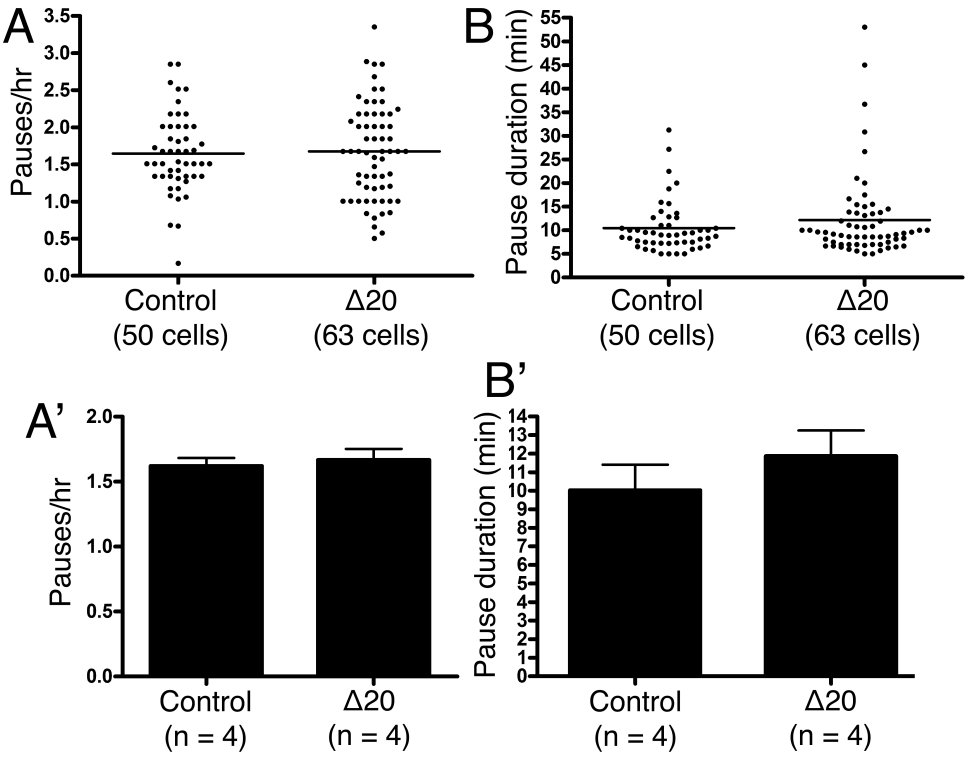

Figure 4.16 ▲ Chronic treatment with Δ20 peptide does not alter pause frequency or duration in SVZ neuroblasts. (A), (A') Frequency of pauses (pauses per hour). (B), (B') Pause duration. (A), (B) All tracked cells, combined across explants. (A'), (B') Means ± SEM with each explant treated as an independent sample.

Δ20 peptide or anti-Nogo-A antibody treatment did not alter directional persistence, a measure of the straightness of a cell's path, calculated as the displacement (distance between the starting and ending points) divided by the total distance traveled (Gertz and Kriegstein, 2015) (Fig. 4.17).

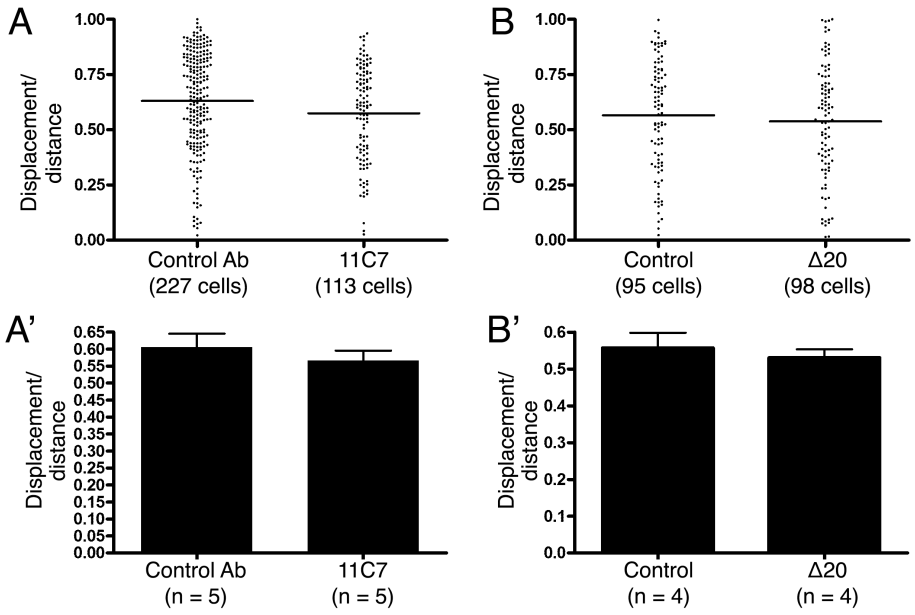

Figure 4.17 ▲ Neither anti-Nogo-A antibody 11C7 nor Δ20 peptide significantly alter directional persistence. (A), (A') Anti-Nogo-A antibody 11C7 versus control antibody. (B),(B') Δ20 peptide versus control peptide. (A), (B) All tracked cells, combined across explants. (A'), (B') Means ± SEM with each explant treated as an independent sample.

Lastly, chronic Δ20 peptide treatment did not significantly alter the average leading process lengths of migrating neuroblasts (Fig. 4.18).

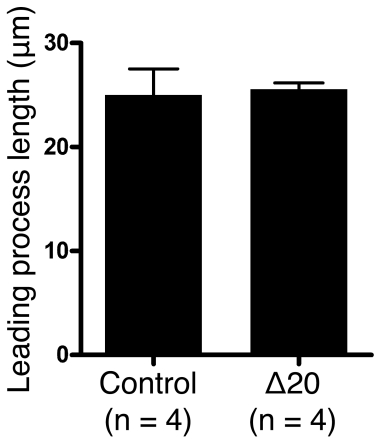

Figure 4.18 ▲ Chronic Δ20 treatment does not significantly alter neuroblast leading process length. Leading process lengths were averaged within each explant, with each explant treated as an independent sample.

DISCUSSION

The results of this study show that Nogo-A is expressed by neuroblasts in the adult rat SVZ, and colocalizes with the endoplasmic reticulum marker calnexin *in vitro*. No evidence for surface expression of Nogo-A was found, suggesting that Nogo-A plays at least a partially cell-autonomous role in these cells. However, we showed that a rich source of myelin resides just lateral to the SVZ that may be available to affect SVZ physiology. Lastly, we found that the chronic administration of exogenous Nogo-A-Δ20 peptide restricted the migration speed of SVZ neuroblasts.

Nogo-A has been detected on the surface of many cell types *in vitro* using live-cell (non-permeabilizing) staining, including oligodendrocytes, primary dorsal root ganglion neurons, and cells from embryonic forebrain-derived neurospheres (Caroni and Schwab, 1988a; Dodd et al., 2005; Mathis et al., 2010). However, while we have shown that

Nogo-A is strongly expressed by SVZ-derived neuroblasts *in vivo* and *in vitro*, its surface expression is not detectable by indirect immunofluorescence. In contrast, other, DCX-negative cell types derived from SVZ explants did in fact show the expected punctate pattern of surface staining. This suggests that this technique is valid for detecting surface expression of Nogo-A. Other methods are available to confirm surface expression, such as biotinylation of surface molecules followed by pulldown and immunoblotting. However this is not amenable to our culture system since 1) SVZ explant cultures contain a mixed population of cells (some of which we now know are surface Nogo-A positive), and 2) relatively few neuroblasts migrate out of the explants and onto the laminin-coated coverslips—likely too few to detect a small amount of surface protein by immunoblotting. If SVZ neuroblasts lack surface expression of Nogo-A, this argues against the model proposed by Rolando and colleagues regarding the role of neuroblast Nogo-A expression in suppressing neural stem cell proliferation and promoting neuroblast migration (Rolando et al., 2012). However, this does not suggest that neuroblasts are not susceptible to Nogo-A signals delivered by other cell types, such as oligodendrocytes.

When we investigated the subcellular localization of Nogo-A, we found extensive colocalization of Nogo-A, βIII tubulin and calnexin throughout the length of the leading process. The most parsimonious interpretation is that Nogo-A, a known ER-associated protein, is distributed throughout the ER, which extends far into the leading process. The functional role of intracellular Nogo-A in SVZ neuroblasts is unknown. However, previous studies have suggested that Nogo-A can act cell-autonomously to regulate neurite

branching and extension and growth cone motility *in vitro* (Kurowska et al., 2014; Montani et al., 2009; Petrinovic et al., 2010). Given the parallels between embryonic and adult SVZ neurogenesis, and the stage-specific expression pattern of Nogo-A in immature neurons, it is possible that intracellular Nogo-A plays a role in the morphogenesis of newborn neurons. Future studies using Nogo-A knockdown siRNA or conditional knockout mice could help to clarify the role of intracellular Nogo-A in SVZ neuroblasts.

The recently characterized receptor for the Nogo-A-Δ20 domain, S1PR2, was also seen in DCX+ neuroblasts, although staining required signal amplification, possibly reflecting a low abundance protein. Specific cellular NgR1 expression, in contrast, was not appreciable in the SVZ, while other cells in the cortex and striatum displayed clear NgR1 immunoreactivity, demonstrating the validity of the staining protocol. This result is at odds with Rolando et al.'s report of NgR1 expression in SVZ neural stem cells in mice, as our immunostaining did not resemble their representative images (Rolando et al., 2012). Beyond a species difference, the reason for this discrepancy is unclear.

In vivo, we showed that the lateral aspect of the SVZ is in contact with or in close proximity to a myelin-rich zone that may be an exogenous source of Nogo-A or other myelin constituents. This band of myelin, which extends rostrally and coalesces into a tube containing a large population of DCX+ neuroblasts in its center, seems well-positioned to be able to signal to migrating neuroblasts. While the consequences of neuroblast-myelin contact are unknown, myelin is not an inert insulator, but rather contains molecules that can signal to other cells. Potentially, this myelin adjacent to the SVZ could be a source of

Nogo-A mediating the effects observed by Rolando et al. (Rolando et al., 2012). Likewise, two other prominent myelin proteins, myelin-associated glycoprotein (MAG) and oligodendrocyte myelin glycoprotein (OMGp) may also play distinct roles in regulating neurogenesis (Li et al., 2009; Martin et al., 2009) (and reviewed in (Xu et al., 2015)). The presence of myelin may act to channel or constrain neuroblast migration, as it has been found to do with developing axons (Schwab and Schnell, 1991). Indeed, axon outgrowth/guidance and neuronal migration share many of the same regulators and behaviors, including guidance cues (for example, slits, netrins, and semaphorins), Rho family GTPases, and actin and microtubule cytoskeletal rearrangements (Govek et al., 2011; Marín et al., 2010). Furthermore, the existence of chemorepellents in the developing brain help prevent the ectopic spread of migrating neurons (Marín et al., 2010). For example, the semaphorins Sema3A and 3F are expressed in the developing striatum and prevent the spread of cortex-bound interneurons into this structure (Marin et al., 2001), and it is possible that a similar mechanism acts to properly channel neuronal migration in the adult SVZ. The sources of the Slit chemorepellents that direct rostral migration in the adult SVZ—the septum and choroid plexus—are both *medial* to the SVZ, suggesting the need for a second chemorepellent source to prevent the ectopic lateral spread of SVZ neuroblasts into the striatum (Nguyen-Ba-Charvet et al., 2004). Once understood, the mechanisms that restrict ectopic migration of adult neuroblasts could possibly be targeted to promote SVZ-based cortical repair.

Rolando and colleagues reported a marked reduction in neuroblast migration when SVZ explants were treated with anti-Nogo-A antibody 11C7, evident just 1 day after plating (Rolando et al., 2012). In contrast, we saw only a slight reduction in migration distance evident only at 7 days after plating. Several differences may account for this discrepancy. First, Rolando et al.'s study used explants from postnatal day 5 (P5) mice, whereas ours were from young adult rats. Beyond the species difference, P5 precedes most myelination in the brain, meaning that explants from P5 mice have not been exposed to myelin, the major source of Nogo-A (Foran and Peterson, 1992). Furthermore, P5 explants much more robustly generate migrating neurons than adult explants, possibly due to an age-related decline in neurogenesis (Wichterle et al., 1997). Indeed, the study by Rolando and colleagues demonstrates much more robust migration from explants 1 day after plating than we ever observed in our culture system (see Fig 4.9).

We found that chronic stimulation with Δ20 peptide led to a modest but statistically significant reduction in the maximum velocity of SVZ neuroblasts. Since Δ20 clustering potentiates its effects on neurite growth inhibition, it is possible that our results underestimate the impact of Nogo-A signaling on SVZ neuroblast motility *in vivo*. In contrast, acute Δ20 peptide treatment did not significantly alter maximum velocity of previously untreated cells in the hours immediately following treatment. These results suggest that the effects of Δ20 on migration may require a longer time course, possibly through effects on gene expression. Alternatively, we cannot rule out that chronic Δ20 stimulation led to long-term receptor desensitization, and that this in turn affected cell

motility. As we applied only a uniform concentration of Δ20, additional unexplored avenues include the influence of Δ20 gradients on neuroblast migration, and assays that incorporate aspects of directed migration (eg., culturing in the presence of physiologically relevant chemoattractant or chemorepellent gradients) to more closely mimic *in vivo* migration. Regardless, these results are in line with a study showing that inhibition of ROCK, a key intracellular mediator of Nogo-A signaling, enhanced migration from adult SVZ-derived neurospheres *in vitro* (Leong et al., 2011). In contrast, pharmacological inhibition of Rac1, a Rho family GTPase also inhibited by Nogo-A signaling, reduced the migraton of SVZ-derived cells (Leong et al., 2011; Niederöst et al., 2002). Within the olfactory bulb, chain migrating neuroblasts dissociate and migrate radially as single cells. Therefore, the singly migrating cells in our explant culture systems, which we tracked exclusively, may be more analogous to radial migration than tangential. This would reconcile our results with Rolando et al.'s finding that Δ20 neutralization with anti-Nogo-A antibodies had no effect on migration specifically from olfactory bulb explants (where migration is mostly radial) (Rolando et al., 2012).

The significance of Nogo-A regulation of neuroblast motility is unclear. If the migration of new neurons is stalled, they could be receptive to niche-derived signals for a longer time, which may influence their fate. For example, in embryonic development, duration of immature neuron exposure to notochord-and floor plate-derived sonic hedgehog contributes to the spatial patterning of the spinal cord (Ribes and Briscoe, 2009). Additionally, the olfactory bulb contains abundant Nogo-A, and neuroblasts can be seen

migrating along Nogo-A positive fibers, which may serve to slow down the locomotion of these cells as they are completing their migration and integrating into the local circuitry. Future studies examining the localization of new OB neurons or their rate of appearance in the OB in Nogo-A knockout mice could shed light on the *in vivo* role of Nogo-A in normal SVZ-OB migration.

CHAPTER FIVE

EFFECTS OF STROKE AND ANTI-NOGO-A TREATMENT ON CELLULAR PROLIFERATION AND NEUROBLAST RESPONSE IN THE SUBVENTRICULAR ZONE

ABSTRACT

Ischemic stroke is a leading cause of adult disability, but there are currently no pharmacological treatments to improve recovery once the acute phase of stroke has passed. Our laboratory has shown that an experimental treatment, neutralizing antibodies against the neurite growth-inhibitory protein Nogo-A, promotes axonal and dendritic remodeling and functional recovery after stroke in adult and aged rats. However, a recent study described a role for Nogo-A in the maintenance of the subventricular zone (SVZ), one of the adult brain's main neurogenic niches, raising the question of whether neurogenesis may be affected by anti-Nogo-A treatment after stroke and play a role in recovery (Rolando et al., 2012). Here, we investigated the consequences of Nogo-A neutralization on cellular proliferation in the SVZ after cortical stroke. After stroke, despite abundant diffusion of treatment antibody into the ipsilateral SVZ, we found no effect of either cortical stroke or treatment on the number of proliferating cells in the SVZ across several time points.

Stroke stimulated neuroblast recruitment from the SVZ, but two weeks of treatment did not alter the density of DCX immunostaining in the SVZ and adjacent striatum. Furthermore, we found no evidence of new neurons generated in the perilesional cortex after stroke, although we did find many newborn cells closely juxtaposed to neuronal cell bodies that without close examination could be mistaken for newborn neurons. These results suggest that cortical neurogenesis does not contribute to functional recovery after stroke and anti-Nogo-A treatment.

INTRODUCTION

Ischemic stroke is a leading cause of adult disability with no pharmacological treatments to restore lost function. Injuries to the adult central nervous system (CNS) are particularly harmful because of the low potential for beneficial reorganization (neuroplasticity) or cell replacement. Neuroplasticity in the adult CNS is potently inhibited by Nogo-A, a transmembrane protein expressed predominantly by oligodendrocytes and their product myelin (Schwab and Strittmatter, 2014). Our laboratory has shown that treatment with neutralizing antibodies against Nogo-A improves functional recovery after stroke in adult and aged rats. This recovery has been associated with axonal and dendritic plasticity from existing neurons in the spared cerebral hemisphere (Kumar and Moon, 2013).

Intriguingly, a recent study reported a role for Nogo-A in the regulation of the subventricular zone (SVZ), one of the adult brain's main neurogenic niches (Rolando et al., 2012). In this study, activation of the Nogo-66 receptor NgR1 was found to inhibit the

proliferation of neural stem cells, while Nogo-A-Δ20 promoted neuroblast migration to the olfactory bulbs (Rolando et al., 2012). As these studies were performed in healthy adult mice, the significance of SVZ regulation by Nogo-A in the context of stroke and anti-Nogo-A antibody treatment is unknown. However, it suggests that the SVZ may be a target of anti-Nogo-A antibody treatment that may stimulate the early steps of cell replacement after injury.

In this study, we investigated the impact of anti-Nogo-A antibody treatment on the neurogenic response to stroke in the SVZ. Using a treatment protocol previously shown to promote functional recovery, we found no evidence that anti-Nogo-A antibody treatment potentiated either cellular proliferation in the SVZ or the density of immature neurons in the SVZ and adjacent striatum after stroke. Unexpectedly, we also saw no effect of stroke itself on cellular proliferation in the SVZ using two different quantification strategies—unbiased stereological cell counts of BrdU+ cells in the SVZ, and quantification of the area of Ki67+ SVZ immunoreactivity. However, we did find evidence of minor neuroblast emigration from the SVZ toward the lesioned cortex. These results suggest that SVZ neurogenesis contributes little to functional recovery after stroke and anti-Nogo-A therapy.

EXPERIMENTAL DESIGN

Quantification of proliferating cells in the SVZ after stroke

BrdU-positive cells were quantified stereologically by using the optical fractionator probe in MBF StereoInvestigator software. Every 6th section between the genu of the

corpus callosum and the crossing of the anterior commissure (8 sections total) was included for analysis. For counting, the SVZ was defined as the dense band of DAPI-stained nuclei in the lateral wall of the lateral ventricles, extending from the dorsal-most point of the lateral ventricle, including the dorsolateral extension of the SVZ, and extending ventrally to the ventral-most point of the lateral ventricle (see Fig. 5.1). Stereological parameters are summarized in table 5.1.

Area of each counting frame	Approximate # of counting sites per section	Disector height	Guard zone thickness	Sampling grid (X x Y, µm)	Section cut thickness	Section evaluation interval
900 µm²	22	25 µm	1.2 µm	57 x 162	40 µm	6

Table 5.1. ▲ Summary of optical fractionator parameters used to quantify BrdU+ cells in the SVZ.

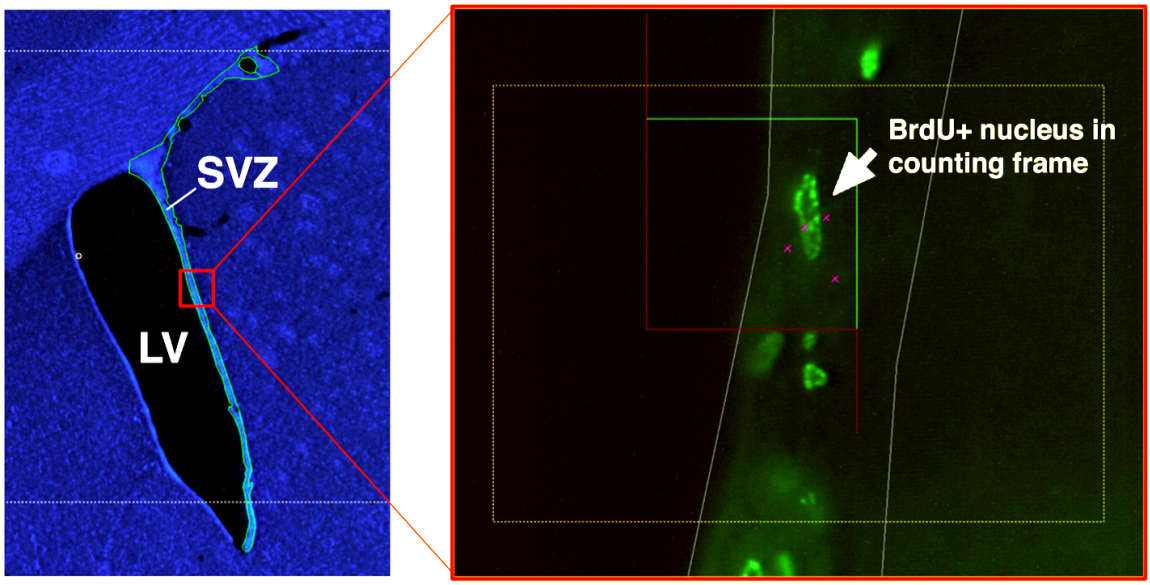

Figure 5.1 ▲ Implementation of the optical fractionator. Left: Low magnification view of DAPI-stained nuclei. A contour (thin green line) was drawn around the SVZ to define the region of interest for cell counting. Right: Higher magnification imge of a BrdU+ nucleus (green) within the counting frame. Magenta x's represent other nuclei outside of the plane of focus that were also located within the counting frame and marked. The left and right images are for demonstration purposes only and were not taken from the same tissue section.

Primary neural stem/progenitor cell culture and quantification

A 4 month old male Long-Evans rat was deeply anesthetized with isoflurane anesthesia and decapitated. The brain was extracted and placed in cold phosphate buffered saline, and then cut into 2 mm coronal sections using a brain matrix. Under a dissecting microscope, the lateral walls of the lateral ventricles were dissected out, minced, and added to a solution of papain (2 mg/mL) in NS-A medium. The tissue was incubated at 34°C with for 30 min, followed by gentle trituration with a fire-polished glass pipet to disperse the cells. After centrifugation, the cell pellet was resuspended in complete medium consisting of NS-A media plus proliferation supplement, 1x antibiotic/antimycotic, heparin (2 ug/mL), EGF (20 ng/mL), and FGF2 (10 ng/mL) and maintained in a 37° C incubator supplemented with 5% CO_2 and 100% humidification. Half media changes were performed every 3-4 days, with passaging after dissociation in Accutase approximately every 7-10 days.

For investigation of cellular proliferation, equal numbers of P6 NSPCs were grown in proliferation media on acid-washed German glass coverslips coated with poly-D-lysine and laminin (10 ug/mL) for 4 days in the presence of 1) anti-BrdU 30 ug/mL, 2) anti-BrdU 27 ug/mL + 11C7 3 ug/mL), or 3) 11C7 30 ug/mL. Cells were then gently rinsed in PBS and fixed for 48 hours in 4% PFA at 4 deg C. Antigen retrieval was performed in 85 deg sodium citrate + 0.05% tween 20 pH 6 for 20 min, followed by 5 min permeabilization in 0.3% Triton X100. Cells were blocked in 10% NGS in PBS for 1 hour at room temperature and incubated with primary antibody (rabbit anti-Ki67, Abcam

Ab16667) at 1:1000 in block overnight at 4 deg. Cells were washed and incubated in secondary antibody (goat anti-rabbit 488, Invitrogen A11070) 1:500 in block for 2 hours at room temperature. Nuclei were visualized with DAPI.

Cells were counted by an investigator blind to treatment group, using the fractionator probe in StereoInvestigator (50x50 um counting frame; ~30 sites per contour). Ki67+ cells and total DAPI+ cells were counted in each counting frame. Data were analyzed by comparing the percentages of Ki67+ cells among treatment groups by one-way ANOVA.

RESULTS

Lesion size is not affected by anti-Nogo-A treatment

As we have previously reported, the total lesion size was not affected by anti-Nogo-A treatment (Fig. 5.2).

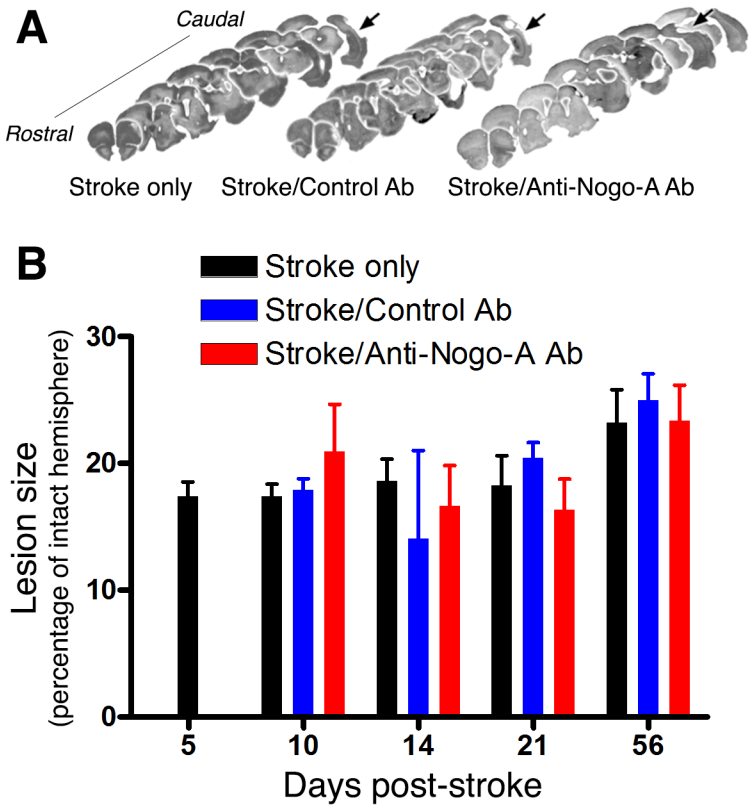

Figure 5.2 ▲ Lesion size is not significantly altered by anti-Nogo-A antibody treatment at any time point assessed. (A) Representative images of stroke lesions (arrows). (B) Lesion sizes, as a percentage of the intact hemisphere, at each time point after stroke (x axis).

	Days post-stroke				
Group	**5**	**10**	**14**	**21**	**56**
Stroke-only	17.38±1.16 (4)	17.40±0.97 (3)	18.57±1.76 (4)	18.25±2.36 (6)	23.20±2.60 (8)
Stroke/ Control Ab	N/A	17.90±0.89 (4)	14.07±6.96 (3)	20.45±1.19 (6)	24.96±2.09 (5)
Stroke/ Anti-Nogo-A	N/A	20.93±3.74 (4)	16.60±3.24 (4)	16.34±2.42 (7)	23.34±2.83 (8)

Table 5.2 ▲ Lesion sizes (percentages). Values are presented as mean (as a percentage of the area of the intact hemisphere) ± SEM, with sample size in parentheses.

Neither stroke nor anti-Nogo-A treatment alter the number of proliferating cells in the SVZ

Cellular proliferation in the SVZ was quantified stereologically at the end of anti-Nogo-A treament (ie., 21 days post-stroke). At this time point, no significant differences were found in the number of BrdU+ cells in the SVZ among sham surgery, stroke-only, stroke plus control antibody or stroke plus anti-Nogo-A antibody groups (Fig 5.3a). To investigate whether there were earlier changes in proliferation, additional time points were added, including 5, 10, and 14 days post-stroke (10- and 14-day post-stroke groups included rats that were treated for only 3 and 7 days, respectively). Again, no evidence was found at any time point for an influence of stroke or treatment on the number of proliferating cells in the SVZ.

Since brain injury is generally associated with an increase in cellular proliferation in the SVZ (Kernie and Parent, 2010), we performed alternative experiments in which we quantified the expression of the endogenous proliferation marker Ki67. In accordance with

our BrdU data, the area of Ki67 immunoreactivity was not significantly different from sham in either the ipsilesional or contralesional SVZ at 10, 14, or 21 days post-stroke (Fig 5.3b).

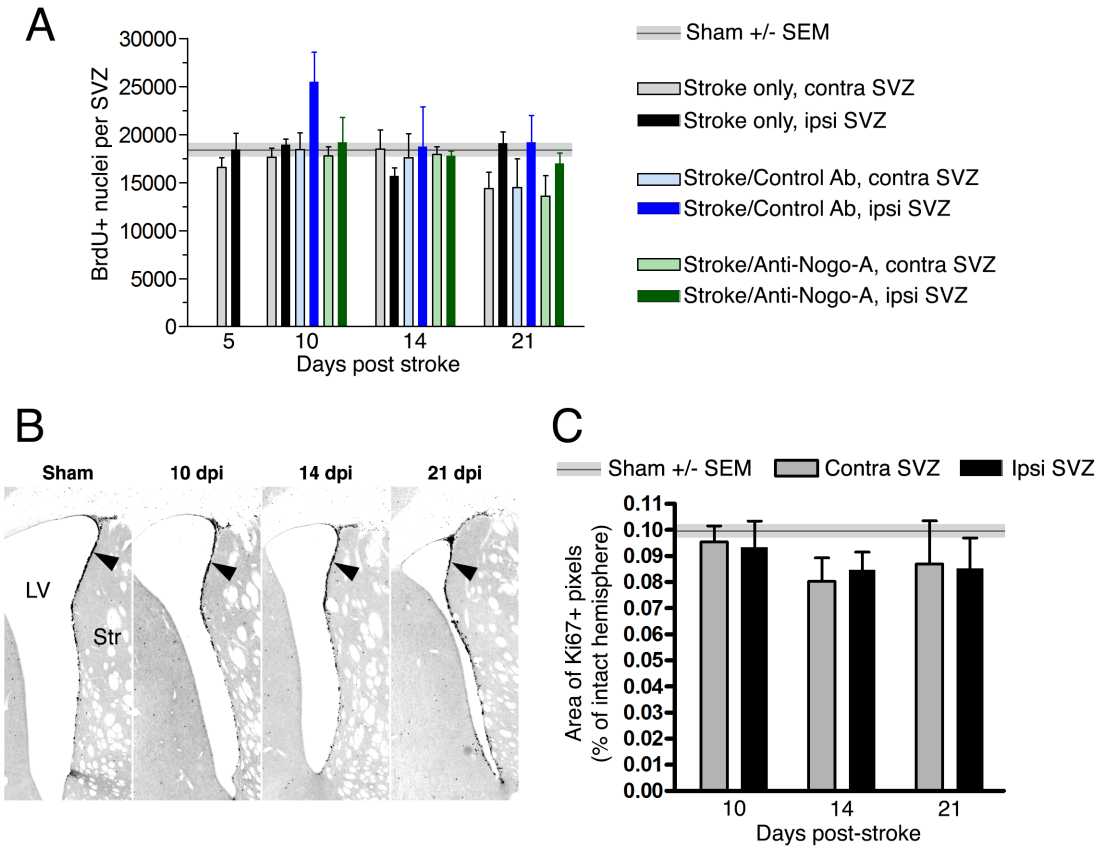

Figure 5.3 ▲ Neither stroke nor anti-Nogo-A treatment significantly alter cellular proliferation in the SVZ at any time point assessed. (A) Unbiased stereological cell counts from the contralesional (contra) and ipsilesional (ipsi) SVZs from sham, 5, 10, 14, and 21 days post-stroke. (B) Representative images of Ki67 immunostaining in the SVZ (arrowhead) from sham and 10, 14, and 21 days post-stroke subjects. LV: lateral ventricle; Str: striatum. (C) Quantification of Ki67-positive pixel area in the SVZ normalized to the area of the intact hemisphere.

	Days post-stroke			
Group	**5**	**10**	**14**	**21**
Sham surgery	N/A	N/A	N/A	18371±741 (4)*
Stroke-only	18453±1696 (3)	18926±576 (3)	15703±830 (2)	19086±1181 (6)
Stroke/Control	N/A	25477±3094 (3)	18729±4158 (3)	19187±2801 (6)
Stroke/ Anti-Nogo-A	N/A	19182±2577 (4)	17800±456 (4)	16996±1080 (7)

Table 5.3a ▲ BrdU cell counts in the *ipsilesional* SVZ after stroke and anti-Nogo-A treatment. Values are presented as mean ± SEM, with sample size in parentheses. *BrdU+ cells in sham brains were counted on only one side.

	Days post-stroke			
Group	**5**	**10**	**14**	**21**
Sham surgery	N/A	N/A	N/A	18371±741 (4)*
Stroke-only	16560±1035 (3)	17637±947 (3)	18476±1980 (2)	14361±1724 (6)
Stroke/Control	N/A	18444±1747 (3)	17591±2500 (3)	14484±2979 (6)
Stroke/ Anti-Nogo-A	N/A	17768±944 (4)	17912±818 (4)	13582±2134 (7)

Table 5.3b ▲ BrdU cell counts in the *contralesional* SVZ after stroke and anti-Nogo-A treatment. Values are presented as mean ± SEM, with sample size in parentheses. *BrdU+ cells in sham brains were counted on only one side.

	Days post-stroke			
Side	**Sham surgery**	**10**	**14**	**21**
Contralesional SVZ	0.09970±0.00227 (4)*	0.09531±0.00621 (3)	0.08024±0.00901 (4)	0.08686±0.01662 (3)
Ipsilesional SVZ		0.09326±0.01008 (3)	0.08458±0.00689 (4)	0.08518±0.01170 (3)

Table 5.4 ▲ Area covered by Ki67+ pixels in the contralesional and ipsilesional SVZ after stroke. Values are presented as mean (as a percentage of the area of the intact hemisphere) ± SEM, with sample size in parentheses. *Ki67+ pixel area in the sham surgery group was established by averaging the values from the SVZs bilaterally.

In agreement with this finding, we also did not find an effect of 11C7 treatment on the number of proliferating primary SVZ neural stem/progenitor cells *in vitro* (Fig. 5.4).

After stroke, immunostaining for the immature neuron marker doublecortin (DCX) revealed numerous cells in the SVZ, as expected, and sparse but distinct DCX+ cells with elongated, migratory morphology located primarily within the white matter tracts of the corpus callosum and external capsule on the ipsilesional side. These cells were typically singly-migrating, rather than in chains, and aligned parallel with the white matter fibers coursing through these regions. Qualitatively, the number of DCX+ that had moved into the corpus callosum seemed to correlate directly with lesion size. The area of DCX+ immunoreactivity in the SVZ and adjacent striatum was quantified after 14 days of anti-Nogo-A treatment (21 days post-stroke). While we observed a trend toward increased DCX+ area in the post-stroke ipsilesional SVZ versus sham, DCX+ pixel area was not significantly altered by anti-Nogo-A treatment (Fig. 5.5).

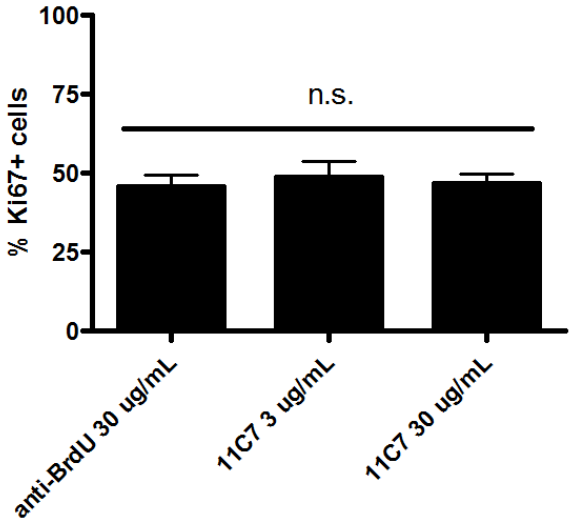

Figure 5.4 ▲ *In vitro* anti-Nogo-A antibody treatment does not significantly alter the number of primary SVZ neural stem/progenitor cells positive for the endogenous proliferation marker Ki67.

The neuroblast response—ie, neuroblasts that had left the SVZ and started migrating ectopically toward the lesion—could be observed even at 8 weeks post-stroke. Notably, one stroke lesion was particularly severe and damaged the dorsolateral striatum, and a robust accumulation of neuroblasts was evident in the dorsal and dorsolateral striatum. While only correlative, these observations suggest differences in the neuroblast response to mixed cortical/striatal stroke versus purely cortical stroke (Fig. 5.6).

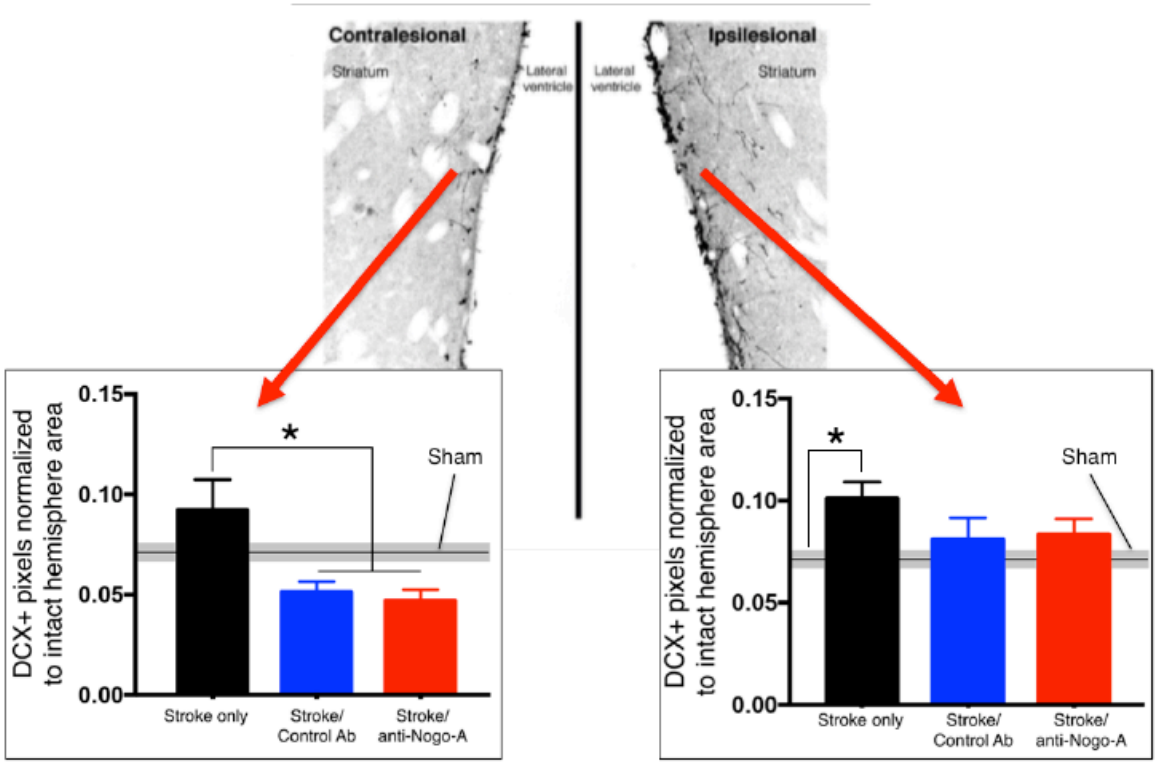

Figure 5.5 ▲ DCX-positive staining density in the SVZ and adjacent striatum is not increased by anti-Nogo-A antibody treatment. Left: Contralesional SVZ/striatum. Staining density was significantly reduced in both control antibody- and anti-Nogo-A antibody-treated groups relative to the untreated/stroke only group. * $p < 0.05$; one way ANOVA and Bonferroni post-hoc tests. Right: Ipsilesional SVZ/striatum. Stroke alone led to a significant increase in DCX staining density which was not potentiated by anti-Nogo-A antibody treatment. * $p < 0.05$ versus sham; unpaired t test.

Group	Contralesional SVZ/striatum	Ipsilesional SVZ/striatum
Sham surgery (4)	0.07114±0.00456	
Stroke-only (6)	0.09205±0.01517	0.10112±0.00809
Stroke/Control (6)	0.05137±0.00519	0.10520±0.02589
Stroke/ Anti-Nogo-A (6)	0.04703±0.00547	0.08332±0.00776

Table 5.5 ▲ Doublecortin positive pixel density at 21 days post-stroke. Values are presented as mean (as a percentage of the area of the intact hemisphere) ± SEM, with sample size in parentheses.

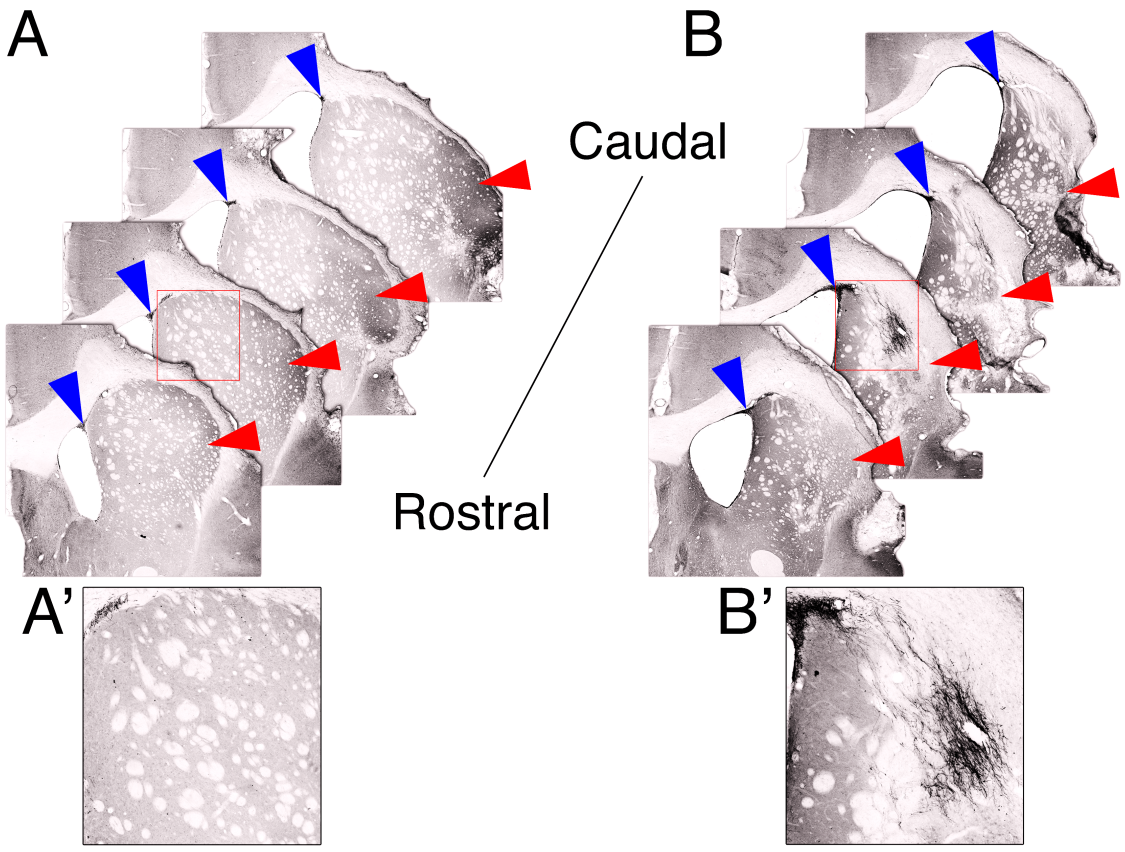

Figure 5.6 ▲ Striatal damage leads to robust neuroblast recruitment. DCX staining, which appears black, is shown from a subject without extensive striatal involvement (A) and with striatal damage (B). (A') and (B') are enlargements of the red boxed areas in (A) and (B), respectively. In (B), DCX+ neuroblasts are seen presumably migrating from the SVZ underneath the corpus callosum and accumulating in the damaged striatum. In contrast, very few DCX+ cells are found in peri-infarct cortex. Blue arrows: SVZ; Red arrows: dorsolateral striatum.

We found no evidence of newborn neurons in perilesional cortex at 8 weeks post-stroke. Numerous BrdU+ cells closely apposed to NeuN+ neuronal cell bodies were observed, which without careful inspection could be mistaken as newborn neurons. Some of these new perineuronal cells were positive for Olig2, identifying these cells as belonging

to the oligodendrocyte lineage (Fig 5.7). These perineuronal cells were found in both perilesional and contralesional cortex.

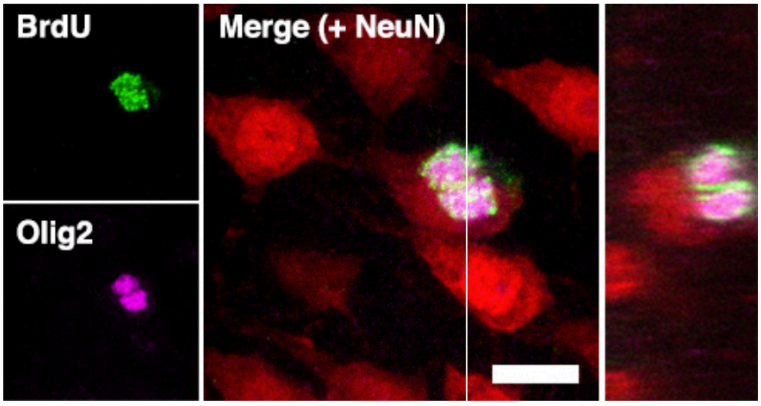

Figure 5.7 ▲ Example of new perineuronal oligodendrocyte-lineage cells generated in the perilesional cortex after stroke. Scale bar: 10 μm. Far right: orthogonal view of the image stack through at the level of the vertical white line shown in the middle panel.

DISCUSSION

To our knowledge, this is the first study to use unbiased stereology to quantify the number of proliferating cells in the SVZ after distal middle cerebral artery occlusion (dMCAO). A previous report used the optical fractionator to quantify SVZ proliferation after distal MCAO in mice, but only in the dorsolateral extension of the SVZ, and not in the lateral wall (Moraga et al., 2014). Furthermore, these results were not compared to a sham surgery group, and while a reduction in BrdU+ cell number is evident at day 14 versus day 7 after ischemia, BrdU was only injected on days 5 and 6 post-stroke, so it is not possible to make any conclusions about cellular proliferation specifically on day 14 (Moraga

et al., 2014). Our estimates of the BrdU+ cell population in the SVZ are consistent with published reports (Lois and Alvarez-Buylla, 1994).

Why striatal but not cortical ischemia appears to upregulate proliferation in the SVZ, per previous reports (for example, (Arvidsson et al., 2002)) is unclear, but a few explanations may be considered. First, the striatum is much closer to the SVZ, and therefore diffusible factors released from the lesion site that may stimulate proliferation would be in greater abundance. The SVZ is also directly innervated by GABAergic fibers from the striatum (Young et al., 2014). As $GABA_A$ receptor activation has been shown to suppress neural stem cell proliferation (Liu et al., 2005), loss of GABAergic input after striatal neuron loss may lead to an increase in neural stem cell proliferation. Lastly, the intraluminal filament model of transient MCAO has been shown to induce hypoxia in the SVZ (Thored et al., 2007), and could possibly mediate direct effects on proliferation.

Treatment with anti-Nogo-A antibodies did not upregulate proliferation in the SVZ after stroke *in vivo* at any time point assessed, nor did it upregulate the proliferation of primary SVZ neural stem/progenitor cells *in vitro*. In the study by Rolando and colleagues, treatment with mAb 11C7 similarly did not lead to changes in cellular proliferation (Rolando et al., 2012). The authors postulated that this is because NgR1, the Nogo-66 receptor, is responsible for inhibiting proliferation, and therefore an antibody targeting the Δ20 domain would not increase proliferation. However, 11C7 treatment has been shown to downregulate surface Nogo-A (Weinmann et al., 2006), thereby indirectly leading to a reduction in the amount of Nogo-66 domain available for signaling. The lack

of an effect of 11C7 on cellular proliferation may be explained by the redundancy of ligands that activate NgR1, including myelin-associated glycoprotein and oligodendrocyte myelin glycoprotein (Schwab and Strittmatter, 2014).

Based on Rolando et al.'s report of stalled neuroblast migration in mice treated with 11C7 *in vivo*, we expected to detect increased neuroblast density in the SVZ and adjacent striatum. However, we saw no effect of 11C7 treatment on the area of DCX+ pixels. Our apparent lack of an *in vivo* effect of 11C7 antibody treatment on neuroblast migration is consistent with our *in vitro* studies of 11C7-treated neuroblasts, showing no effects on neuroblast locomotion speed, pause properties, or directional persistence, and with the lack of Nogo-A surface staining in SVZ-derived neuroblasts (Chapter 4). Potentially, the presence of the stroke injury accounts for the discrepancy between our findings *in vivo*.

Proliferative "satellite" glial cells in the cortex have been recognized in the literature (Kornack and Rakic, 2001; Kuhn et al., 1997; Levison et al., 1999). In our study, we identified newly generated Olig2+ perineuronal oligodendrocytes in both perilesional and contralateral cortices. The significance of their most striking feature—an extremely close association with neuronal cell bodies, sometimes to the point of indentation—is not well understood. Unlike canonical myelinating oligodendrocytes, perineuronal oligodendrocytes express the glutamate converting enzyme glutamine synthetase, indicating a potential role in glutamate metabolism (D'Amelio et al., 1990). Potentially relevant in the context of ischemia, perineuronal oligodendrocytes have been implicated in neuroprotection in a mouse model of demyelinating disease via upregulated synthesis of lipocalin-type

prostaglandin D synthase, which produces the anti-apoptotic prostaglandin D2 (Liang et al., 2005; Taniike et al., 2002). As we did not have a matched sham surgery group, we cannot assess whether ischemia itself increases the production of new perineuronal oligodendrocytes. However, it is possible that the production of these cells may help to buffer their adjacent neurons against future ischemic insults, and deserves further examination.

CHAPTER SIX

HIPPOCAMPAL NEUROGENESIS AFTER STROKE AND ANTI-NOGO-A TREATMENT

ABSTRACT

Ischemic stroke is a leading cause of adult disability, including cognitive impairment. Our laboratory has shown that treatment with function-blocking antibodies against the neurite growth inhibitory protein Nogo-A promotes functional recovery after stroke in adult and aged rats, including enhancing spatial memory performance, for which the hippocampus is critically important. Since spatial memory has been linked to hippocampal neurogenesis, we investigated whether anti-Nogo-A treatment increases hippocampal neurogenesis after stroke. After inducing permanent middle cerebral artery occlusion in adult rats, we measured cellular proliferation in the dentate gyrus at 5, 10, 14, and 21 days post-stroke, as well as the number of newborn neurons at 8 weeks post-stroke in untreated, control antibody-treated, and anti-Nogo-A-treated groups. We found that stroke alone transiently increased cellular proliferation and increased neurogenesis in the ipsilesional granule cell layer of the dentate gyrus. Treatment with both anti-Nogo-A and control antibodies increased the accumulation of new microglia/macrophages in the

dentate granule cell layer, but neither treatment increased cellular proliferation or the number of newborn neurons above stroke-only levels. These results suggest that enhanced neurogenesis is not a key determinant of spatial memory recovery after stroke and anti-Nogo-A immunotherapy.

INTRODUCTION

Cognitive impairment is a recognized sequela of ischemic stroke (Gottesman and Hillis, 2010). Our laboratory has shown that treatment with function-blocking antibodies against the neurite growth-inhibitory protein Nogo-A (anti-Nogo-A immunotherapy) improves spatial memory performance after stroke in aged rats (Gillani et al., 2010), but a cellular mechanism of efficacy has not yet been identified. We and others have previously demonstrated that anti-Nogo-A immunotherapy stimulates dendritic and axonal remodeling and increases dendritic spine density in the contralesional sensorimotor cortex after stroke (Lindau et al., 2014; Papadopoulos et al., 2002; 2006; Seymour et al., 2005; Tsai et al., 2007; 2011; Wiessner et al., 2003). These neuroplastic changes may underlie the sensorimotor recovery seen in anti-Nogo-A treated animals (Lindau et al., 2014; Papadopoulos et al., 2002; 2006; Seymour et al., 2005; Tsai et al., 2007; 2011; Wiessner et al., 2003) (reviewed in (Kumar and Moon, 2013)), as silencing of newly sprouted axonal connections ablates the sensorimotor recovery promoted by anti-Nogo-A treatment (Wahl et al., 2014). However, no changes in dendritic complexity or spine density were found in anti-Nogo-A-treated animals in pyramidal neurons of CA1 or CA3 or in dentate granule cells, despite spatial memory improvement, suggesting an alternate mechanism of efficacy

(Gillani et al., 2010). We and other groups have likewise reported that anti-Nogo-A treatment enhances recovery from hemispatial neglect after aspiration lesion of the medial agranular cortex (Brenneman et al., 2008) and recovery of cognitive function after traumatic brain injury (Lenzlinger et al., 2005; Marklund et al., 2007), positioning Nogo-A as a promising therapeutic target for improving cognition after brain injury.

Several studies have suggested a correlation between hippocampal neurogenesis and spatial memory performance on the Morris water maze (reviewed by (Garthe and Kempermann, 2013)), and interventions that increase neurogenesis have also been shown to improve Morris water maze performance after brain injury, including stroke (Meng et al., 2014; Wurm et al., 2007). Whether Nogo-A plays a direct role in adult hippocampal neurogenesis is unknown. However, a previous study reported that mice deficient for the Nogo receptor NgR1 exhibit increased hippocampal neurogenesis and reduced cognitive impairment after traumatic brain injury (Tong et al., 2013). Furthermore, at the molecular level, key intracellular mediators of Nogo-A signaling—namely the small GTPase RhoA and its effector kinase ROCK (Schwab and Strittmatter, 2014)— play a suppressive role in hippocampal neurogenesis ((Christie et al., 2013; Keung et al., 2011), reviewed in (Vadodaria and Jessberger, 2013)). Nogo-A signaling has also been shown to inhibit nerve growth factor-mediated CREB phosphorylation *in vitro* (Joset et al., 2010), whereas CREB phosphorylation is important for the maturation and survival of newborn dentate granule cells, including after stroke (Jagasia et al., 2009; Zhu et al., 2004). These studies raise the question of whether antibody-mediated Nogo-A neutralization could lead

to alterations in neurogenesis, which may in turn contribute to cognitive recovery after stroke.

The goal of this study was to determine whether Nogo-A neutralization enhanced post-stroke hippocampal neurogenesis. Our results showed that while infusion of both anti-Nogo-A and control antibodies led to the appearance of new microglia/macrophages in the hippocampus, Nogo-A neutralization did not affect the number of newborn neurons in the dentate gyrus after stroke. Therefore, enhanced neurogenesis is unlikely to contribute to the improvement in spatial memory observed after stroke and anti-Nogo-A immunotherapy.

EXPERIMENTAL DESIGN

Cellular proliferation

For each time point, six 40 μm sections per subject encompassing the dorsal DG (every 12th section beginning at the rostral appearance of the dentate granule cell layer, between approximately -2 and -4.8 mm with respect to bregma (Paxinos and Watson, 1998)) were immunostained for BrdU and examined using bright-field microscopy on a Leica DM4000B microscope. Cell counts were performed by manually counting the number of BrdU+ nuclei in the subgranular zone (SGZ) and basal layers of the granule cell layer (GCL) (approximately < 3 nuclei from the interface between the dentate granule cell layer and polymorphic layer) bilaterally.

To account for potential differences in SGZ/GCL size between subjects, counts were normalized to SGZ length (adapted from (Imbimbo et al., 2010; Lee et al., 2012)),

measured for each section at the interface of the GCL and polymorphic layer using MBF StereoInvestigator software (MBF Bioscience, Williston, VT).

BrdU+ cell counts at 8 weeks post stroke

Due to repeated BrdU injections, many more BrdU+ cells were present in the GCL than were present for assessing proliferation after a single BrdU injection. Therefore, we employed an automated counting procedure to quantify the total number of BrdU+ cells. A total of six 40 μm sections (every 12th section beginning at the rostral appearance of the dentate granule cell layer) was stained for BrdU, lightly counterstained with toluidine blue to identify the dentate gyrus, mounted and coverslipped. The hippocampus of each section was digitized using Neurolucida software (MBF Bioscience) using a 5x objective and imported into ImageJ (Schindelin et al., 2012). Automated cell counts were performed by selecting the entire GCL, thresholding to select only BrdU+ nuclei and not toluidine blue-counterstained cells, and using the 'Analyze Particles' command. The counts for each section were added and multiplied by 12 to estimate the total number of BrdU+ cells per dentate gyrus per subject. Counts were further normalized to GCL volume using Cavalieri's principle (see below).

Measurement of GCL volume

The toluidine blue-stained tissue sections used for measuring total BrdU+ cells at 8 weeks post-stroke (6 sections total per subject) were imaged in MBF StereoInvestigator

software. The Cavalieri Estimator probe was applied to measure GCL area and estimate the total volume of the GCL within the dorsal DG encompassed by the six sections.

Quantification of newborn cell phenotypes

A total of three 40 μm sections (every 24th section beginning at the rostral appearance of the GCL and proceeding caudally) were stained for BrdU plus NeuN, Iba1, or Sox2, counterstained with DAPI, and examined on a Leica SPE confocal microscope using a 63x/1.3 NA oil immersion objective.

Due to the dense cellularity of the GCL and poor penetration of the NeuN antibody that confounded co-expression analysis in the middle of the tissue section, analysis of BrdU/NeuN co-labeling was restricted to near the outer surfaces of the tissue where NeuN expression was unambiguous. Approximately 50 cells per dentate gyrus per side were examined in each subject. Workflow was as follows: BrdU-positive cells were identified by first scanning the tissue with the appropriate excitation laser until positive nuclei were identified. Then a single optical section was acquired with 1 Airy unit pinhole size, and channels merged to identify 1) total BrdU+ cells, and 2) the number of BrdU+ cells that were positive for either NeuN, Iba1, or Sox2. When co-labeling was not clear from a single optical section, z-stacks were acquired to disambiguate the labels.

Estimates of the total numbers of new neurons were calculated by multiplying the total number of BrdU+ cells by the proportion of BrdU+ cells expressing each marker.

Treatment antibody fluorescence intensity

Three tissue sections through the dorsal DG (a 1 in 24 series) from an untreated, 7-day treated (three subjects each from control antibody and anti-Nogo-A groups) and 8 weeks post-stroke (three subjects each from control antibody and anti-Nogo-A groups) were washed in sodium phosphate buffer and incubated in DyLight-488-conjugated donkey anti-mouse (rat serum protein adsorbed) secondary antibody (Jackson Immunoresearch, West Grove, PA; 1:200 in PB/0.4% Triton X100) for 90 minutes at room temperature. Sections were washed in PB and then mounted on gelatin subbed slides and coverslipped in Fluoromount G. Z stacks through the entire thickness of each tissue section were acquired using a 10x objective on a Leica SPE confocal microscope at equivalent parts of the DG in each tissue section. All image acquisition settings were kept constant. Image stacks were imported into ImageJ and compressed to maximum intensity Z projections. The mean gray value of the tissue was then measured in each section using ImageJ and averaged to yield a single intensity value for each hippocampus per subject. The mean gray value of the tissue that did not receive antibody treatment was considered the amount of non-specific background fluorescence.

RESULTS

Nogo-A is expressed by immature neurons in the normal adult dentate gyrus (DG)

To determine whether neural precursor cells in the subgranular zone and granule cell layer (GCL) of the DG may be potential direct cellular targets of anti-Nogo-A immunotherapy, we performed double-label immunofluorescent staining using the Nogo-A-specific antibody 11C7 and antibodies to cell type-specific markers (Figs 6.1 and 6.2). Strong Nogo-A expression was found in immature (doublecortin [DCX]-positive) neurons in various stages of development. Both radially-oriented (more mature) cells with more complex arborizations (Fig 6.2a) and tangentially-oriented (transitioning, less mature progenitors) (Fig 6.2b) (Kempermann et al., 2004) were positive for Nogo-A. Nogo-A expression was especially enriched in the apical dendrites of radially-oriented DCX+ cells.

In contrast, Nogo-A expression by mature dentate granule cells within the GCL was not appreciable by immunofluorescence (Fig 6.2c), consistent with a previous report (Huber et al., 2002), suggesting transient expression of Nogo-A during the development of adult-born dentate granule cells. Robust Nogo-A expression was observed in large, pyramidal NeuN+ cells at the GCL/polymorphic layer interface (putative basket cells) (Fig 2C, arrowhead), while Nogo-A was not detectable in GFAP+ putative stem cells or astrocytes of the subgranular zone (Fig 6.2d).

A recently identified receptor for the Nogo-A Δ20 domain, sphingosine-1-phosphate receptor 2 (Kempf et al., 2014), was found to be widely expressed in the DG GCL (as reported in (Akahoshi et al., 2011)), including in DCX+ cells (Fig 6.2e).

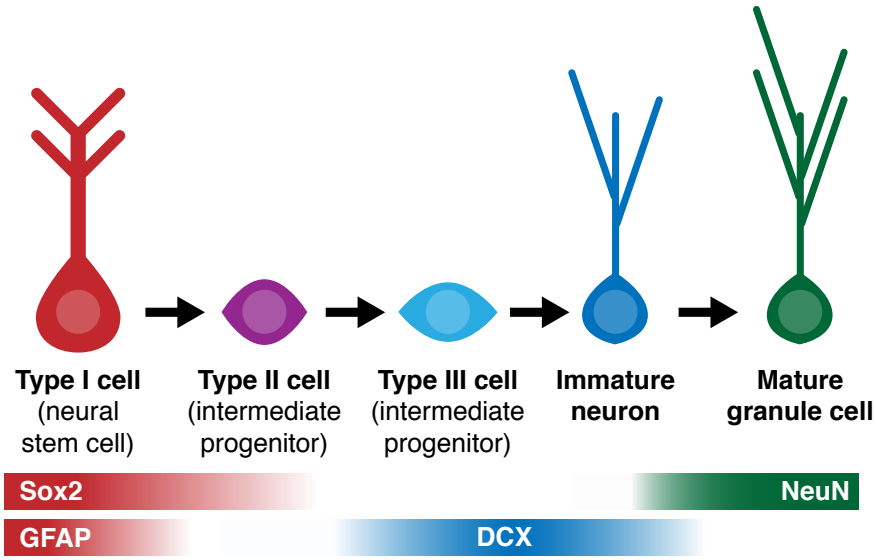

Figure 6.1 ▲ Simplified diagram of cell lineage progression and stage-specific expression of markers (Sox2, GFAP, DCX, NeuN) referenced in this study.

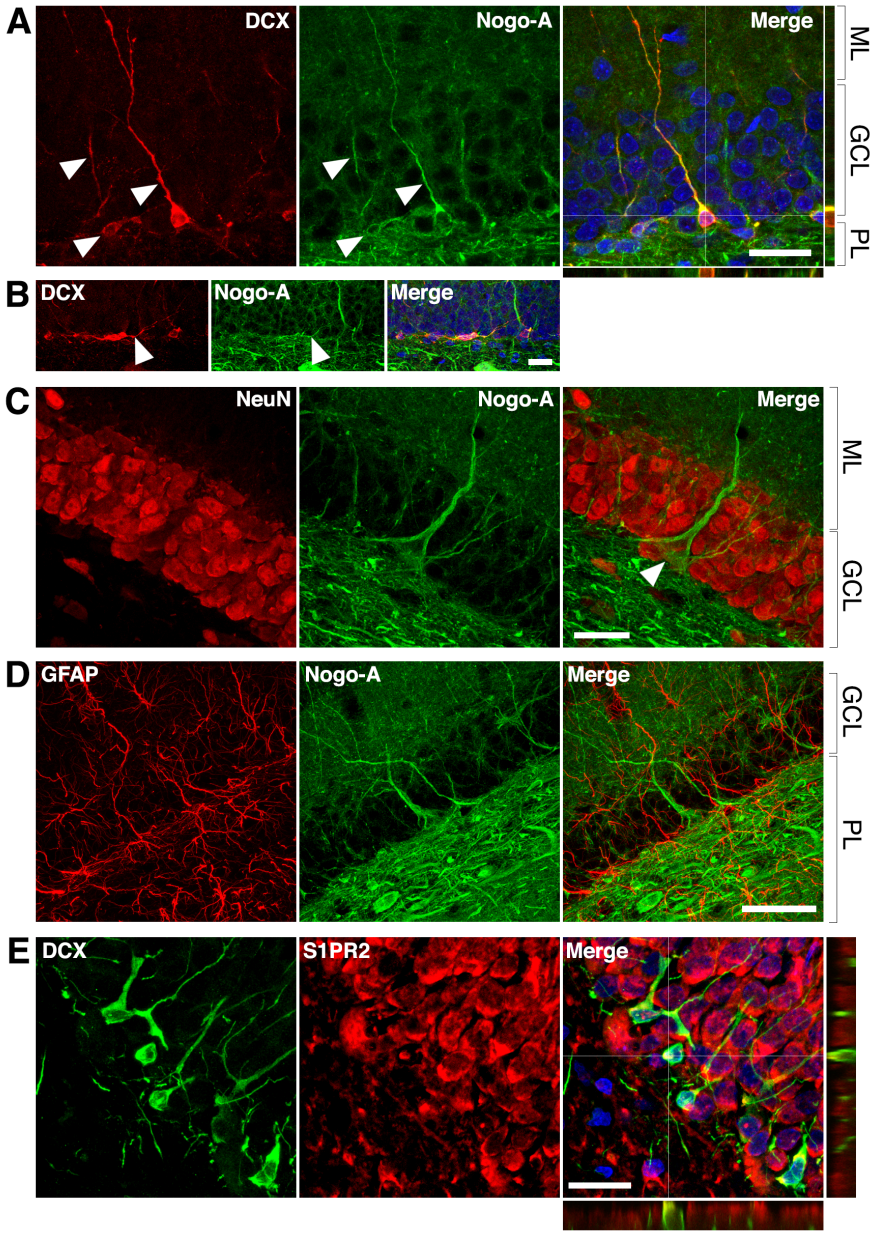

Figure 6.2 ▲ Nogo-A is expressed by immature neurons in the adult dentate gyrus. (A) Nogo-A is expressed in the processes and somata of immature neurons (arrowheads), which are also positive for doublecortin (DCX). Scale bar: 25 μm. (B) Horizontally-oriented DCX+/Nogo-A+ neuroblast. Scale bar: 25 μm. (C) Nogo-A expression is not appreciable in NeuN+ mature granule cells, the majority of NeuN+ cells in the GCL. However, putative basket cells (arrow) label strongly for Nogo-A. Scale bar: 25 μm. (D) Nogo-A immunoreactivity was not detected in GFAP+ stem cells or astrocytes. Scale bar: 50 μm. (E) Broad expression pattern

of S1PR2 in the GCL, including DCX+ immature neurons. Scale bar: 20 μm. ML: molecular layer; GCL: granule cell layer; PL: polymorphic layer.

Lesion size is not affected by antibody treatment at any time point assessed

Stroke lesions in all experimental groups were similar in location, encompassing the dorsolateral cortex and extending from primary motor cortex rostrally through auditory and visual cortices caudally (Fig 5.2). Little to no infarction of the underlying white matter or subcortical structures was evident, consistent with previous observations using this model (Gillani et al., 2010). At all time points, the hippocampus was grossly intact upon brain cryosectioning, but occasionally appeared distorted on the side ipsilateral to the stroke lesion, possibly due to distention of the cerebral ventricles. Lesion sizes (typically 17-25% of the contralesional hemisphere) were not different among the three treatment groups at any time point assessed (10, 14, 21, or 56 days post-stroke) (Fig 5.2).

Infused treatment antibodies penetrate the hippocampus

Treatment antibodies penetrated into the hippocampal parenchyma as assessed by immunofluorescent staining for mouse IgG after 3 days of treatment (Fig 6.3). Treatment antibody was detected in the hippocampus after 3, 7, and 14 days of treatment. Five weeks after pump removal (7 weeks after treatment initiation), both control and anti-Nogo-A antibodies appeared to have been substantially cleared, and were no longer detectable by immunofluorescence above background levels in the DG.

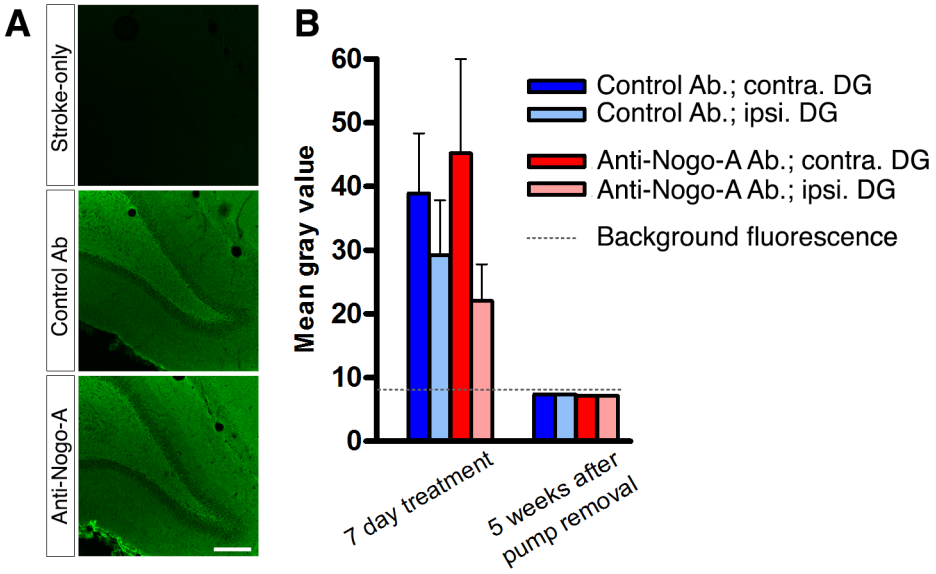

Figure 6.3 ▲ Anti-Nogo-A antibody penetrates the hippocampus. (A) Immunostaining for mouse IgG after 3 days of infusion shows diffuse, uniform penetration of anti-Nogo-A and control antibodies in the dentate gyrus (DG), whereas only tissue autofluorescence is evident in untreated MCAO rats. Scale bar: 200 μm. (B) Quantification of mean fluorescence intensity shows expected elevated signal intensity 7 days after beginning treatment, whereas at 5 weeks after treatment cessation, the signal is not detectable above nonspecific background fluorescence by direct immunofluorescence (n=3 rats per treatment group per time point). DG: Dentate gyrus.

Stroke, but not anti-Nogo-A treatment, potentiates cellular proliferation in the DG

Cellular proliferation was measured by injecting rats with a single dose of BrdU and euthanizing two hours later (Fig 6.4). Baseline proliferative activity in the SGZ and basal layers of the GCL, as measured in sham surgery groups, was generally found to be low (3.00 ± 0.19 BrdU+ cells/mm) (Fig 6.4, top panel). The number of proliferating cells was then measured at 5, 10, 14, and 21 days post-MCAO. Since treatment began 7 days post-stroke, data obtained at 5 days post-stroke includes only stroke-only subjects. The majority

of BrdU+ nuclei appeared to be localized to the SGZ and basal GCL layers. Five days after stroke, the number of proliferating cells in the ipsilesional DG increased over 3-fold (10.91 ± 0.41 BrdU+ cells/mm; $p < 0.0001$ vs. sham, two-tailed t test) and had declined to baseline by 10 days post-stroke (2.21 ± 0.27 BrdU+ cells/mm). The number of proliferating cells in the contralesional DG trended toward a more modest elevation above sham at 5 days post-stroke (5.76 ± 1.50 BrdU+ cells/mm, $p = 0.118$ vs sham). The proliferating cells at 5 days post-stroke were generally localized in dense clusters, suggesting derivation from common progenitors. Nearly all proliferating cells at this time point (69/70 cells in the ipsilesional DG and 60/60 cells in the contralesional DG across 4 different rats) were found to be at least weakly Sox2-positive (Fig 5D), suggesting that the majority of these proliferating cells were activated stem cells and/or intermediate progenitors. We found no significant effect of antibody treatment on the number of proliferating cells at any time point assessed (Fig. 6.4).

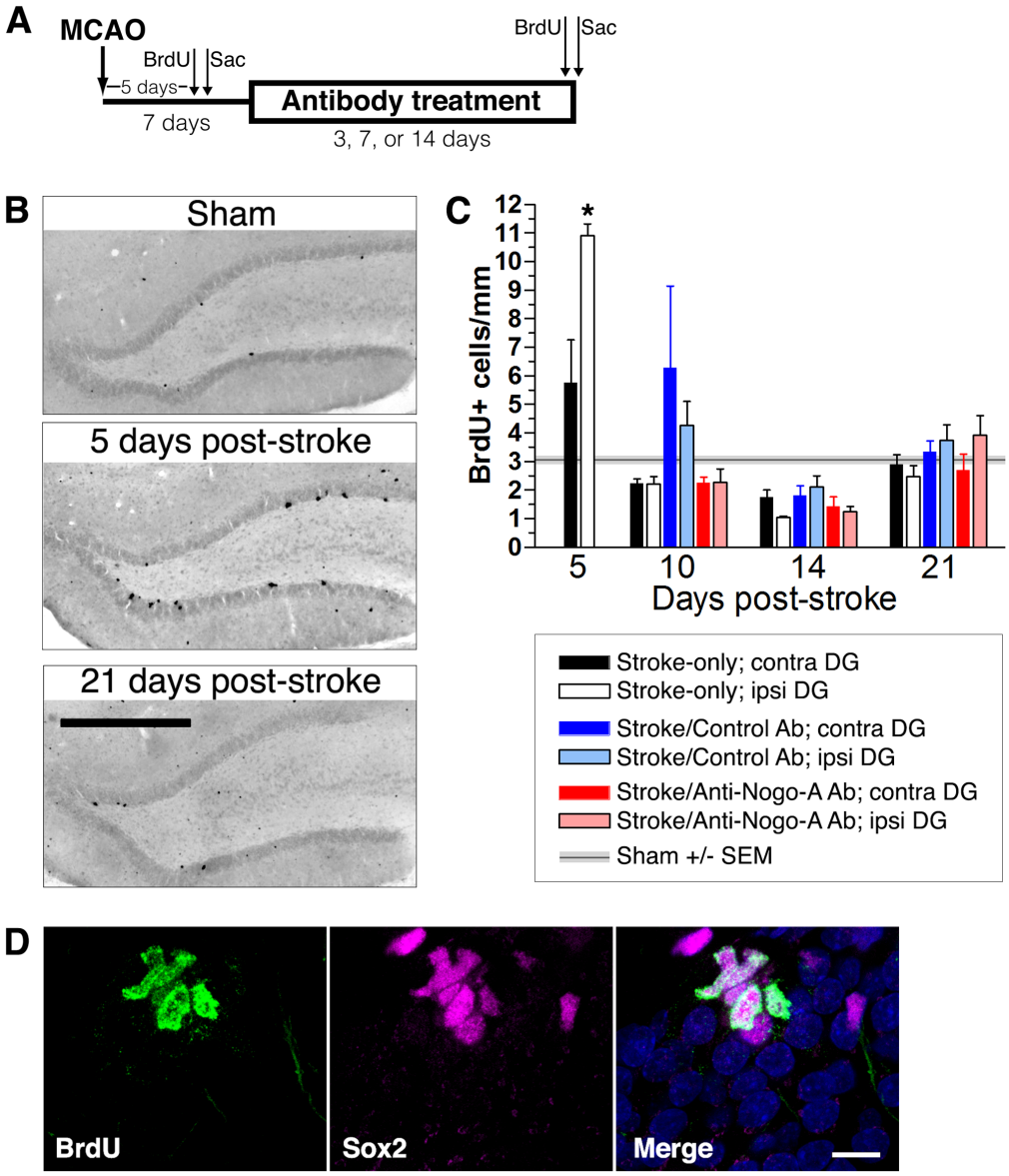

Figure 6.4 ▲ Stroke induces a transient increase in cellular proliferation in the dentate gyrus (DG) that is not altered by anti-Nogo-A treatment. (A) Overview of BrdU injection strategy to measure cellular proliferation. (B) Representative images of BrdU immunoreactivity in the ipsilesional DG of sham and stroke-only subjects at 5 and 21 days post-stroke. Numerous clusters of BrdU+ nuclei in the SGZ and basal GCL were visible at 5 days post-stroke, which were not apparent in sham or 21 days post-stroke groups. Scale bar: 500 µm. (C) Total numbers of BrdU+ nuclei in the SGZ and basal GCL normalized to SGZ length. * $p < 0.05$ vs. sham. Error bars indicate SEM. (D) Representative image of a cluster of Sox2+/BrdU+ cells in a stroke-only (untreated) subject at 5 days post-stroke, indicating proliferation of stem

cells and/or intermediate progenitor cells. Nuclei are visualized in merged image with DAPI counterstain. Scale bar: 10 μm. DG: Dentate gyrus.

	Days post-stroke			
Group	**5 dpi**	**10 dpi**	**14 dpi**	**21 dpi**
Sham	N/A	N/A	N/A	3.00 ± 0.19 (4)
Stroke-only (ipsi. DG)	10.91 ± 0.41 (4)	2.21 ± 0.27 (3)	1.04 ± 0.05 (2)	2.48 ± 0.38 (6)
Stroke-only (contra. DG)	5.76 ± 1.50 (4)	2.23 ± 0.17 (3)	1.75 ± 0.25 (2)	2.86 ± 0.34 (6)
Stroke/ Control Ab (ipsi. DG)	N/A	4.27 ± 0.84 (3)	2.12 ± 0.39 (3)	4.13 ± 0.54 (6)
Stroke/ Control Ab (contra. DG)	N/A	6.23 ± 2.87 (3)	1.81 ± 0.35 (3)	3.26 ± 0.38 (6)
Stroke/ Anti-Nogo-A Ab (ipsi. DG)	N/A	2.261 ± 0.480 (4)	1.25 ± 0.18 (4)	4.39 ± 0.69 (7)
Stroke/ Anti-Nogo-A Ab (contra. DG)	N/A	2.269 ± 0.183 (4)	1.43 ± 0.33 (4)	3.05 ± 0.56 (7)

Table 6.1 ▲ Cellular proliferation (cells/mm ± SEM) at each time point assessed (dpi: days post-injury). Sample sizes are in parentheses.

Both control and anti-Nogo-A antibody treatment stimulate the accumulation of new microglia/macrophages, but not new neurons, in the dentate granule cell layer (GCL)

To analyze the phenotypes of newborn cells, rats were administered multiple injections of BrdU beginning 7 days after stroke and euthanized 7 weeks thereafter (Fig 6.5). Stroke itself led to a significant increase in the total number of BrdU-positive cells (ie, cells that had proliferated between days 7 and 11 post-stroke and survived approximately 6-7 weeks thereafter) in the ipsilesional (7716 ± 446 cells/mm^3) compared

to contralesional (4582 ± 431 cells/mm^3) GCL. In both control antibody and anti-Nogo-A treatment groups, more BrdU+ cells were found in the GCL compared to the stroke-only group, but were also more generally distributed throughout the DG. However, the proportion of BrdU+ cells co-labeled for NeuN (ie., new neurons) in the GCL was lower in antibody-treated groups, such that the total numbers of newborn neurons, specifically, was not statistically different among groups.

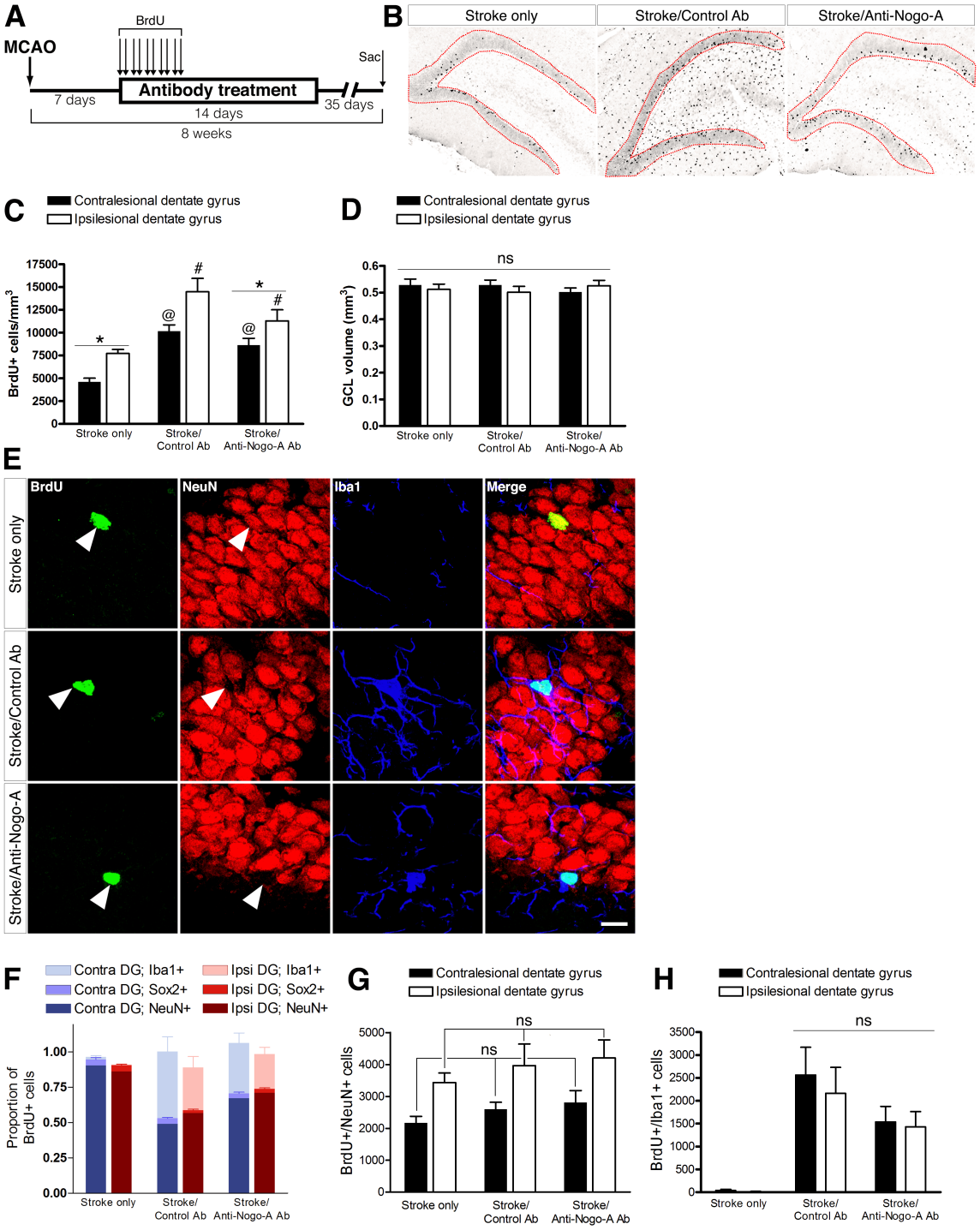
A
MCAO
BrdU
Sac
7 days
Antibody treatment
35 days
14 days
8 weeks
B
Stroke only
Stroke/Control Ab
Stroke/Anti-Nogo-A
C
Contralesional dentate gyrus
Ipsilesional dentate gyrus
BrdU+ cells/mm3
Stroke only
Stroke/ Control Ab
Stroke/ Anti-Nogo-A Ab
D
Contralesional dentate gyrus
Ipsilesional dentate gyrus
ns
GCL volume (mm3)
Stroke only
Stroke/ Control Ab
Stroke/ Anti-Nogo-A Ab
E
BrdU
NeuN
Iba1
Merge
Stroke only
Stroke/Control Ab
Stroke/Anti-Nogo-A
F
Contra DG; Iba1+
Contra DG; Sox2+
Contra DG; NeuN+
Ipsi DG; Iba1+
Ipsi DG; Sox2+
Ipsi DG; NeuN+
Proportion of BrdU+ cells
Stroke only
Stroke/ Control Ab
Stroke/ Anti-Nogo-A Ab
G
Contralesional dentate gyrus
Ipsilesional dentate gyrus
ns
ns
BrdU+/NeuN+ cells
Stroke only
Stroke/ Control Ab
Stroke/ Anti-Nogo-A Ab
H
Contralesional dentate gyrus
Ipsilesional dentate gyrus
ns
BrdU+/Iba1+ cells
Stroke only
Stroke/ Control Ab
Stroke/ Anti-Nogo-A Ab

Fig 6.5 ▲ Both anti-Nogo-A and control antibody treatment induce long-lasting accumulation of new microglia/macrophages without altering neurogenesis. (A) Overview of BrdU injection strategy to measure differentiation and survival of proliferating cells. (B) Representative images of BrdU immunoreactivity in the ipsilesional dentate gyrus at 8 weeks post-stroke. The GCL, in which cells were counted, is outlined in red. Widespread newborn cells are evident in both control and anti-Nogo-A antibody groups. (C) Total BrdU+ nuclei in the contralesional (black bars) and ipsilesional (white bars) GCLs. * $p < 0.05$, ipsilesional vs contralesional DG (within treatment group); @ $p < 0.05$, vs stroke-only contralesional DG; # $p < 0.05$, vs stroke-only ipsilesional DG. (D) The volume of the GCL in which BrdU+ nuclei were counted (in panel 'C') was not significantly different among groups. (E) Representative image of newborn neurons (BrdU+/NeuN+) and microglia/macrophages (BrdU+/Iba1+) in the GCL. Scale bar: 10 μm. (F) Proportions of newborn cells of each phenotype (neuron [NeuN+], microglia/macrophage [Iba1+], neural stem/progenitor cell or astrocyte [Sox2+]). (G) Total number of new neurons in the GCL. (H) Total number of new microglia/macrophages in the GCL. All error bars indicate SEM.

Group	Ipsilesional DG	Contralesional DG
Stroke-only (8)	7715 ± 446	4582 ± 431
Stroke/Control Ab (5)	14467 ± 1479	10137 ± 716
Stroke/Anti-Nogo-A Ab (8)	11383 ± 1197	8473 ± 726

Table 6.2a ▲ BrdU+ cell density (cells/mm^2) in the dentate gyrus at 8 weeks post-stroke, ± SEM. Sample sizes are in parentheses.

Group	NeuN+	Iba1+	Sox2+
Stroke-only (8)	0.860 ± 0.032	0.0025 ± 0.0025	0.0459 ± 0.0078
Stroke/Control Ab (5)	0.567 ± 0.099	0.304 ± 0.077	0.0198 ± 0.0088
Stroke/Anti-Nogo-A Ab (8)	0.709 ± 0.051	0.246 ± 0.049	0.0276 ± 0.0083

Table 6.2b ▲ Newborn cell phenotype proportions in the ipsilesional DG (± SEM). Sample sizes are in parentheses.

Group	NeuN+	Iba1+	Sox2+
Stroke-only (8)	0.903 ± 0.019	0.018 ± 0.010	0.0418 ± 0.0142
Stroke/Control Ab (5)	0.490 ± 0.040	0.474 ± 0.104	0.0402 ± 0.0065
Stroke/Anti-Nogo-A Ab (8)	0.671 ± 0.074	0.356 ± 0.072	0.0346 ± 0.0097

Table 6.2c ▲ Newborn cell phenotype proportions in the contralesional DG (± SEM). Sample sizes are in parentheses.

Group	Ipsilesional DG	Contralesional DG
Stroke-only (8)	3430 ± 299	2167 ± 207
Stroke/Control Ab (5)	3962 ± 678	2597 ± 217
Stroke/Anti-Nogo-A Ab (8)	4202 ± 569	2802 ± 378

Table 6.2d ▲ Total new neuron numbers ± SEM. Sample sizes are in parentheses.

Group	Ipsilesional DG	Contralesional DG
Stroke-only (8)	10 ± 10	40 ± 22
Stroke/Control Ab (5)	2162 ± 567	2562 ± 608
Stroke/Anti-Nogo-A Ab (8)	1430 ± 334	1535 ± 342

Table 6.2e ▲ Total new microglia/macrophages ± SEM. Sample sizes are in parentheses.

Group	Ipsilesional DG	Contralesional DG
Stroke-only (8)	170 ± 22	94 ± 32
Stroke/Control Ab (5)	141 ± 66	226 ± 55
Stroke/Anti-Nogo-A Ab (8)	151 ± 42	143 ± 45

Table 6.2f ▲ Total new Sox2+ cells ± SEM. Sample sizes are in parentheses.

DISCUSSION

Anti-Nogo-A immunotherapy improves spatial memory after stroke in aged rats, but a cellular mechanism of efficacy has not been identified (Gillani et al., 2010). This study was conducted to determine whether Nogo-A neutralization enhances post-stroke neurogenesis in the dentate gyrus.

We first performed multiple-label immunofluorecent staining to determine whether Nogo-A is expressed by neural precursor cells in the adult DG, thereby identifying possible direct treatment targets. Nogo-A was found to be expressed by doublecortin (DCX)-positive immature neurons, but not stem cells or mature dentate granule cells. To our knowledge, this is the first report of Nogo-A expression in immature neurons of the adult dentate gyrus. This transient expression suggests a stage-specific role of Nogo-A expression in adult hippocampal neuronal development, similar to what has been reported in the adult subventricular zone (Rolando et al., 2012) and during embryonic and early postnatal development (Aloy et al., 2007; Huber et al., 2002; Mathis et al., 2010; Mingorance-Le Meur et al., 2007; Schwab, 2010). Notably, per many of these reports, Nogo-A is expressed by migratory neurons. While we do not directly address the normal physiological role of cell surface and/or intracellular Nogo-A in DG neurogenesis here, we may infer from these previous studies that Nogo-A could play a role in migration of neuronal precursors in the adult DG (Deng et al., 2010; Sun et al., 2015) or in the morphogenesis of new DG neurons (Kurowska et al., 2014; Petrinovic et al., 2013a).

Examining treatment antibody distribution, we showed that intracerebroventricularly infused antibody entered the hippocampal parenchyma, but was undetectable by immunofluorescence five weeks after cessation of treatment. Therefore, direct exposure of target tissue to infused antibody is transient. As we did not analyze antibody distribution at earlier time points after treatment cessation, we cannot conclude that complete antibody clearance requires the full five weeks. However, our findings are in line with a previous report noting a reduction in anti-Nogo-A antibody in the brain parenchyma just one week after the end of treatment (Marklund et al., 2007). These results raise the possibility that rapid clearance of the antibody from the brain may limit the full potential of anti-Nogo-A antibodies to promote functional recovery, and that a longer treatment duration may be further clinically beneficial.

After inducing a large cortical stroke, we measured the number of proliferating cells after various time points with or without antibody treatment. We found that the number of proliferating cells was elevated above sham level at only the earliest time point we analyzed, 5 days post-stroke. This early, transient increase in cellular proliferation after focal ischemia is similar to data reported previously by other groups (Matsumori et al., 2006; Takasawa et al., 2002). However, anti-Nogo-A treatment did not significantly alter the number of proliferating cells in the subgranular zone (SGZ) and basal granule cell layer (GCL) at any time point. The mechanisms responsible for stimulating proliferation after cortical injury are not well understood. One study found that spreading depression, which can be triggered by stroke, was sufficient to increase proliferation and neurogenesis in the

SGZ (Röther et al., 1996; Urbach et al., 2008). Notably, in our hands the proliferative responses of the SGZ and SVZ to dMCAO were different: whereas stroke induced an early, transient, ~3 fold increase in cell proliferation in the SGZ, no such effect was found in the SVZ (see Chapter 5).

We then investigated the types of cells that were produced after stroke and survived long-term. We found that the proportion of long-lived newborn cells that were positive for NeuN (ie., new neurons) was approximately 86-90% in the stroke-only group, similar to findings in a previous report (Kluska et al., 2005). Given the increase in total BrdU+ cells in the ipsilesional GCL, this indicates a significant increase in the number of new neurons in the ipsilesional versus contralesional DG. This result is consistent with reports of increased hippocampal neurogenesis in numerous animal models of stroke, including transient global ischemia (Kee et al., 2001; Liu et al., 1998), transient middle cerebral artery occlusion (Jin et al., 2001; Zhu et al., 2003; 2004), photothrombotic cortical stroke (Kluska et al., 2005), and distal middle cerebral artery occlusion (Matsumori et al., 2006). In contrast, only a small number of BrdU+ cells at 8 weeks post-stroke were Sox2-positive. Sox2 is expressed by both astrocytes and neural stem cells in the adult rat brain (Komitova and Eriksson, 2004). However, the fact that we found so few Sox2+ cells at 8 weeks post-stroke, after finding that the majority of proliferating cells at 5 days post-stroke were Sox2-positive, suggests that 1) post-stroke astrogliosis in the GCL was minimal, 2) normally self-renewing Sox2+ stem cells did not self-renew, and/or 3) this population of proliferative cells had progressed past a self-renewal stage at the time of BrdU

incorporation. This could be reconciled if non-renewing progenitors, rather than self-renewing neural stem cells, are the predominant proliferative cell type after stroke.

Both control antibody- and anti-Nogo-A-treated groups exhibited robust accumulation of new Iba1-positive microglia/macrophages in the GCL. In contrast, newborn microglia/macrophages were found very rarely in the GCL of stroke-only subjects. Several potential mechanisms behind the observed accumulation of new microglia/macrophages may be considered. First, the absence of differences in lesion size between treated and untreated groups argues against a direct effect of the lesion itself. Cannulae for antibody delivery are implanted in the lateral cerebral ventricle, and may in rare cases puncture the hippocampal fimbria. However, the fact that BrdU+ cells were generally elevated bilaterally and more uniformly distributed, rather than clustered around a cannula track, makes it unlikely that the observed response was a reaction to mechanical injury. Infusion of mouse antibody into the rat CNS could potentially induce a microglial/macrophage response through either recognition of the antibody as a foreign protein, or binding and activation of microglia/macrophage-expressed Fc receptors. Antibody immunogenicity in human patients should be reduced by the use of human antibodies (Nelson et al., 2010), which are currently in use in anti-Nogo-A clinical trials for spinal cord injury and have so far shown an encouraging safety profile (Zörner and Schwab, 2010). While to our knowledge direct demonstration of rat FcR-mouse IgG binding has not been demonstrated, cross-species FcR binding has been reported between

more phylogenetically distant species (Lubeck et al., 1985), and FcR cross linking has been shown to stimulate macrophage proliferation (Luo et al., 2010).

The mechanism responsible for improved spatial memory after stroke and anti-Nogo-A treatment is not yet fully understood. While our previous work did not find an effect of anti-Nogo-A treatment on dendritic complexity in CA1, CA3, or DG GCL neurons, a subsequent study noted dendritic alterations in these subfields after acute treatment of hippocampal slice cultures with anti-Nogo-A antibody (Zagrebelsky et al., 2010). These changes were evident after just 4 days of antibody treatment, a much shorter time course than in our previous study, in which histological analysis was performed 10 weeks after the end of treatment. Therefore, it is possible that *in vivo* anti-Nogo-A antibody treatment after stroke leads to rapid changes in dendritic growth that may be pruned back over time.

Intriguingly, several studies have shown that Nogo-A and its receptors NgR1 and S1PR2 can regulate cognitive function and synaptic plasticity. Transgenic Nogo-A knockdown rats exhibit subtle spatial memory deficits in certain tasks (Petrasek et al., 2014a; 2014b), while mice overexpressing NgR1 show impaired spatial memory performance in the Morris water maze (Karlsson et al., 2016), suggesting that the proper balance of Nogo-A signaling, including during development, is necessary for optimal cognitive function. These effects may also depend on whether Nogo-A signaling perturbation is chronic (as in the case of Nogo-A- or NgR1-transgenic animals), or acute (after neutralizing antibody or blocking peptide treatment). For example, CA3-CA1 LTP

was unaffected by null mutation of NgR1 (in the absence of FGF2) (Lee et al., 2008), whereas acute application of an NgR1 blocking antibody enhanced LTP (Delekate et al., 2011). However, both Nogo-A knockdown rats (Tews et al., 2013) and acute hippocampal slices treated with anti-Nogo-A antibodies (Delekate et al., 2011; Kellner et al., 2016) exhibited enhanced CA3-CA1 LTP, suggesting different roles of the ligand (Nogo-A) and receptor (NgR1) in the proper development and function of hippocampal circuitry. Given these findings, it is possible that Nogo-A neutralization improves spatial memory after stroke through a mechanism involving enhanced synaptic plasticity.

Lastly, it is possible that other properties related to newborn neuron function that we did not examine, including connectivity, synaptogenesis, or morphogenesis, rather than the total number of newborn neurons, may be altered by Nogo-A neutralization. The Nogo receptor NgR1 negatively regulates synaptogenesis and dendritic complexity during hippocampal development (Wills et al., 2012), raising the possibility of a similar role in adult hippocampal neurogenesis. Future studies examining these changes in adult-born neurons after anti-Nogo-A treatment may be enlightening.

In conclusion, our results suggest that hippocampal neurogenesis does not contribute substantially to anti-Nogo-A therapy-mediated spatial memory recovery after stroke, and indicate that other mechanisms are likely to underlie this recovery. These results add to our understanding of the scope and limitations of anti-Nogo-A immunotherapy, which are vitally important as anti-Nogo-A antibodies continue to be used in human clinical trials.

CHAPTER SEVEN

GENERAL DISCUSSION

SUMMARY AND DISCUSSION OF RESULTS

These results show that infusion of anti-Nogo-A neutralizing antibodies does not appreciably alter the neurogenic response to ischemic stroke. Therefore, the contribution of neurogenesis to recovery after stroke and anti-Nogo-A treatment is likely minimal. However, these studies provided new insights into the functions of Nogo-A within the adult brain's major neurogenic niches.

We first defined the expression pattern of Nogo-A and its receptors in the subventricular zone (SVZ) and dentate gyrus (DG). Common to both areas was strong expression of Nogo-A in doublecortin (DCX)-positive immature neurons. S1PR2 immunoreactivity could be found in DCX-positive cells as well. In contrast, clear evidence of NgR1 expression in the SVZ was not found by immunofluorescence. In migrating neuroblasts, we noted that Nogo-A was particularly enriched throughout the leading process, an observation previously made in tangentially migrating embryonic neural precursors (Mingorance-Le Meur et al., 2007). This was more deeply examined in SVZ explant culture *in vitro*, where we showed that Nogo-A colocalizes with the endoplasmic

reticulum marker calnexin throughout the length of the leading process. Through live cell staining with two different anti-Nogo-A antibodies *in vitro*, we found that DCX+ SVZ-derived neuroblasts did not show appreciable surface staining.

These results suggest that neuroblast-associated Nogo-A plays a cell autonomous role, rather than signaling to neighboring cells. However, it does not mean that neuroblasts are not subject to Nogo-A signaling from exogenous sources. Indeed, we noted the presence of a myelin-rich zone immediately adjacent to the SVZ that appears well-situated to signal to the SVZ. In examining the motility of SVZ-derived neuroblasts *in vitro*, we found that exogenous Nogo-A-Δ20 peptide led to a reduction in maximum velocity, showing that while these cells do not express surface Nogo-A, they are still subject to its regulatory influences. Consistent with a lack of cell surface expression, anti-Nogo-A antibody treatment did not significantly alter any property of neuroblast motility that we investigated, including speed, pauses, and directional persistence.

After stroke, we treated adult rats with anti-Nogo-A antibodies using a treatment delay (7 days) that promoted functional recovery in our previous studies. This allowed us to correlate effects on neurogenesis with previously observed sensorimotor and cognitive recovery. However, we found that anti-Nogo-A treatment had no effect on the number of proliferating cells in the SVZ or DG at any time point assessed, or on neuroblast density in the SVZ (Chapter 5) or the number of new neurons produced in the granule cell layer of the DG (Chapter 6). Both anti-Nogo-A and control antibody treatment appeared to stimulate an immune response, leading to the accumulation of new microglia/macrophages

in the dentate gyrus. Unexpectedly, stroke itself potentiated cellular proliferation in the dentate gyrus, but not the subventricular zone. Therefore, it is unlikely that neurogenesis plays a major role in recovery of sensorimotor or cognitive function after stroke and anti-Nogo-A treatment.

In some respects, these results reflect favorably on the applicability of anti-Nogo-A treatment to human stroke patients with sensorimotor and/or cognitive deficits. Subventricular zone neurogenesis is comparatively much less robust in humans than in rodents, and the ultimate fate of proliferating cells in the human SVZ is unclear. Furthermore, neurogenesis declines sharply with age even in rodents, and most strokes occur in the aged population (Heine et al., 2004; Jin et al., 2003; Knoth et al., 2010; Mozaffarian et al., 2016). That anti-Nogo-A treatment does not rely on neurogenesis to promote recovery suggests that this process would not need to be targeted to improve recovery in humans. Still, as anti-Nogo-A antibody has been in clinical trials for spinal cord injury (Zörner and Schwab, 2010) and a trial for stroke is in the planning phases, it is critical to understand the full scope of anti-Nogo-A on the brain. This includes whether it stimulates any of the various components of neurogenesis, including proliferation, migration, and neuronal survival.

FUTURE DIRECTIONS

The basic biology of Nogo-A in adult neurogenesis deserves further exploration. Neurogenesis is not just a target for repair after brain injury, but has been implicated in other conditions such as cancer, epilepsy, and depression. Revealing the role of Nogo-A in

neurogenesis could provide novel insights into these diseases. Specifically, the significance of stage-specific Nogo-A expression in adult-born neurons is unknown. As surface expression of Nogo-A, at least in the SVZ, is minimal, this may be best investigated using genetic methods. Conditional knockout mice, in which Nogo-A is knocked out specifically in adult neural stem cells, followed by migration, morphogenesis, and behavioral assays, would go a long way in answering this question.

We noted a stark difference in the recruitment of DCX+ neuroblasts to the perilesional cortex versus ischemic striatum (Fig 5.6). This discrepancy calls for further investigation. Is it simply a matter of distance from the lesion to the SVZ? While this is a possibility, large cortical lesions can be directly dorsal to the SVZ. In these cases, only the corpus callosum separates the SVZ from the lesion cavity. Do chemotactic factors diffuse adequately to the SVZ? Is the corpus callosum a permissive substrate for migration from the SVZ to the cortex? After stroke, only a small fraction of the total number of SVZ neuroblasts appears to be diverted and move into the corpus callosum and external capsule toward the cortical lesion. Notably, the few neuroblasts that do migrate in to the corpus callosum appear to mainly align with the direction of the fibers in this area (ie, medio-laterally), while direct migration to the cortex would require dorsal migration (Fig 7.1). In contrast, neuroblasts migrating toward the ischemic striatum appear to take a more direct route. Does the corpus callosum contain repulsive or migration-inhibitory factors, or prevent adequate adhesion? This scenario draws parallels with myelin-associated inhibitors of axon outgrowth. Lastly, neuroblasts migrate along blood vessels in both the healthy

brain (during radial migration in the olfactory bulb) and in the injured brain, (toward the ischemic striatum) (Bovetti et al., 2007; Thored et al., 2007; Yamashita et al., 2006). Is the orientation of the vasculature in the corpus callosum conducive to direct radial migration from the SVZ toward the cortex?

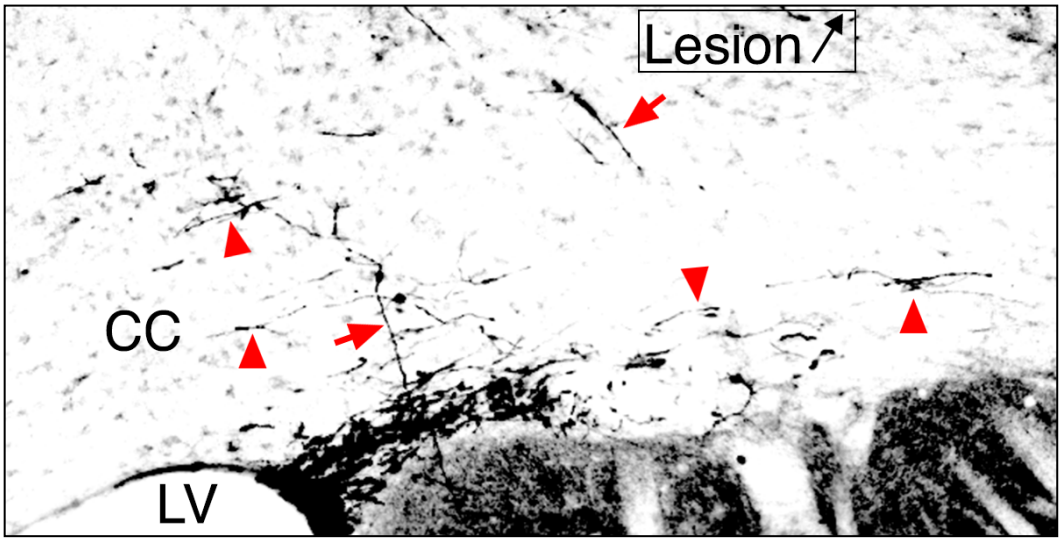

Figure 7.1 ▲ Doublecortin-positive cells in the corpus callosum (CC) after stroke. Most DCX+ neuroblasts align with the fibers coursing through the CC (red arrowheads), with some exceptions (red arrows).

In the adult brain's main neurogenic niches, newborn neurons are able to extend axons and dendrites apparently unimpeded. Why these cells are uniquely able to circumvent the same growth constraints as developmentally born CNS neurons is unknown, and is deserving of further research. Furthermore, robust axon growth from transplanted neural stem cells into adult CNS white matter *in vivo* has been reported (Lu et al., 2012; 2014). In fact, one study remarked that "initial axon outgrowth preferentially

occurred through white matter" of the spinal cord (Lu et al., 2012). This suggests that these new neural stem cell-derived neurons respond differently to the adult CNS. Myelin-associated glycoprotein (MAG) *promotes* axon outgrowth from young neurons (less than P3-4), but *inhibits* axon outgrowth from older neurons. A reduction in cAMP in older neurons is thought to underlie this switch. (Cai et al., 2001; Mukhopadhyay et al., 1994). Could myelin-associated "inhibitors" such as MAG or Nogo-A also promote the growth of adult-born CNS neurons in a cAMP-dependent manner? Additional open questions include whether, at the neurite outgrowth phase, adult-born neurons express receptors for myelin-associated inhibitors, and if so, whether these receptors couple to the same signaling pathways (ie., RhoA, ROCK) that restrict axon outgrowth in adult neurons. Understanding how immature neurons grow so well in the adult CNS could open up new avenues for neural repair.

Lastly, hundreds of studies have been published regarding injury-induced neurogenesis. However, widely variable methodology and reporting have made it difficult to make unified statements about the exact nature of the neurogenic response to different injuries. For example, "proliferation" may be measured in one study (such as this dissertation) through a single BrdU injection 2 hours before sacrifice, while another study uses multiple injections over the course of days, at which point other influences such as survival and migration begin to creep in. The current gold standard for ectopic, injury-induced neurogenesis is co-labelling of BrdU with a mature neuron marker, eg NeuN. This strategy requires that 1) a neural progenitor proliferates, and that 2) this proliferation

is captured in the window in which BrdU is administered. However, proliferation is not necessary for the generation of a new neuron. For example, a recent report (albeit, one in need of independent confirmation) reported that astrocytes could transdifferentiate into neurons after striatal ischemia (Duan et al., 2015). In this case, proliferation is not a prerequisite for neurogenesis. New methods to globally detect the appearance of new neurons that do not rely on BrdU incorporation, combined with whole-brain imaging (eg., CLARITY (Chung et al., 2013)) would be both higher throughput and more comprehensive than current techniques and provide a powerful, more accurate picture of injury-induced neurogenesis.

APPENDIX A: PILOT STUDY ON TREATMENT ANTIBODY DISTRIBUTION

INTRODUCTION

Anti-Nogo-A antibody treatment promotes functional recovery after stroke when delivered by osmotic pump via the intracerebroventricular (ICV) (Markus et al., 2005) or intrathecal (Lindau et al., 2014; Tsai et al., 2007) routes. While effective, these routes are less desirable for human patients, as they involve surgery and its potential complications. Therefore, a less invasive but still effective route would be ideal for use in the clinic.

Presumably, anti-Nogo-A antibody would not need to be distributed equally throughout the entire CNS to be effective. If this treatment works by disinhibiting plasticity at the level of a sprouting grown cone, localized antibody application should be effective. Anti-Nogo-induced axon sprouting occurs preferentially into areas that are deafferented or otherwise injured, such as the dorsolateral striatum, pons, and red nucleus (Kartje et al., 1999; Papadopoulos et al., 2002; Wenk et al., 1999). Sprouting into the deafferented thalamus has not been reported after stroke and anti-Nogo-A treatment, although it has been reported after neonatal lesions, whose neuroplastic response tends to mimic what is seen in anti-Nogo-A-treated adults (Yu et al., 1995). These deafferented areas undergo an inflammatory response, which can lead to blood brain barrier dysfunction (da Fonseca et al., 2014). Drugs infused into the cerebrospinal fluid are rapidly cleared into the bloodstream (Pardridge, 2011), and direct diffusion of antibodies through the tortuous interstitial spaces of the brain parenchyma is slow and inefficient (Wolak et al., 2015). These points raise the question of whether anti-Nogo-A antibody may reach its sites of

action through the bloodstream, and therefore if intravenous administration may be a less invasive but still effective route.

In this pilot study, we explored the relationship between BBB permeability and treatment antibody diffusion to determine whether intravenous antibody treatment could be efficacious. We found evidence of intracerebroventricularly infused antibody in the plasma, and qualitatively, treatment antibody accumulation appeared to correlate with sites of inflammation and BBB permeability after stroke. Furthermore, clearance of infused treatment antibodies from the brain appeared to be essentially complete 5 weeks after treatment cessation.

EXPERIMENTAL DESIGN

Assessment of treatment antibody distribution

Tissue sections were incubated in biotinylated anti-mouse antibodies that had been adsorbed against rat serum proteins, and processed for peroxidase-nickel DAB detection with an ABC kit as previously described. Tissue sections were then scanned at high resolution on a flatbed scanner and imported into Adobe Photoshop CS6. Control tissue sections from untreated rats were also processed in parallel and all contrast adjustments applied equally to all tissue.

Plasma collection and dot blot

At sacrifice, blood was withdrawn from the right atrium and stored on ice in EDTA tubes, then spun down. Plasma was transferred to different tubes and stored at minus 80° C until analysis. For dot blotting, a PVDF membrane was wet in methanol,

then dH2O and TBS. The membrane was placed on a piece of filter paper dampened with TBS, and 2 uL of undiluted plasma samples were spotted (from 2 different untreated rats, and 3 different rats each from control antibody- and 11C7-treated rats, all after 7 days of treatment). The membrane was allowed to dry and then re-wet for 20 min with methanol containing 3% H_2O_2 to inactivate peroxidases within the samples. The membrane was then blocked in 2% non-fat milk in TBS/0.05% Tween 20 for 90 min, then blocked in Vector Avidin/Biotin block (2 drops avidin in 10 mL TBS for 15 min, rinsed in TBS, then 2 drops biotin in 10 mL TBS for 15 min, then rinsed.) The membrane was then incubated in biotinylated donkey anti mouse (rat adsorbed), 1:5000 in TBS/Tween, for 90 min, washed, and incubated in Vector ABC (1 drop each in 10 mL TBS/Tween) for 90 min. After washing in TBS, the membrane was incubated in Pico ECL, and developed on film for 60 sec.

Qualitative assessment of blood-brain barrer (BBB) permeability

BBB permeability was defined by the extravasation of rat immunoglobulins into the brain parenchyma (Saunders et al., 2015). Tissue from sham surgery and stroke-only subjects from various time points was subject to inactivation of endogenous peroxidases by incubation in 3% H_2O_2, washed, and then incubated in a biotinylated anti-rat IgG antibody. After washing, the tissue was incubated in avidin-biotin-peroxidase complex (ABC) and then reacted in nickel-enhanced DAB. Tissue sections were then scanned at high resolution and imported into ImageJ. To better visualize the distibution of reaction

product, a lookup table was applied to the image, essentially generating a heat map indicating stronger or weaker staining.

RESULTS

Treatment antibody, infused into the ipsilateral cerebral ventricle, could be found in the brain parenchyma by immunohistochemistry as early as 3 days after the start of treatment (the earliest time point we examined) (Fig A.1). Staining tended to be stronger on the ipsilateral side, especially in the septum, striatum, hippocampus, thalamus, and cortex adjacent to the lesion. Five weeks after the end of treatment, the antibody appeared to have been substantially cleared from the brain parenchyma.

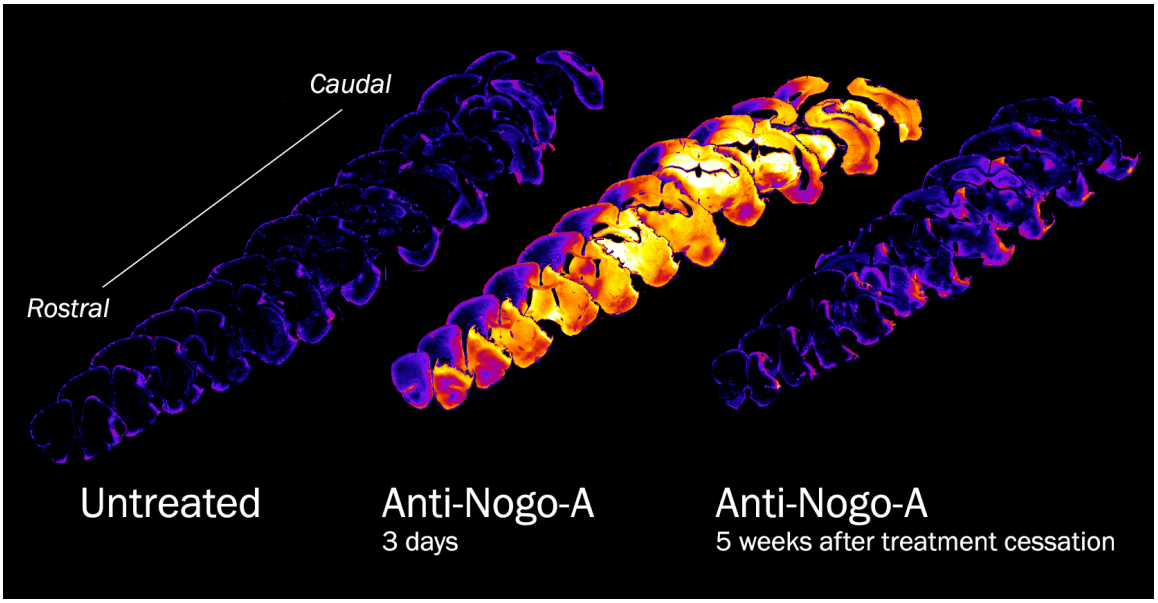

Figure A.1 ▲ Immunostaining for mouse IgG in an untreated (left), 3 day anti-Nogo-A treated (middle), and 5 weeks post-anti-Nogo-A treatment cessation (right) brain.

Blood samples were collected from rats upon euthanasia and dot blotted for evidence of mouse IgG in the plasma. As expected, plasma from untreated rats did not react with an anti-mouse IgG antibody (Fig A.2, top). However, strong signals were observed in the plasma from both control and anti-Nogo-A-treated rats, suggesting the presence of treatment antibody in the blood (Fig A.2, middle and bottom).

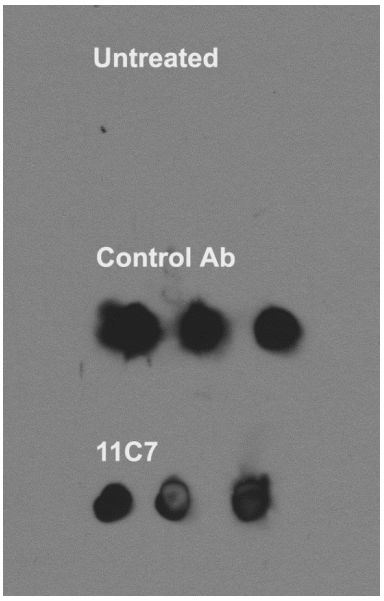

Figure A.2 ▲ Dot blot of mouse IgG in rat plasma after 7 days of intracerebroventricular treatment. No reactivity was visible in untreated rat plasma (n=2), whereas clear reactivity is seen in both control (n=3) and anti-Nogo-A antibody- (n=3) treated rats.

We examined inflammation by staining for ED1, a lysosomal protein expressed by activated microglia and macrophages. Abundant ED1 immunoreactivity was observed in areas of axonal degeneration including the dorsolateral striatum and thalamus, even at 8 weeks post-stroke (Fig A.3).

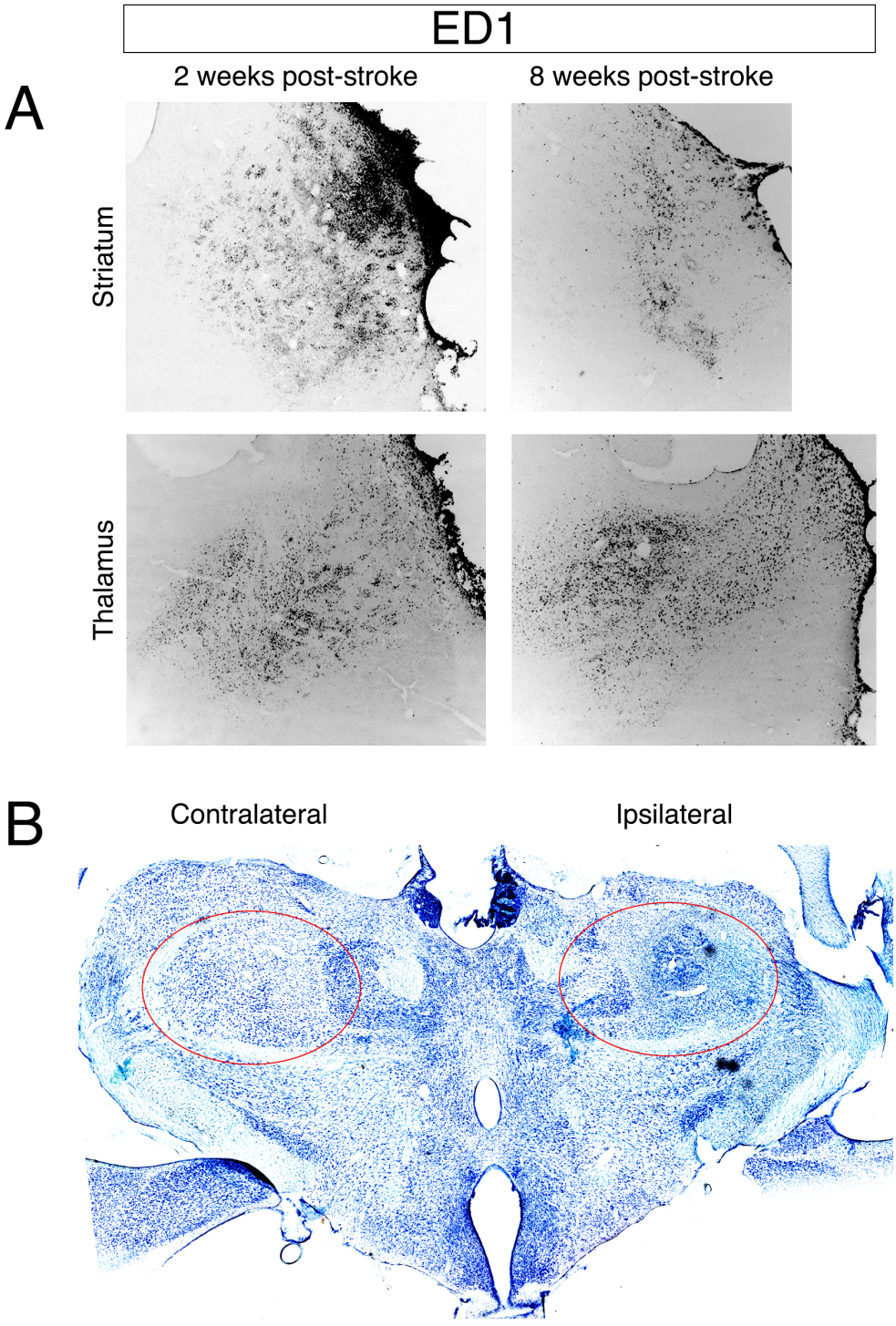

Figure A.3 ▲ Inflammation in the striatum and thalamus after cortical stroke. (A) Low magnification images of ED1 immunoreactivity in the ipsilesional striatum (top) and

thalamus (bottom) at 2 weeks (left) and 8 weeks (right) post-stroke. (B) Low magnification image of the thalamus (Nissl stain) at 8 weeks post stroke demonstrating cellular infiltration and disorganization in the ipsilateral versus contralateral VPL/VPM (red ovals).

Lastly, we examined the collection of rat IgG in the brain parenchyma by immunohistochemistry to identify sites of blood brain barrier (BBB) permeability. Rat IgG was seen in known areas of BBB permeability, including the hypothalamus, median eminence, and septum. Additionally, evidence of IgG extravasation was seen in sites with high levels of ED1 staining, including the perilesional cortex and ipsilesional dorsolateral striatum and thalamus (Fig A.4). These areas (septum, hypothalamus, striatum, thalamus, perilesional cortex) also appeared to show the strongest signals for the distribution of infused treatment antibody. Unexpectedly, the staining intensity of anti-Nogo-A antibodies was typically weaker in the white matter than in the surrounding gray matter.

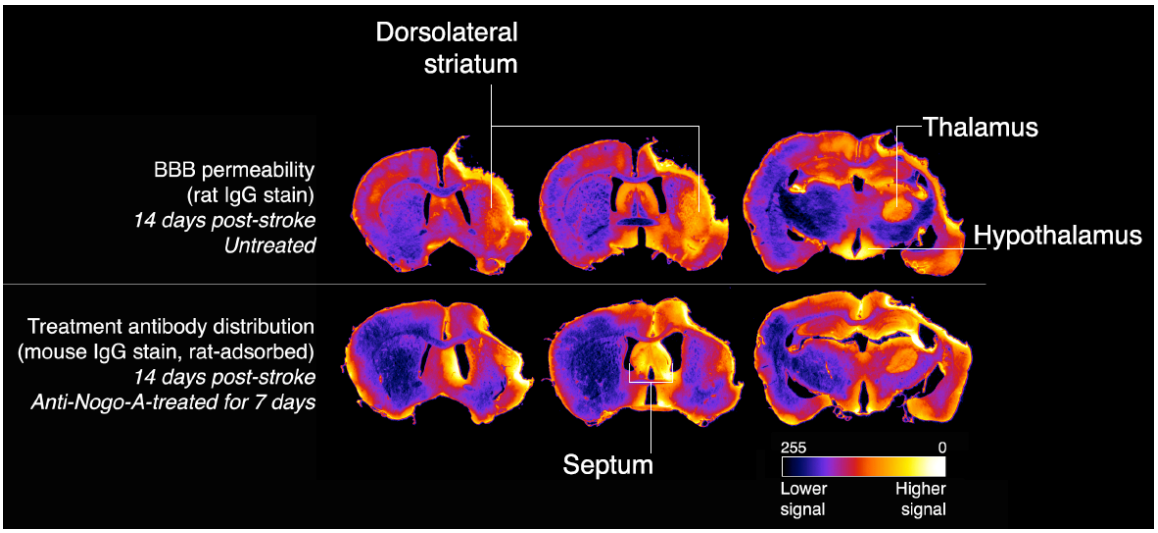

Figure A.4 ▲ Correlation between rat IgG extravasation (top) and treatment antibody localization (bottom) at 14 days post-stroke. DAB reaction product intensities have been converted to heat maps to better visualize the staining distribution.

DISCUSSION

The results of this study show that the localization of ICV-infused treatment antibody in the tissue parenchyma correlates with sites of inflammation and BBB breakdown.

As we infused the antibody into the ipsilesional ventricle, we cannot say whether stronger antibody penetration into the ipsilesional side is due to proximity of the infusion cannula or inflammation. If this same pattern of antibody distribution were found after *contralateral* ICV or intrathecal infusion, this would provide evidence for blood-to-brain spread.

Due to the rapid clearance of drugs from the cerebrospinal fluid (CSF) to the plasma, CSF injection has been compared to a "slow intravenous infusion" (Christy and

Fishman, 1961; Pardridge, 2011). Macromolecule diffusion from the CSF (which circulates around the ventricles and outer surfaces of the brain) to the extracellular fluid of the brain's tortuous interstitial spaces (typically the site of drug action) is limited (Kamali-Zare and Nicholson, 2013; Wolak and Thorne, 2013; Wolak et al., 2015). Furthermore, antibodies, once in the brain parenchyma, are rapidly effluxed to the blood through Fc-receptor mediated transport (Schlachetzki et al., 2002; Zhang and Pardridge, 2001). Therefore, it appears that direct infusion of anti-Nogo-A treatment antibody into the CSF is an inefficient means of delivery.

There are several implications of determining the exact route by which anti-Nogo-A antibody enters the brain and diffuses to its sites of action. First, this may suggest more clinically preferable routes of administration, such as intravenous (IV). Second, if ICV-delivered antibody does indeed reach its site of action via a circuitous route into the bloodstream and then back into the brain at sites of BBB permeability, this suggests that BBB permeability facilitates the beneficial effects of anti-Nogo-A antibody. This leads to the intriguing questions of whether BBB healing could limit the time frame in which anti-Nogo-A is effective, and if so, whether interventions to disrupt the BBB locally (such as focused ultrasound (Konofagou et al., 2012)) could help re-open a window for treatment efficacy in chronic stroke patients. Future studies should establish 1) whether antibody distribution patterns after ICV administration are different in the stroke-injured versus normal brain, 2) the brain distribution pattern of IV-infused antibody, and 3) whether IV treatment is effective in promoting functional recovery.

APPENDIX B:

R SCRIPTS FOR CELL TRACKING

The following R script was written by Ian Vaagenes, PhD. It is used to extract information about the motility of SVZ-derived neuroblasts that had been analyzed with the ImageJ plugin TrackMate and saved as .csv files.

```
library(ggplot2)
library(ggthemes)
library(dplyr)
library(reshape)
datm <- read.csv(file.choose())

###add columns for cumulative distance and frame by frame distance
uniq_neurons<-unique(datm$TRACK_ID)
datm$distance<-rep(NA,nrow(datm))
datm$cum_distance<-rep(NA,nrow(datm))
datm$velocity<-rep(NA,nrow(datm))

big_list<-list()
index<-0

for(i in uniq_neurons){
  #i = uniq_neurons[2]
  temp<-filter(datm, TRACK_ID == i)

  for(j in 2:nrow(temp)){
    temp$distance[j]<-sqrt(((temp$POSITION_X[j]-temp$POSITION_X[j-
1])^2)+((temp$POSITION_Y[j]-temp$POSITION_Y[j-1])^2))
    temp$velocity[j]<-sqrt(((temp$POSITION_X[j]-temp$POSITION_X[j-
1])^2)+((temp$POSITION_Y[j]-temp$POSITION_Y[j-1])^2))/300
  }
  index<-index+1
  temp$distance[is.na(temp$distance)] <- 0
  temp$cum_distance<-cumsum(temp$distance)

  big_list[[index]]<-temp
}

datm <- data.frame(do.call(rbind, big_list))
###########
###functions needed####
velocity_function <- function(test){
  indicator <- 0
  counter<-1
  df <- NULL
  for(i in 1:nrow(test)){
    #print(i)
    if(test$pause[i]==1){
      #print(i)
      indicator <- test$cum_distance[i]
    }else{
      #print(i)
      if(test$pause[i+1] == 1 | is.na(test$pause[i+1]) == T){
        #print(i)
        df<-c(df,((test$cum_distance[i]-indicator)/(counter*5)))
        counter<-1
      }else{
```

```
        counter <-1+counter
      }
    }
  }
  return(data.frame(df))
}
##distance during movement function
distance_function <- function(test){
  indicator <- 0
  counter<-1
  df <- NULL
  for(i in 1:nrow(test)){
    #print(i)
    if(test$pause[i]==1){
      #print(i)
      indicator <- test$cum_distance[i]
    }else{
      #print(i)
      if(test$pause[i+1] == 1 | is.na(test$pause[i+1]) == T){
        #print(test$value[i])
        df<-c(df,(test$cum_distance[i]-indicator))
        counter<-1
      }else{
        counter <-1+counter
      }
    }
  }
  return(data.frame(df))
}
##pause duration
pause_duration_function <- function(test){
  counter<-1
  df <- NULL
  for(i in 1:nrow(test)){
    #print(i)
    if(test$pause[i]==0){
      counter <- 1
    }else{
      #print(i)
      if(test$pause[i+1] == 0 | is.na(test$pause[i+1]) == T){
        #print(i)
        df<-c(df,counter)
        counter<-1
      }else{
        counter <-1+counter
      }
    }
  }
  return(data.frame(df))
}

##move duration
move_duration_function <- function(test){
  counter<-1
  df <- NULL
  for(i in 1:nrow(test)){
    #print(i)
    if(test$pause[i]==1){
      counter <- 1
```

```
      }else{
        #print(i)
        if(test$pause[i+1] == 1 | is.na(test$pause[i+1]) == T){
          #print(i)
          df<-c(df,counter)
          counter<-1
        }else{
          counter <-1+counter
        }
      }
    }
    return(data.frame(df))
  }

  run_diff <- function(x){
    diffs <- rep(NA, length(x))
    for(i in 2:length(x)){
      diffs[i]<-abs(x[i] - x[i-1])
    }
    return(as.data.frame(diffs))
  }
  #############
  #############
  #############
  #create pause function 0.4566
  pause <- function(x){
    ifelse(x >= 0.4566, 0, 1)}
  ############################
  ############
  ############
  ############

  datm1 <- datm
    diffs<-datm %>% group_by(TRACK_ID) %>% do(run_diff(.$cum_distance))

    datm$diffs <- diffs$diffs
    datm$pause <- pause(datm$diffs)
  datm2 <- datm
  #need to delete the first and last behavior(movement or pause) because
their lengths are censored

  #head(datm)
  #delete first and last behavior
  #get indices for end of beginning run and start of last run
  neurons<-unique(datm$TRACK_ID)
  biglist <- list()

  for(i in 1:length(neurons)){
    temp1 <- filter(datm, TRACK_ID == paste(neurons[i]))
    temp2<-rle(temp1$pause)
    start_index<-temp2$lengths[2] + temp2$lengths[1] + 1
    end_index<-length(temp1$pause) - temp2$lengths[length(temp2$lengths)]
    biglist[[i]]<-temp1[start_index:end_index,]
    }
  #use for duration
  datm <- data.frame(do.call(rbind, biglist))
  #need first pause for average velocity but discard last behavior
  biglist <- list()
```

```
      for(i in 1:length(neurons)){
        temp1 <- filter(datm2, TRACK_ID == paste(neurons[i]))
        temp2<-rle(temp1$pause)
        #start_index<-temp2$lengths[2] + temp2$lengths[1] + 1
        end_index<-length(temp1$pause) - temp2$lengths[length(temp2$lengths)]
        biglist[[i]]<-temp1[1:end_index,]
      }
      #use only for velocity
      datm_for_velocity <- data.frame(do.call(rbind, biglist))
      datm_for_velocity <-
datm_for_velocity[which(!is.na(datm_for_velocity$pause)),]
      #compute avg pause duration and total pause number
      runs_function <- function(){
        avg_pause_duration <- rep(NA, length(neurons))
        total_pause_number <- rep(NA, length(neurons))
        for(i in 1:length(neurons)){
          temp <- filter(datm, TRACK_ID == paste(neurons[i]))
          temp1<- rle(temp$pause)
          avg_pause_duration[i] <- mean(temp1$lengths[temp1$values==1], na.rm =
T)
          total_pause_number[i] <- length(temp1$lengths[temp1$values==1])
        }
        return(data.frame(avg_pause_duration, total_pause_number, neurons))
      }


      #get velocity


      velocity_by_move<-group_by(datm_for_velocity, TRACK_ID) %>%
do(velocity_function(.))
      #testing velocity funciton
      for(i in 1:length(neurons)){
        df<-filter(datm_for_velocity, TRACK_ID == neurons[i])
        print(neurons[i])
        print(velocity_function(df))
      }


      ###
      pause_durations<-group_by(datm, TRACK_ID) %>%
do(pause_duration_function(.))

      distance_by_move <- group_by(datm, TRACK_ID) %>% do(distance_function(.))

      movement_durations <- group_by(datm, TRACK_ID) %>%
do(move_duration_function(.))

      #create main dataframe
      avg_velocity <- group_by(velocity_by_move, TRACK_ID) %>%
        summarise(average_velocity = mean(df))
      names(avg_velocity)[1]<-"neurons"
      maindf<-runs_function()
      #maindf$treatment <- noquote(sapply(strsplit(logs[l], " "), "[[", 2))
      #maindf$explant_number = noquote(sapply(strsplit(logs[l], " "), "[[", 1))
      maindf<-inner_join(avg_velocity, maindf)
      avg_move_durations <- group_by(movement_durations, TRACK_ID) %>%
        summarise(average_move_duration = mean(df))
      names(avg_move_durations)[1]<-"neurons"
```

```
      maindf<-inner_join(maindf, avg_move_durations)

      ##function to get directional persistence
      group_by(datm1, TRACK_ID) %>%
        filter(row_number()==1 | row_number()==n()) %>%
        select(TRACK_ID, POSITION_X, POSITION_Y, cum_distance) %>%
        summarise(total.displacement = sqrt(diff(POSITION_X)^2 +
diff(POSITION_Y)^2), cumulative.distance.travelled = max(cum_distance)) %>%
        mutate(directional.persistence = total.displacement /
cumulative.distance.travelled) %>%
        select(neurons = TRACK_ID, directional.persistence) %>%
        inner_join(.,maindf) -> maindf


      ##to copy into excel, you could save as csv and import or just use the
following and paste

      write.csv(maindf, file="maindf.csv",row.names=FALSE,quote=FALSE)
      write.table(maindf, "clipboard", sep = "\t", row.names = F)
```

REFERENCES

Akahoshi, N., Ishizaki, Y., Yasuda, H., Murashima, Y. L., Shinba, T., Goto, K., et al. (2011). Frequent spontaneous seizures followed by spatial working memory/anxiety deficits in mice lacking sphingosine 1-phosphate receptor 2. *Epilepsy Behav* 22, 659–665. doi:10.1016/j.yebeh.2011.09.002.

Allen, E. (1912). The cessation of mitosis in the central nervous system of the albino rat. *J. Comp. Neurol.*

Aloy, E. M., Weinmann, O., Pot, C., Kasper, H., Dodd, D. A., Rülicke, T., et al. (2007). Synaptic destabilization by neuronal Nogo-A. *Brain Cell Bio* 35, 137–157. doi:10.1007/s11068-007-9014-3.

Altman, J. (1962). Are new neurons formed in the brains of adult mammals? *Science* 135, 1127–1128.

Altman, J. (1963). Autoradiographic investigation of cell proliferation in the brains of rats and cats. *Anat. Rec.* 145, 573–591.

Altman, J., and Das, G. D. (1965). Autoradiographic and histological evidence of postnatal hippocampal neurogenesis in rats. *J. Comp. Neurol.*

Arvidsson, A., Collin, T., Kirik, D., Kokaia, Z., and Lindvall, O. (2002). Neuronal replacement from endogenous precursors in the adult brain after stroke. *Nat Med* 8, 963–970. doi:10.1038/nm747.

Atwal, J. K., Pinkston-Gosse, J., Syken, J., Stawicki, S., Wu, Y., Shatz, C., et al. (2008). PirB is a functional receptor for myelin inhibitors of axonal regeneration. *Science* 322, 967–970. doi:10.1126/science.1161151.

Bacigaluppi, M., Comi, G., and Hermann, D. M. (2010). Animal models of ischemic stroke. Part two: modeling cerebral ischemia. *Open Neurol J* 4, 34–38. doi:10.2174/1874205X01004020034.

Bandtlow, C., Zachleder, T., and Schwab, M. E. (1990). Oligodendrocytes arrest neurite growth by contact inhibition. *J. Neurosci.* 10, 3837–3848.

Benner, E. J., Luciano, D., Jo, R., Abdi, K., Paez-Gonzalez, P., Sheng, H., et al. (2013). Protective astrogenesis from the SVZ niche after injury is controlled by Notch modulator Thbs4. *Nature* 497, 369–373. doi:10.1038/nature12069.

Bergmann, O., Spalding, K. L., and Frisén, J. (2015). Adult Neurogenesis in Humans. *Cold Spring Harbor Perspectives in Biology* 7, a018994. doi:10.1101/cshperspect.a018994.

Bovetti, S., Hsieh, Y.-C., Bovolin, P., Perroteau, I., Kazunori, T., and Puche, A. C. (2007). Blood vessels form a scaffold for neuroblast migration in the adult olfactory bulb. *Journal of Neuroscience* 27, 5976–5980. doi:10.1523/JNEUROSCI.0678-07.2007.

Bowers, M., and Jessberger, S. (2016). Linking adult hippocampal neurogenesis with human physiology and disease. *Dev. Dyn.* doi:10.1002/dvdy.24396.

Bregman, B. S., Kunkel-Bagden, E., Schnell, L., Dai, H. N., Gao, D., and Schwab, M. E. (1995). Recovery from spinal cord injury mediated by antibodies to neurite growth inhibitors. *Nature* 378, 498–501. doi:10.1038/378498a0.

Brenneman, M. M., Wagner, S. J., Cheatwood, J. L., Heldt, S. A., Corwin, J. V., Reep, R. L., et al. (2008). Nogo-A inhibition induces recovery from neglect in rats. *Behav. Brain Res.* 187, 262–272. doi:10.1016/j.bbr.2007.09.018.

Cadelli, D., and Schwab, M. E. (1991). Regeneration of Lesioned Septohippocampal Acetylcholinesterase-positive Axons is Improved by Antibodies Against the Myelin-associated Neurite Growth Inhibitors NI-35/250. *Eur. J. Neurosci.* 3, 825–832.

Cai, D., Qiu, J., Cao, Z., McAtee, M., Bregman, B. S., and Filbin, M. T. (2001). Neuronal cyclic AMP controls the developmental loss in ability of axons to regenerate. *Journal of Neuroscience* 21, 4731–4739.

Caltharp, S. A., Pira, C. U., Mishima, N., Youngdale, E. N., McNeill, D. S., Liwnicz, B. H., et al. (2007). NOGO-A induction and localization during chick brain development indicate a role disparate from neurite outgrowth inhibition. *BMC Dev. Biol.* 7, 32. doi:10.1186/1471-213X-7-32.

Cameron, H. A., and McKay, R. D. (2001). Adult neurogenesis produces a large pool of new granule cells in the dentate gyrus. *J. Comp. Neurol.* 435, 406–417.

Capilla-Gonzalez, V., Lavell, E., Quiñones-Hinojosa, A., and Guerrero-Cazares, H. (2015). Regulation of subventricular zone-derived cells migration in the adult brain. *Adv. Exp. Med. Biol.* 853, 1–21. doi:10.1007/978-3-319-16537-0_1.

Carmichael, S. T. (2005). Rodent models of focal stroke: size, mechanism, and purpose. *NeuroRx* 2, 396–409. doi:10.1602/neurorx.2.3.396.

Caroni, P., and Schwab, M. E. (1988a). Antibody against myelin-associated inhibitor of neurite growth neutralizes nonpermissive substrate properties of CNS white matter. *Neuron* 1, 85–96.

Caroni, P., and Schwab, M. E. (1988b). Two membrane protein fractions from rat central myelin with inhibitory properties for neurite growth and fibroblast spreading. *The Journal of Cell Biology* 106, 1281–1288.

Castro, A. J. (1975). Ipsilateral corticospinal projections after large lesions of the cerebral hemisphere in neonatal rats. *Exp. Neurol.* 46, 1–8.

Chen, M. S., Huber, A. B., van der Haar, M. E., Frank, M., Schnell, L., Spillmann, A. A., et al. (2000). Nogo-A is a myelin-associated neurite outgrowth inhibitor and an antigen for monoclonal antibody IN-1. *Nature* 403, 434–439. doi:10.1038/35000219.

Chen, S. T., Hsu, C. Y., Hogan, E. L., Maricq, H., and Balentine, J. D. (1986). A model of focal ischemic stroke in the rat: reproducible extensive cortical infarction. *Stroke* 17, 738–743.

Christian, K. M., Song, H., and Ming, G.-L. (2014). Functions and dysfunctions of adult hippocampal neurogenesis. *Annu. Rev. Neurosci.* 37, 243–262. doi:10.1146/annurev-neuro-071013-014134.

Christie, K. J., Turbic, A., and Turnley, A. M. (2013). Adult hippocampal neurogenesis, Rho kinase inhibition and enhancement of neuronal survival. *Neuroscience* 247, 75–83. doi:10.1016/j.neuroscience.2013.05.019.

CHRISTY, N. P., and FISHMAN, R. A. (1961). Studies of the blood-cerebrospinal fluid barrier to cortisol in the dog. *J. Clin. Invest.* 40, 1997–2006. doi:10.1172/JCI104426.

Chung, K., Wallace, J., Kim, S.-Y., Kalyanasundaram, S., Andalman, A. S., Davidson, T. J., et al. (2013). Structural and molecular interrogation of intact biological systems. *Nature* 497, 332–337. doi:10.1038/nature12107.

Clelland, C. D., Choi, M., Romberg, C., Clemenson, G. D., Fragniere, A., Tyers, P., et al. (2009). A functional role for adult hippocampal neurogenesis in spatial pattern separation. *Science* 325, 210–213. doi:10.1126/science.1173215.

Cramer, S. C. (2008). Repairing the human brain after stroke: I. Mechanisms of spontaneous recovery. *Ann Neurol.* 63, 272–287. doi:10.1002/ana.21393.

Craveiro, L. M., Weinmann, O., Roschitzki, B., Gonzenbach, R. R., Zörner, B., Montani, L., et al. (2013). Infusion of anti-Nogo-A antibodies in adult rats increases growth and synapse related proteins in the absence of behavioral alterations. 250C, 52–68. doi:10.1016/j.expneurol.2013.09.015.

Curtis, M. A., Kam, M., Nannmark, U., Anderson, M. F., Axell, M. Z., Wikkelso, C., et al. (2007a). Human neuroblasts migrate to the olfactory bulb via a lateral ventricular extension. *Science* 315, 1243–1249. doi:10.1126/science.1136281.

Curtis, M. A., Kam, M., Nannmark, U., Faull, R. L. M., and Eriksson, P. S. (2007b). Response to Comment on "Human Neuroblasts Migrate to the Olfactory Bulb via a Lateral Ventricular Extension." *Science* 318, 393c–393c. doi:10.1126/science.1145164.

D'Amelio, F., Eng, L. F., and Gibbs, M. A. (1990). Glutamine synthetase immunoreactivity is present in oligodendroglia of various regions of the central nervous system. *Glia* 3, 335–341. doi:10.1002/glia.440030504.

da Fonseca, A. C. C., Matias, D., Garcia, C., Amaral, R., Geraldo, L. H., Freitas, C., et al. (2014). The impact of microglial activation on blood-brain barrier in brain diseases. *Front Cell Neurosci* 8, 362. doi:10.3389/fncel.2014.00362.

David, S., and Aguayo, A. J. (1981). Axonal elongation into peripheral nervous system "bridges" after central nervous system injury in adult rats. *Science* 214, 931–933.

Delekate, A., Zagrebelsky, M., Kramer, S., Schwab, M. E., and Korte, M. (2011). NogoA restricts synaptic plasticity in the adult hippocampus on a fast time scale. *Proc. Natl. Acad. Sci. U.S.A.* 108, 2569–2574. doi:10.1073/pnas.1013322108/-/DCSupplemental.

Deng, W., Aimone, J. B., and Gage, F. H. (2010). New neurons and new memories: how does adult hippocampal neurogenesis affect learning and memory? *Nat Rev Neurosci* 11, 339–350. doi:10.1038/nrn2822.

Dodd, D. A., Niederoest, B., Bloechlinger, S., Dupuis, L., Loeffler, J.-P., and Schwab, M. E. (2005). Nogo-A, -B, and -C are found on the cell surface and interact together in many different cell types. *J. Biol. Chem.* 280, 12494–12502. doi:10.1074/jbc.M411827200.

Doetsch, F., García-Verdugo, J. M., and Alvarez-Buylla, A. (1997). Cellular composition and three-dimensional organization of the subventricular germinal zone in the adult mammalian brain. *J. Neurosci.* 17, 5046–5061.

Duan, C.-L., Liu, C.-W., Shen, S.-W., Yu, Z., Mo, J.-L., Chen, X.-H., et al. (2015).

Striatal astrocytes transdifferentiate into functional mature neurons following ischemic brain injury. *Glia* 63, 1660–1670. doi:10.1002/glia.22837.

Eadie, B. D., Redila, V. A., and Christie, B. R. (2005). Voluntary exercise alters the cytoarchitecture of the adult dentate gyrus by increasing cellular proliferation, dendritic complexity, and spine density. *J. Comp. Neurol.* 486, 39–47. doi:10.1002/cne.20493.

Emberson, J., Lees, K. R., Lyden, P., Blackwell, L., Albers, G., Bluhmki, E., et al. (2014). Effect of treatment delay, age, and stroke severity on the effects of intravenous thrombolysis with alteplase for acute ischaemic stroke: a meta-analysis of individual patient data from randomised trials. *Lancet* 384, 1929–1935. doi:10.1016/S0140-6736(14)60584-5.

Eriksson, P. S., Perfilieva, E., Björk-Eriksson, T., Alborn, A. M., Nordborg, C., Peterson, D. A., et al. (1998). Neurogenesis in the adult human hippocampus. *Nat Med* 4, 1313–1317. doi:10.1038/3305.

Ernst, A., Alkass, K., Bernard, S., Salehpour, M., Perl, S., Tisdale, J., et al. (2014). Neurogenesis in the striatum of the adult human brain. *Cell* 156, 1072–1083. doi:10.1016/j.cell.2014.01.044.

Faiz, M., Sachewsky, N., Gascón, S., Bang, K. W. A., Morshead, C. M., and Nagy, A. (2015). Adult Neural Stem Cells from the Subventricular Zone Give Rise to Reactive Astrocytes in the Cortex after Stroke. *Cell Stem Cell* 17, 624–634. doi:10.1016/j.stem.2015.08.002.

Feigin, V. L., Forouzanfar, M. H., Krishnamurthi, R., Mensah, G. A., Connor, M., Bennett, D. A., et al. (2014). Global and regional burden of stroke during 1990–2010: findings from the Global Burden of Disease Study 2010. *The Lancet* 383, 245–255. doi:10.1016/S0140-6736(13)61953-4.

Foran, D. R., and Peterson, A. C. (1992). Myelin acquisition in the central nervous system of the mouse revealed by an MBP-Lac Z transgene. *J. Neurosci.* 12, 4890–4897.

Fournier, A. E., GrandPré, T., and Strittmatter, S. M. (2001). Identification of a receptor mediating Nogo-66 inhibition of axonal regeneration. *Nature* 409, 341–346. doi:10.1038/35053072.

Garcion, E., Halilagic, A., Faissner, A., and ffrench-Constant, C. (2004). Generation of an environmental niche for neural stem cell development by the extracellular matrix molecule tenascin C. *Development* 131, 3423–3432. doi:10.1242/dev.01202.

Garthe, A., and Kempermann, G. (2013). An old test for new neurons: refining the

Morris water maze to study the functional relevance of adult hippocampal neurogenesis. *Front Neurosci* 7, 63. doi:10.3389/fnins.2013.00063.

Gertz, C. C., and Kriegstein, A. R. (2015). Neuronal Migration Dynamics in the Developing Ferret Cortex. *Journal of Neuroscience* 35, 14307–14315. doi:10.1523/JNEUROSCI.2198-15.2015.

Giachino, C., De Marchis, S., Giampietro, C., Parlato, R., Perroteau, I., Schütz, G., et al. (2005). cAMP response element-binding protein regulates differentiation and survival of newborn neurons in the olfactory bulb. *Journal of Neuroscience* 25, 10105–10118. doi:10.1523/JNEUROSCI.3512-05.2005.

Gillani, R. L., Tsai, S.-Y., Wallace, D. G., O'Brien, T. E., Arhebamen, E., Tole, M., et al. (2010). Cognitive recovery in the aged rat after stroke and anti-Nogo-A immunotherapy. *Behav. Brain Res.* 208, 415–424. doi:10.1016/j.bbr.2009.12.015.

Gladstone, D. J., Black, S. E., Hakim, A. M., Heart and Stroke Foundation of Ontario Centre of Excellence in Stroke Recovery (2002). Toward wisdom from failure: lessons from neuroprotective stroke trials and new therapeutic directions. *Stroke* 33, 2123–2136. doi:10.1161/01.STR.0000025518.34157.51.

Goings, G. E., Wibisono, B. L., and Szele, F. G. (2002). Cerebral cortex lesions decrease the number of bromodeoxyuridine-positive subventricular zone cells in mice. *Neuroscience Letters* 329, 161–164.

Goldman, S. A., and Nottebohm, F. (1983). Neuronal production, migration, and differentiation in a vocal control nucleus of the adult female canary brain. in.

Gottesman, R. F., and Hillis, A. E. (2010). Predictors and assessment of cognitive dysfunction resulting from ischaemic stroke. *The Lancet Neurology* 9, 895–905. doi:10.1016/S1474-4422(10)70164-2.

Govek, E.-E., Hatten, M. E., and Van Aelst, L. (2011). The role of Rho GTPase proteins in CNS neuronal migration. *Devel Neurobio* 71, 528–553. doi:10.1002/dneu.20850.

GrandPré, T., Nakamura, F., Vartanian, T., and Strittmatter, S. M. (2000). Identification of the Nogo inhibitor of axon regeneration as a Reticulon protein. *Nature*.

Grünewald, E., Kinnell, H. L., Porteous, D. J., and Thomson, P. A. (2009). GPR50 interacts with neuronal NOGO-A and affects neurite outgrowth. *Mol. Cell. Neurosci.* 42, 363–371. doi:10.1016/j.mcn.2009.08.007.

Gu, H., Yu, S. P., Gutekunst, C.-A., Gross, R. E., and Wei, L. (2013). Inhibition of the

Rho signaling pathway improves neurite outgrowth and neuronal differentiation of mouse neural stem cells. *Int J Physiol Pathophysiol Pharmacol* 5, 11–20.

Gu, W., Brännström, T., and Wester, P. (2000). Cortical neurogenesis in adult rats after reversible photothrombotic stroke. *Journal of Cerebral Blood Flow & Metabolism* 20, 1166–1173. doi:10.1097/00004647-200008000-00002.

Guo, X., Zahir, T., Mothe, A., Shoichet, M. S., Morshead, C. M., Katayama, Y., et al. (2012). The effect of growth factors and soluble Nogo-66 receptor protein on transplanted neural stem/progenitor survival and axonal regeneration after complete transection of rat spinal cord. *Cell Transplant* 21, 1177–1197. doi:10.3727/096368911X612503.

Haybaeck, J., Llenos, I. C., Dulay, R. J., Bettermann, K., Miller, C. L., Wälchli, T., et al. (2012). Expression of nogo-a is decreased with increasing gestational age in the human fetal brain. *Dev. Neurosci.* 34, 402–416. doi:10.1159/000343143.

Heine, V. M., Maslam, S., Joëls, M., and Lucassen, P. J. (2004). Prominent decline of newborn cell proliferation, differentiation, and apoptosis in the aging dentate gyrus, in absence of an age-related hypothalamus-pituitary-adrenal axis activation. *Neurobiol. Aging* 25, 361–375. doi:10.1016/S0197-4580(03)00090-3.

Herold, S., Jagasia, R., Merz, K., Wassmer, K., and Lie, D. C. (2011). CREB signalling regulates early survival, neuronal gene expression and morphological development in adult subventricular zone neurogenesis. *Mol. Cell. Neurosci.* 46, 79–88. doi:10.1016/j.mcn.2010.08.008.

Hu, F., and Strittmatter, S. M. (2008). The N-terminal domain of Nogo-A inhibits cell adhesion and axonal outgrowth by an integrin-specific mechanism. *Journal of Neuroscience* 28, 1262–1269. doi:10.1523/JNEUROSCI.1068-07.2008.

Huber, A. B., Weinmann, O., Brösamle, C., Oertle, T., and Schwab, M. E. (2002). Patterns of Nogo mRNA and protein expression in the developing and adult rat and after CNS lesions. *Journal of Neuroscience* 22, 3553–3567.

Huttner, H. B., Bergmann, O., Salehpour, M., Rácz, A., Tatarishvili, J., Lindgren, E., et al. (2014). The age and genomic integrity of neurons after cortical stroke in humans. *Nat Neurosci* 17, 801–803. doi:10.1038/nn.3706.

Imbimbo, B. P., Giardino, L., Sivilia, S., Giuliani, A., Gusciglio, M., Pietrini, V., et al. (2010). CHF5074, a novel gamma-secretase modulator, restores hippocampal neurogenesis potential and reverses contextual memory deficit in a transgenic mouse model of Alzheimer's disease. *J. Alzheimers Dis.* 20, 159–173. doi:10.3233/JAD-2010-

1366.

Jagasia, R., Steib, K., Englberger, E., Herold, S., Faus-Kessler, T., Saxe, M., et al. (2009). GABA-cAMP response element-binding protein signaling regulates maturation and survival of newly generated neurons in the adult hippocampus. *Journal of Neuroscience* 29, 7966–7977. doi:10.1523/JNEUROSCI.1054-09.2009.

James, R., Kim, Y., Hockberger, P. E., and Szele, F. G. (2011). Subventricular zone cell migration: lessons from quantitative two-photon microscopy. *Front Neurosci* 5, 30. doi:10.3389/fnins.2011.00030.

Jiang, W., Gu, W., Brännström, T., Rosqvist, R., and Wester, P. (2001). Cortical neurogenesis in adult rats after transient middle cerebral artery occlusion. *Stroke* 32, 1201–1207. doi:10.1161/01.STR.32.5.1201.

Jin, K., Minami, M., Lan, J. Q., Mao, X. O., Batteur, S., Simon, R. P., et al. (2001). Neurogenesis in dentate subgranular zone and rostral subventricular zone after focal cerebral ischemia in the rat. *Proc. Natl. Acad. Sci. U.S.A.* 98, 4710–4715.

Jin, K., Sun, Y., Xie, L., Batteur, S., Mao, X. O., Smelick, C., et al. (2003). Neurogenesis and aging: FGF-2 and HB-EGF restore neurogenesis in hippocampus and subventricular zone of aged mice. *Aging Cell* 2, 175–183.

Jin, K., Wang, X., Xie, L., Mao, X. O., and Greenberg, D. A. (2010). Transgenic ablation of doublecortin-expressing cells suppresses adult neurogenesis and worsens stroke outcome in mice. *Proceedings of the National Academy of Sciences* 107, 7993–7998. doi:10.1073/pnas.1000154107.

Jin, K., Wang, X., Xie, L., Mao, X. O., Zhu, W., Wang, Y., et al. (2006). Evidence for stroke-induced neurogenesis in the human brain. *Proc. Natl. Acad. Sci. U.S.A.* 103, 13198–13202. doi:10.1073/pnas.0603512103.

Josephson, A., Widenfalk, J., Widmer, H. W., Olson, L., and Spenger, C. (2001). NOGO mRNA expression in adult and fetal human and rat nervous tissue and in weight drop injury. *Exp. Neurol.* 169, 319–328. doi:10.1006/exnr.2001.7659.

Joset, A., Dodd, D. A., Halegoua, S., and Schwab, M. E. (2010). Pincher-generated Nogo-A endosomes mediate growth cone collapse and retrograde signaling. *The Journal of Cell Biology* 188, 271–285. doi:10.1083/jcb.200906089.

Kamali-Zare, P., and Nicholson, C. (2013). Brain extracellular space: geometry, matrix and physiological importance. *Basic Clin Neurosci* 4, 282–286.

Karlsson, T. E., Smedfors, G., Brodin, A. T. S., Aberg, E., Mattsson, A., Högbeck, I., et al. (2016). NgR1: A Tunable Sensor Regulating Memory Formation, Synaptic, and Dendritic Plasticity. *Cerebral Cortex* 26, 1804–1817. doi:10.1093/cercor/bhw007.

Kartje, G. L., Schulz, M. K., Lopez Yunez, A., Schnell, L., and Schwab, M. E. (1999). Corticostriatal plasticity is restricted by myelin-associated neurite growth inhibitors in the adult rat. *Ann Neurol.* 45, 778–786.

Kee, N. J., Preston, E., and Wojtowicz, J. M. (2001). Enhanced neurogenesis after transient global ischemia in the dentate gyrus of the rat. *Exp Brain Res* 136, 313–320. doi:10.1007/s002210000591.

Kellner, Y., Fricke, S., Kramer, S., Iobbi, C., Wierenga, C. J., Schwab, M. E., et al. (2016). Nogo-A controls structural plasticity at dendritic spines by rapidly modulating actin dynamics. *Hippocampus*. doi:10.1002/hipo.22565.

Kelly-Hayes, M., Beiser, A., Kase, C. S., Scaramucci, A., D'Agostino, R. B., and Wolf, P. A. (2003). The influence of gender and age on disability following ischemic stroke: the Framingham study. *J Stroke Cerebrovasc Dis* 12, 119–126. doi:10.1016/S1052-3057(03)00042-9.

Kempermann, G., Jessberger, S., Steiner, B., and Kronenberg, G. (2004). Milestones of neuronal development in the adult hippocampus. *Trends in Neurosciences* 27, 447–452. doi:10.1016/j.tins.2004.05.013.

Kempf, A., and Schwab, M. E. (2013). Nogo-A represses anatomical and synaptic plasticity in the central nervous system. *Physiology (Bethesda)* 28, 151–163. doi:10.1152/physiol.00052.2012.

Kempf, A., Tews, B., Arzt, M. E., Weinmann, O., Obermair, F. J., Pernet, V., et al. (2014). The Sphingolipid Receptor S1PR2 Is a Receptor for Nogo-A Repressing Synaptic Plasticity. *PLoS Biol* 12, e1001763. doi:10.1371/journal.pbio.1001763.s006.

Kerever, A., Schnack, J., Vellinga, D., Ichikawa, N., Moon, C., Arikawa-Hirasawa, E., et al. (2007). Novel extracellular matrix structures in the neural stem cell niche capture the neurogenic factor fibroblast growth factor 2 from the extracellular milieu. *Stem Cells* 25, 2146–2157. doi:10.1634/stemcells.2007-0082.

Kernie, S. G., and Parent, J. M. (2010). Forebrain neurogenesis after focal Ischemic and traumatic brain injury. *Neurobiology of Disease* 37, 267–274. doi:10.1016/j.nbd.2009.11.002.

Keung, A. J., de Juan-Pardo, E. M., Schaffer, D. V., and Kumar, S. (2011). Rho GTPases

mediate the mechanosensitive lineage commitment of neural stem cells. *Stem Cells* 29, 1886–1897. doi:10.1002/stem.746.

Kimura, A., Ohmori, T., Kashiwakura, Y., Ohkawa, R., Madoiwa, S., Mimuro, J., et al. (2008). Antagonism of sphingosine 1-phosphate receptor-2 enhances migration of neural progenitor cells toward an area of brain. *Stroke* 39, 3411–3417. doi:10.1161/STROKEAHA.108.514612.

Kimura, A., Ohmori, T., Ohkawa, R., Madoiwa, S., Mimuro, J., Murakami, T., et al. (2007). Essential roles of sphingosine 1-phosphate/S1P1 receptor axis in the migration of neural stem cells toward a site of spinal cord injury. *Stem Cells* 25, 115–124. doi:10.1634/stemcells.2006-0223.

Kluska, M. M., Witte, O. W., Bolz, J., and Redecker, C. (2005). Neurogenesis in the adult dentate gyrus after cortical infarcts: effects of infarct location, N-methyl-D-aspartate receptor blockade and anti-inflammatory treatment. *Neuroscience* 135, 723–735. doi:10.1016/j.neuroscience.2005.06.082.

Knoth, R., Singec, I., Ditter, M., Pantazis, G., Capetian, P., Meyer, R. P., et al. (2010). Murine features of neurogenesis in the human hippocampus across the lifespan from 0 to 100 years. *PLoS ONE* 5, e8809. doi:10.1371/journal.pone.0008809.

Komitova, M., and Eriksson, P. S. (2004). Sox-2 is expressed by neural progenitors and astroglia in the adult rat brain. *Neuroscience Letters* 369, 24–27. doi:10.1016/j.neulet.2004.07.035.

Komitova, M., Mattsson, B., Johansson, B. B., and Eriksson, P. S. (2005). Enriched environment increases neural stem/progenitor cell proliferation and neurogenesis in the subventricular zone of stroke-lesioned adult rats. *Stroke* 36, 1278–1282. doi:10.1161/01.STR.0000166197.94147.59.

Konofagou, E. E., Tung, Y.-S., Choi, J., Deffieux, T., Baseri, B., and Vlachos, F. (2012). Ultrasound-induced blood-brain barrier opening. *Curr Pharm Biotechnol* 13, 1332–1345.

Kornack, D. R., and Rakic, P. (2001). Cell proliferation without neurogenesis in adult primate neocortex. *Science* 294, 2127–2130. doi:10.1126/science.1065467.

Kuhn, H. G., Winkler, J., Kempermann, G., Thal, L. J., and Gage, F. H. (1997). Epidermal growth factor and fibroblast growth factor-2 have different effects on neural progenitors in the adult rat brain. *J. Neurosci.* 17, 5820–5829.

Kumar, P., and Moon, L. D. F. (2013). Therapeutics targeting Nogo-A hold promise for

stroke restoration. *CNS Neurol Disord Drug Targets* 12, 200–208.

Kurowska, Z., Brundin, P., Schwab, M. E., and Li, J. Y. (2014). Intracellular Nogo-A facilitates initiation of neurite formation in mouse midbrain neurons in vitro. *Neuroscience* 256, 456–466. doi:10.1016/j.neuroscience.2013.10.029.

Lacar, B., Parylak, S. L., Vadodaria, K. C., Sarkar, A., and Gage, F. H. (2014). Increasing the resolution of the adult neurogenesis picture. *F1000Prime Rep* 6, 8. doi:10.12703/P6-8.

Lazarini, F., and Lledo, P.-M. (2011). Is adult neurogenesis essential for olfaction? *Trends Neurosci.* 34, 20–30. doi:10.1016/j.tins.2010.09.006.

Lazarini, F., Mouthon, M.-A., Gheusi, G., de Chaumont, F., Olivo-Marin, J.-C., Lamarque, S., et al. (2009). Cellular and behavioral effects of cranial irradiation of the subventricular zone in adult mice. *PLoS ONE* 4, e7017. doi:10.1371/journal.pone.0007017.

Lee, H., Raiker, S. J., Venkatesh, K., Geary, R., Robak, L. A., Zhang, Y., et al. (2008). Synaptic function for the Nogo-66 receptor NgR1: regulation of dendritic spine morphology and activity-dependent synaptic strength. *Journal of Neuroscience* 28, 2753–2765. doi:10.1523/JNEUROSCI.5586-07.2008.

Lee, S.-T., Chu, K., Jung, K.-H., Kim, J. H., Huh, J.-Y., Yoon, H., et al. (2012). miR-206 regulates brain-derived neurotrophic factor in Alzheimer disease model. *Ann Neurol.* 72, 269–277. doi:10.1002/ana.23588.

Leker, R. R., Soldner, F., Velasco, I., Gavin, D. K., Androutsellis-Theotokis, A., and McKay, R. D. G. (2007). Long-lasting regeneration after ischemia in the cerebral cortex. *Stroke* 38, 153–161. doi:10.1161/01.STR.0000252156.65953.a9.

Lenzlinger, P. M., Shimizu, S., Marklund, N., Thompson, H. J., Schwab, M. E., Saatman, K. E., et al. (2005). Delayed inhibition of Nogo-A does not alter injury-induced axonal sprouting but enhances recovery of cognitive function following experimental traumatic brain injury in rats. *Neuroscience* 134, 1047–1056. doi:10.1016/j.neuroscience.2005.04.048.

Leong, S. Y., Faux, C. H., Turbic, A., Dixon, K. J., and Turnley, A. M. (2011). The Rho kinase pathway regulates mouse adult neural precursor cell migration. *Stem Cells* 29, 332–343. doi:10.1002/stem.577.

Levison, S. W., Young, G. M., and Goldman, J. E. (1999). Cycling cells in the adult rat neocortex preferentially generate oligodendroglia. *J. Neurosci. Res.* 57, 435–446.

Li, X., Fu, Q.-L., Jing, X.-L., Liao, X.-X., Zeng, A.-H., Xiong, Y., et al. (2009). Myelin-associated glycoprotein inhibits the neuronal differentiation of neural progenitors. *Neuroreport* 20, 708–712. doi:10.1097/WNR.0b013e32832aa942.

Liang, X., Wu, L., Hand, T., and Andreasson, K. (2005). Prostaglandin D2 mediates neuronal protection via the DP1 receptor. *J. Neurochem.* 92, 477–486. doi:10.1111/j.1471-4159.2004.02870.x.

Liao, H., Duka, T., Teng, F. Y. H., Sun, L., Bu, W.-Y., Ahmed, S., et al. (2004). Nogo-66 and myelin-associated glycoprotein (MAG) inhibit the adhesion and migration of Nogo-66 receptor expressing human glioma cells. *J. Neurochem.* 90, 1156–1162. doi:10.1111/j.1471-4159.2004.02573.x.

Lim, D. A., and Alvarez-Buylla, A. (2016). The Adult Ventricular-Subventricular Zone (V-SVZ) and Olfactory Bulb (OB) Neurogenesis. *Cold Spring Harbor Perspectives in Biology* 8. doi:10.1101/cshperspect.a018820.

Lindau, N. T., Bänninger, B. J., Gullo, M., Good, N. A., Bachmann, L. C., Starkey, M. L., et al. (2014). Rewiring of the corticospinal tract in the adult rat after unilateral stroke and anti-Nogo-A therapy. *Brain* 137, 739–756. doi:10.1093/brain/awt336.

Lindvall, O., and Kokaia, Z. (2015). Neurogenesis following Stroke Affecting the Adult Brain. *Cold Spring Harbor Perspectives in Biology* 7. doi:10.1101/cshperspect.a019034.

Liu, J., Solway, K., Messing, R. O., and Sharp, F. R. (1998). Increased neurogenesis in the dentate gyrus after transient global ischemia in gerbils. *J. Neurosci.* 18, 7768–7778.

Liu, X., Wang, Q., Haydar, T. F., and Bordey, A. (2005). Nonsynaptic GABA signaling in postnatal subventricular zone controls proliferation of GFAP-expressing progenitors. *Nat Neurosci* 8, 1179–1187. doi:10.1038/nn1522.

Lo, E. H., Dalkara, T., and Moskowitz, M. A. (2003). Mechanisms, challenges and opportunities in stroke. *Nat Rev Neurosci* 4, 399–415. doi:10.1038/nrn1106.

Lois, C., and Alvarez-Buylla, A. (1994). Long-distance neuronal migration in the adult mammalian brain. *Science* 264, 1145–1148.

Lu, P., Wang, Y., Graham, L., McHale, K., Gao, M., Wu, D., et al. (2012). Long-distance growth and connectivity of neural stem cells after severe spinal cord injury. *Cell* 150, 1264–1273. doi:10.1016/j.cell.2012.08.020.

Lu, P., Woodruff, G., Wang, Y., Graham, L., Hunt, M., Wu, D., et al. (2014). Long-distance axonal growth from human induced pluripotent stem cells after spinal cord

injury. *Neuron* 83, 789–796. doi:10.1016/j.neuron.2014.07.014.

Lubeck, M. D., Steplewski, Z., Baglia, F., Klein, M. H., Dorrington, K. J., and Koprowski, H. (1985). The interaction of murine IgG subclass proteins with human monocyte Fc receptors. *J. Immunol.* 135, 1299–1304.

Luo, Y., Pollard, J. W., and Casadevall, A. (2010). Fcgamma receptor cross-linking stimulates cell proliferation of macrophages via the ERK pathway. *J. Biol. Chem.* 285, 4232–4242. doi:10.1074/jbc.M109.037168.

Macas, J., Nern, C., Plate, K. H., and Momma, S. (2006). Increased generation of neuronal progenitors after ischemic injury in the aged adult human forebrain. *Journal of Neuroscience* 26, 13114–13119. doi:10.1523/JNEUROSCI.4667-06.2006.

Marin, O., Yaron, A., Bagri, A., Tessier-Lavigne, M., and Rubenstein, J. L. (2001). Sorting of striatal and cortical interneurons regulated by semaphorin-neuropilin interactions. *Science* 293, 872–875. doi:10.1126/science.1061891.

Marín, O., Valiente, M., Ge, X., and Tsai, L.-H. (2010). Guiding neuronal cell migrations. *Cold Spring Harbor Perspectives in Biology* 2, a001834. doi:10.1101/cshperspect.a001834.

Marklund, N., Bareyre, F. M., Royo, N. C., Thompson, H. J., Mir, A. K., Grady, M. S., et al. (2007). Cognitive outcome following brain injury and treatment with an inhibitor of Nogo-A in association with an attenuated downregulation of hippocampal growth-associated protein-43 expression. *J. Neurosurg.* 107, 844–853. doi:10.3171/JNS-07/10/0844.

Markus, T. M., Tsai, S.-Y., Bollnow, M. R., Farrer, R. G., O'Brien, T. E., Kindler-Baumann, D. R., et al. (2005). Recovery and brain reorganization after stroke in adult and aged rats. *Ann Neurol.* 58, 950–953. doi:10.1002/ana.20676.

Marlier, Q., Verteneuil, S., and Vandenbosch, R. (2015). Mechanisms and Functional Significance of Stroke-Induced Neurogenesis. *Frontiers in …* 9, 19. doi:10.3389/fnins.2015.00458.

Martin, I., Andres, C. R., Védrine, S., Tabagh, R., Michelle, C., Jourdan, M.-L., et al. (2009). Effect of the oligodendrocyte myelin glycoprotein (OMgp) on the expansion and neuronal differentiation of rat neural stem cells. *Brain Res.* 1284, 22–30. doi:10.1016/j.brainres.2009.05.070.

Martí-Fàbregas, J., Romaguera-Ros, M., Gómez-Pinedo, U., Martínez-Ramírez, S., Jiménez-Xarrié, E., Marín, R., et al. (2010). Proliferation in the human ipsilateral

subventricular zone after ischemic stroke. *Neurology* 74, 357–365. doi:10.1212/WNL.0b013e3181cbccec.

Mathis, C., Schröter, A., Thallmair, M., and Schwab, M. E. (2010). Nogo-a regulates neural precursor migration in the embryonic mouse cortex. *Cerebral Cortex* 20, 2380–2390. doi:10.1093/cercor/bhp307.

Matsumori, Y., Matsumori, Y., Hong, S. M., Hong, S. M., Fan, Y., Fan, Y., et al. (2006). Enriched environment and spatial learning enhance hippocampal neurogenesis and salvages ischemic penumbra after focal cerebral ischemia. *Neurobiology of Disease* 22, 187–198. doi:10.1016/j.nbd.2005.10.015.

Mazya, M., Egido, J. A., Ford, G. A., Lees, K. R., Mikulik, R., Toni, D., et al. (2012). Predicting the risk of symptomatic intracerebral hemorrhage in ischemic stroke treated with intravenous alteplase: safe Implementation of Treatments in Stroke (SITS) symptomatic intracerebral hemorrhage risk score. *Stroke* 43, 1524–1531. doi:10.1161/STROKEAHA.111.644815.

Meng, Y., Chopp, M., Zhang, Y., Liu, Z., An, A., Mahmood, A., et al. (2014). Subacute intranasal administration of tissue plasminogen activator promotes neuroplasticity and improves functional recovery following traumatic brain injury in rats. *PLoS ONE* 9, e106238. doi:10.1371/journal.pone.0106238.

Menn, B., Garcia-Verdugo, J.-M., Yaschine, C., Gonzalez-Perez, O., Rowitch, D., and Alvarez-Buylla, A. (2006). Origin of oligodendrocytes in the subventricular zone of the adult brain. *Journal of Neuroscience* 26, 7907–7918. doi:10.1523/JNEUROSCI.1299-06.2006.

Mercier, F., Kitasako, J. T., and Hatton, G. I. (2002). Anatomy of the brain neurogenic zones revisited: fractones and the fibroblast/macrophage network. *J. Comp. Neurol.* 451, 170–188. doi:10.1002/cne.10342.

Mi, S., Lee, X., Shao, Z., Thill, G., Ji, B., Relton, J., et al. (2004). LINGO-1 is a component of the Nogo-66 receptor/p75 signaling complex. *Nat Neurosci* 7, 221–228. doi:10.1038/nn1188.

Mingorance, A., Fontana, X., Solé, M., Burgaya, F., Ureña, J. M., Teng, F. Y. H., et al. (2004). Regulation of Nogo and Nogo receptor during the development of the entorhino-hippocampal pathway and after adult hippocampal lesions. *Mol. Cell. Neurosci.* 26, 34–49. doi:10.1016/j.mcn.2004.01.001.

Mingorance-Le Meur, A., Zheng, B., Soriano, E., and del Río, J. A. (2007). Involvement of the myelin-associated inhibitor Nogo-A in early cortical development and neuronal

maturation. *Cereb. Cortex* 17, 2375–2386. doi:10.1093/cercor/bhl146.

Mokin, M., Rojas, H., and Levy, E. I. (2016). Randomized trials of endovascular therapy for stroke - impact on stroke care. *Nature Publishing Group* 12, 86–94. doi:10.1038/nrneurol.2015.240.

Montani, L., Gerrits, B., Gehrig, P., Kempf, A., Dimou, L., Wollscheid, B., et al. (2009). Neuronal Nogo-A modulates growth cone motility via Rho-GTP/LIMK1/cofilin in the unlesioned adult nervous system. *J. Biol. Chem.* 284, 10793–10807. doi:10.1074/jbc.M808297200.

Moraga, A., Pradillo, J. M., Cuartero, M. I., Hernández-Jiménez, M., Oses, M., Moro, M. A., et al. (2014). Toll-like receptor 4 modulates cell migration and cortical neurogenesis after focal cerebral ischemia. *FASEB J.* doi:10.1096/fj.14-252452.

Moreno, M. M., Linster, C., Escanilla, O., Sacquet, J., Didier, A., and Mandairon, N. (2009). Olfactory perceptual learning requires adult neurogenesis. *Proceedings of the National Academy of Sciences* 106, 17980–17985. doi:10.1073/pnas.0907063106.

Morshead, C. M., and van der Kooy, D. (1992). Postmitotic death is the fate of constitutively proliferating cells in the subependymal layer of the adult mouse brain. *J. Neurosci.* 12, 249–256.

Moskowitz, M. A., Lo, E. H., and Iadecola, C. (2010). The science of stroke: mechanisms in search of treatments. *Neuron* 67, 181–198. doi:10.1016/j.neuron.2010.07.002.

Mozaffarian, D., Benjamin, E. J., Go, A. S., Arnett, D. K., Blaha, M. J., Cushman, M., et al. (2016). Heart Disease and Stroke Statistics-2016 Update: A Report From the American Heart Association. *Circulation* 133, e38–e360. doi:10.1161/CIR.0000000000000350.

Mukhopadhyay, G., Doherty, P., Walsh, F. S., Crocker, P. R., and Filbin, M. T. (1994). A novel role for myelin-associated glycoprotein as an inhibitor of axonal regeneration. *Neuron* 13, 757–767.

Munger, S. D., Leinders-Zufall, T., and Zufall, F. (2009). Subsystem organization of the mammalian sense of smell. *Annu. Rev. Physiol.* 71, 115–140. doi:10.1146/annurev.physiol.70.113006.100608.

Nelson, A. L., Dhimolea, E., and Reichert, J. M. (2010). Development trends for human monoclonal antibody therapeutics. *Nat Rev Drug Discov* 9, 767–774. doi:10.1038/nrd3229.

Ng, Y. S., Stein, J., Ning, M., and Black-Schaffer, R. M. (2007). Comparison of clinical characteristics and functional outcomes of ischemic stroke in different vascular territories. *Stroke* 38, 2309–2314. doi:10.1161/STROKEAHA.106.475483.

Nguyen-Ba-Charvet, K. T., Picard-Riera, N., Tessier-Lavigne, M., Baron-Van Evercooren, A., Sotelo, C., and Chédotal, A. (2004). Multiple roles for slits in the control of cell migration in the rostral migratory stream. *Journal of Neuroscience* 24, 1497–1506. doi:10.1523/JNEUROSCI.4729-03.2004.

Niederöst, B., Oertle, T., Fritsche, J., McKinney, R. A., and Bandtlow, C. E. (2002). Nogo-A and myelin-associated glycoprotein mediate neurite growth inhibition by antagonistic regulation of RhoA and Rac1. *Journal of Neuroscience* 22, 10368–10376.

Nocentini, S., Reginensi, D., Garcia, S., Carulla, P., Moreno-Flores, M. T., Wandosell, F., et al. (2012). Myelin-associated proteins block the migration of olfactory ensheathing cells: an in vitro study using single-cell tracking and traction force microscopy. *Cell. Mol. Life Sci.* 69, 1689–1703. doi:10.1007/s00018-011-0893-1.

Noori, H. R., and Fornal, C. A. (2011). The appropriateness of unbiased optical fractionators to assess cell proliferation in the adult hippocampus. *Front Neurosci* 5, 140. doi:10.3389/fnins.2011.00140.

Oertle, T., van der Haar, M. E., Bandtlow, C. E., Robeva, A., Burfeind, P., Buss, A., et al. (2003). Nogo-A inhibits neurite outgrowth and cell spreading with three discrete regions. *Journal of Neuroscience* 23, 5393–5406.

Ohab, J. J., Fleming, S., Blesch, A., and Carmichael, S. T. (2006). A neurovascular niche for neurogenesis after stroke. *Journal of Neuroscience* 26, 13007–13016. doi:10.1523/JNEUROSCI.4323-06.2006.

Okamoto, H., Takuwa, N., Yokomizo, T., Sugimoto, N., Sakurada, S., Shigematsu, H., et al. (2000). Inhibitory regulation of Rac activation, membrane ruffling, and cell migration by the G protein-coupled sphingosine-1-phosphate receptor EDG5 but not EDG1 or EDG3. *Mol. Cell. Biol.* 20, 9247–9261.

Osada, M., Yatomi, Y., Ohmori, T., Ikeda, H., and Ozaki, Y. (2002). Enhancement of sphingosine 1-phosphate-induced migration of vascular endothelial cells and smooth muscle cells by an EDG-5 antagonist. *Biochem. Biophys. Res. Commun.* 299, 483–487.

Papadopoulos, C. M., Tsai, S.-Y., Alsbiei, T., O'Brien, T. E., Schwab, M. E., and Kartje, G. L. (2002). Functional recovery and neuroanatomical plasticity following middle cerebral artery occlusion and IN-1 antibody treatment in the adult rat. *Ann Neurol.* 51, 433–441. doi:10.1002/ana.10144.

Papadopoulos, C. M., Tsai, S.-Y., Cheatwood, J. L., Bollnow, M. R., Kolb, B. E., Schwab, M. E., et al. (2006). Dendritic plasticity in the adult rat following middle cerebral artery occlusion and Nogo-a neutralization. *Cereb. Cortex* 16, 529–536. doi:10.1093/cercor/bhi132.

Pardridge, W. M. (2011). Drug transport in brain via the cerebrospinal fluid. *Fluids Barriers CNS* 8, 7. doi:10.1186/2045-8118-8-7.

Parent, J. M., Vexler, Z. S., Gong, C., Derugin, N., and Ferriero, D. M. (2002). Rat forebrain neurogenesis and striatal neuron replacement after focal stroke. *Ann Neurol.* 52, 802–813. doi:10.1002/ana.10393.

Paxinos, G., and Watson, C. (1998). The Rat Brain in Stereotaxic Coordinates, 4th Ed. Academic Press.

Peretto, P., Merighi, A., Fasolo, A., and Bonfanti, L. (1997). Glial tubes in the rostral migratory stream of the adult rat. *Brain Res. Bull.* 42, 9–21.

Peterson, D. A. (1999). Quantitative histology using confocal microscopy: implementation of unbiased stereology procedures. *Methods* 18, 493–507. doi:10.1006/meth.1999.0818.

Petrasek, T., Prokopova, I., Bahnik, S., Schönig, K., Berger, S., Vales, K., et al. (2014a). Nogo-A downregulation impairs place avoidance in the Carousel maze but not spatial memory in the Morris water maze. *Neurobiol Learn Mem* 107, 42–49. doi:10.1016/j.nlm.2013.10.015.

Petrasek, T., Prokopova, I., Sladek, M., Weissova, K., Vojtechova, I., Bahnik, S., et al. (2014b). Nogo-A-deficient Transgenic Rats Show Deficits in Higher Cognitive Functions, Decreased Anxiety, and Altered Circadian Activity Patterns. *Front Behav Neurosci* 8, 90. doi:10.3389/fnbeh.2014.00090.

Petrinovic, M. M., Duncan, C. S., Bourikas, D., Weinman, O., Montani, L., Schroeter, A., et al. (2010). Neuronal Nogo-A regulates neurite fasciculation, branching and extension in the developing nervous system. *Development* 137, 2539–2550. doi:10.1242/dev.048371.

Petrinovic, M. M., Hourez, R., Aloy, E. M., Dewarrat, G., Gall, D., Weinmann, O., et al. (2013a). Neuronal Nogo-A negatively regulates dendritic morphology and synaptic transmission in the cerebellum. *Proceedings of the National Academy of Sciences* 110, 1083–1088. doi:10.1073/pnas.1214255110.

Petrinovic, M. M., Hourez, R., Aloy, E. M., Dewarrat, G., Gall, D., Weinmann, O., et

al. (2013b). Neuronal Nogo-A negatively regulates dendritic morphology and synaptic transmission in the cerebellum. *Proc. Natl. Acad. Sci. U.S.A.* 110, 1083–1088. doi:10.1073/pnas.1214255110/-/DCSupplemental/pnas.201214255SI.pdf.

Prinjha, R., Moore, S. E., Vinson, M., Blake, S., Morrow, R., Christie, G., et al. (2000). Inhibitor of neurite outgrowth in humans. *Nature* 403, 383–384. doi:10.1038/35000287.

Quiñones-Hinojosa, A., and Chaichana, K. (2007). The human subventricular zone: A source of new cells and a potential source of brain tumors. 205, 313–324. doi:10.1016/j.expneurol.2007.03.016.

Quiñones-Hinojosa, A., Sanai, N., Soriano-Navarro, M., Gonzalez-Perez, O., Mirzadeh, Z., Gil-Perotin, S., et al. (2006). Cellular composition and cytoarchitecture of the adult human subventricular zone: a niche of neural stem cells. *J. Comp. Neurol.* 494, 415–434. doi:10.1002/cne.20798.

Raber, J., Fan, Y., Matsumori, Y., Liu, Z., Weinstein, P. R., Fike, J. R., et al. (2004). Irradiation attenuates neurogenesis and exacerbates ischemia-induced deficits. *Ann Neurol.* 55, 381–389. doi:10.1002/ana.10853.

Raiker, S. J., Lee, H., Baldwin, K. T., Duan, Y., Shrager, P., and Giger, R. J. (2010). Oligodendrocyte-myelin glycoprotein and Nogo negatively regulate activity-dependent synaptic plasticity. *Journal of Neuroscience* 30, 12432–12445. doi:10.1523/JNEUROSCI.0895-10.2010.

Raineteau, O., Z'Graggen, W. J., Thallmair, M., and Schwab, M. E. (1999). Sprouting and regeneration after pyramidotomy and blockade of the myelin-associated neurite growth inhibitors NI 35/250 in adult rats. *Eur. J. Neurosci.* 11, 1486–1490.

Ramasamy, S., Yu, F., Hong Yu, Y., Srivats, H., Dawe, G. S., and Ahmed, S. (2014). NogoR1 and PirB signaling stimulates neural stem cell survival and proliferation. *Stem Cells* 32, 1636–1648. doi:10.1002/stem.1645.

Reginensi, D., Carulla, P., Nocentini, S., Seira, O., Serra-Picamal, X., Torres-Espín, A., et al. (2015). Increased migration of olfactory ensheathing cells secreting the Nogo receptor ectodomain over inhibitory substrates and lesioned spinal cord. *Cell. Mol. Life Sci.* 72, 2719–2737. doi:10.1007/s00018-015-1869-3.

Ribes, V., and Briscoe, J. (2009). Establishing and interpreting graded Sonic Hedgehog signaling during vertebrate neural tube patterning: the role of negative feedback. *Cold Spring Harbor Perspectives in Biology* 1, a002014. doi:10.1101/cshperspect.a002014.

Richardson, P. M., McGuinness, U. M., and Aguayo, A. J. (1980). Axons from CNS neurons regenerate into PNS grafts. *Nature* 284, 264–265.

Rolando, C., Parolisi, R., Boda, E., Schwab, M. E., Rossi, F., and Buffo, A. (2012). Distinct roles of Nogo-a and Nogo receptor 1 in the homeostatic regulation of adult neural stem cell function and neuroblast migration. *Journal of Neuroscience* 32, 17788–17799. doi:10.1523/JNEUROSCI.3142-12.2012.

Röther, J., de Crespigny, A. J., D'Arceuil, H., and Mosley, M. E. (1996). MR detection of cortical spreading depression immediately after focal ischemia in the rat. *Journal of Cerebral Blood Flow & Metabolism* 16, 214–220. doi:10.1097/00004647-199603000-00005.

Sahay, A., Scobie, K. N., Hill, A. S., O'Carroll, C. M., Kheirbek, M. A., Burghardt, N. S., et al. (2011). Increasing adult hippocampal neurogenesis is sufficient to improve pattern separation. *Nature* 472, 466–470. doi:10.1038/nature09817.

Sanai, N., Berger, M. S., Garcia-Verdugo, J.-M., and Alvarez-Buylla, A. (2007). Comment on "Human neuroblasts migrate to the olfactory bulb via a lateral ventricular extension". *Science* 318, 393–author reply 393. doi:10.1126/science.1145011.

Sanai, N., Nguyen, T., Ihrie, R. A., Mirzadeh, Z., Tsai, H.-H., Wong, M., et al. (2011). Corridors of migrating neurons in the human brain and their decline during infancy. *Nature* 478, 382–386. doi:10.1038/nature10487.

Sanai, N., Tramontin, A. D., Quiñones-Hinojosa, A., Barbaro, N. M., Gupta, N., Kunwar, S., et al. (2004). Unique astrocyte ribbon in adult human brain contains neural stem cells but lacks chain migration. *Nature* 427, 740–744. doi:10.1038/nature02301.

Saunders, N. R., Dziegielewska, K. M., Møllgård, K., and Habgood, M. D. (2015). Markers for blood-brain barrier integrity: how appropriate is Evans blue in the twenty-first century and what are the alternatives? *Front Neurosci* 9, 385. doi:10.3389/fnins.2015.00385.

Schindelin, J., Arganda-Carreras, I., Frise, E., Kaynig, V., Longair, M., Pietzsch, T., et al. (2012). Fiji: an open-source platform for biological-image analysis. *Nat. Methods* 9, 676–682. doi:10.1038/nmeth.2019.

Schlachetzki, F., Zhu, C., and Pardridge, W. M. (2002). Expression of the neonatal Fc receptor (FcRn) at the blood-brain barrier. *J. Neurochem.* 81, 203–206.

Schmandke, A., Schmandke, A., and Schwab, M. E. (2014). Nogo-A: Multiple Roles in CNS Development, Maintenance, and Disease. *Neuroscientist* 20, 372–386. doi:10.1177/1073858413516800.

Schnell, L., and Schwab, M. E. (1990). Axonal regeneration in the rat spinal cord produced by an antibody against myelin-associated neurite growth inhibitors. *Nature* 343, 269–272. doi:10.1038/343269a0.

Schwab, M. E. (2010). Functions of Nogo proteins and their receptors in the nervous system. *Nat Rev Neurosci* 11, 799–811. doi:10.1038/nrn2936.

Schwab, M. E., and Caroni, P. (1988). Oligodendrocytes and CNS myelin are nonpermissive substrates for neurite growth and fibroblast spreading in vitro. *J. Neurosci.* 8, 2381–2393.

Schwab, M. E., and Schnell, L. (1991). Channeling of developing rat corticospinal tract axons by myelin-associated neurite growth inhibitors. *J. Neurosci.* 11, 709–721.

Schwab, M. E., and Strittmatter, S. M. (2014). Nogo limits neural plasticity and recovery from injury. *Curr. Opin. Neurobiol.* 27, 53–60. doi:10.1016/j.conb.2014.02.011.

Schwab, M. E., and Thoenen, H. (1985). Dissociated neurons regenerate into sciatic but not optic nerve explants in culture irrespective of neurotrophic factors. *J. Neurosci.* 5, 2415–2423.

Seymour, A. B., Andrews, E. M., Tsai, S.-Y., Markus, T. M., Bollnow, M. R., Brenneman, M. M., et al. (2005). Delayed treatment with monoclonal antibody IN-1 1 week after stroke results in recovery of function and corticorubral plasticity in adult rats. *Journal of Cerebral Blood Flow & Metabolism* 25, 1366–1375. doi:10.1038/sj.jcbfm.9600134.

Shao, Z., Browning, J. L., Lee, X., Scott, M. L., Shulga-Morskaya, S., Allaire, N., et al. (2005). TAJ/TROY, an orphan TNF receptor family member, binds Nogo-66 receptor 1 and regulates axonal regeneration. *Neuron* 45, 353–359. doi:10.1016/j.neuron.2004.12.050.

Spalding, K. L., Bergmann, O., Alkass, K., Bernard, S., Salehpour, M., Huttner, H. B., et al. (2013). Dynamics of hippocampal neurogenesis in adult humans. *Cell* 153, 1219–1227. doi:10.1016/j.cell.2013.05.002.

Spillmann, A. A., Amberger, V. R., and Schwab, M. E. (1997). High molecular weight protein of human central nervous system myelin inhibits neurite outgrowth: an effect which can be neutralized by the monoclonal antibody IN-1. *Eur. J. Neurosci.* 9, 549–

555.

Su, Z., Cao, L., Zhu, Y., Liu, X., Huang, Z., Huang, A., et al. (2007). Nogo enhances the adhesion of olfactory ensheathing cells and inhibits their migration. *J. Cell. Sci.* 120, 1877–1887. doi:10.1242/jcs.03448.

Sun, F., Wang, X., Mao, X., Xie, L., and Jin, K. (2012). Ablation of neurogenesis attenuates recovery of motor function after focal cerebral ischemia in middle-aged mice. *PLoS ONE* 7, e46326. doi:10.1371/journal.pone.0046326.g005.

Sun, G. J., Zhou, Y., Stadel, R. P., Moss, J., Yong, J. H. A., Ito, S., et al. (2015). Tangential migration of neuronal precursors of glutamatergic neurons in the adult mammalian brain. *Proceedings of the National Academy of Sciences* 112, 9484–9489. doi:10.1073/pnas.1508545112.

Takasawa, K.-I., Kitagawa, K., Yagita, Y., Sasaki, T., Tanaka, S., Matsushita, K., et al. (2002). Increased proliferation of neural progenitor cells but reduced survival of newborn cells in the contralateral hippocampus after focal cerebral ischemia in rats. *J. Cereb. Blood Flow Metab.* 22, 299–307. doi:10.1097/00004647-200203000-00007.

Tang, X., Falls, D. L., Li, X., Lane, T., and Luskin, M. B. (2007). Antigen-retrieval procedure for bromodeoxyuridine immunolabeling with concurrent labeling of nuclear DNA and antigens damaged by HCl pretreatment. *Journal of Neuroscience* 27, 5837–5844. doi:10.1523/JNEUROSCI.5048-06.2007.

Taniike, M., Mohri, I., Eguchi, N., Beuckmann, C. T., Suzuki, K., and Urade, Y. (2002). Perineuronal oligodendrocytes protect against neuronal apoptosis through the production of lipocalin-type prostaglandin D synthase in a genetic demyelinating model. *Journal of Neuroscience* 22, 4885–4896.

Taupin, P. (2007). BrdU immunohistochemistry for studying adult neurogenesis: paradigms, pitfalls, limitations, and validation. *Brain Res Rev* 53, 198–214. doi:10.1016/j.brainresrev.2006.08.002.

Tews, B., Schönig, K., Arzt, M. E., Clementi, S., Rioult-Pedotti, M.-S., Zemmar, A., et al. (2013). Synthetic microRNA-mediated downregulation of Nogo-A in transgenic rats reveals its role as regulator of synaptic plasticity and cognitive function. *Proceedings of the National Academy of Sciences* 110, 6583–6588. doi:10.1073/pnas.1217665110.

Thallmair, M., Metz, G. A., Z'Graggen, W. J., Raineteau, O., Kartje, G. L., and Schwab, M. E. (1998). Neurite growth inhibitors restrict plasticity and functional recovery following corticospinal tract lesions. *Nat Neurosci* 1, 124–131. doi:10.1038/373.

Thiede-Stan, N. K., Tews, B., Albrecht, D., Ristic, Z., Ewers, H., and Schwab, M. E. (2015). Tetraspanin-3 is an organizer of the multi-subunit Nogo-A signaling complex. *J. Cell. Sci.* 128, 3583–3596. doi:10.1242/jcs.167981.

Thored, P., Wood, J., Arvidsson, A., Cammenga, J., Kokaia, Z., and Lindvall, O. (2007). Long-term neuroblast migration along blood vessels in an area with transient angiogenesis and increased vascularization after stroke. *Stroke* 38, 3032–3039. doi:10.1161/STROKEAHA.107.488445.

Tong, J., Liu, W., Wang, X., Han, X., Hyrien, O., Samadani, U., et al. (2013). Inhibition of Nogo-66 receptor 1 enhances recovery of cognitive function after traumatic brain injury in mice. *J. Neurotrauma* 30, 247–258. doi:10.1089/neu.2012.2493.

Tsai, S.-Y., Markus, T. M., Andrews, E. M., Cheatwood, J. L., Emerick, A. J., Mir, A. K., et al. (2007). Intrathecal treatment with anti-Nogo-A antibody improves functional recovery in adult rats after stroke. *Exp Brain Res* 182, 261–266. doi:10.1007/s00221-007-1067-0.

Tsai, S.-Y., Papadopoulos, C. M., Schwab, M. E., and Kartje, G. L. (2011). Delayed anti-nogo-a therapy improves function after chronic stroke in adult rats. *Stroke* 42, 186–190. doi:10.1161/STROKEAHA.110.590083.

Turnley, A. M., Basrai, H. S., and Christie, K. J. (2014). Is integration and survival of newborn neurons the bottleneck for effective neural repair by endogenous neural precursor cells? *Front Neurosci* 8, 29. doi:10.3389/fnins.2014.00029.

Urbach, A., Redecker, C., and Witte, O. W. (2008). Induction of neurogenesis in the adult dentate gyrus by cortical spreading depression. *Stroke* 39, 3064–3072. doi:10.1161/STROKEAHA.108.518076.

Vadodaria, K. C., and Jessberger, S. (2013). Maturation and integration of adult born hippocampal neurons: signal convergence onto small Rho GTPases. *Front Synaptic Neurosci* 5, 4. doi:10.3389/fnsyn.2013.00004.

Valley, M. T., Mullen, T. R., Schultz, L. C., Sagdullaev, B. T., and Firestein, S. (2009). Ablation of mouse adult neurogenesis alters olfactory bulb structure and olfactory fear conditioning. *Front Neurosci* 3, 51. doi:10.3389/neuro.22.003.2009.

Voeltz, G. K., Prinz, W. A., Shibata, Y., Rist, J. M., and Rapoport, T. A. (2006). A class of membrane proteins shaping the tubular endoplasmic reticulum. *Cell* 124, 573–586. doi:10.1016/j.cell.2005.11.047.

Wahl, A. S., Omlor, W., Rubio, J. C., Chen, J. L., Zheng, H., Schröter, A., et al. (2014).

Neuronal repair. Asynchronous therapy restores motor control by rewiring of the rat corticospinal tract after stroke. *Science* 344, 1250–1255. doi:10.1126/science.1253050.

Wang, B., Xiao, Z., Chen, B., Han, J., Gao, Y., Zhang, J., et al. (2008). Nogo-66 promotes the differentiation of neural progenitors into astroglial lineage cells through mTOR-STAT3 pathway. *PLoS ONE* 3, e1856. doi:10.1371/journal.pone.0001856.

Wang, C., You, Y., Qi, D., Zhou, X., Wang, L., Wei, S., et al. (2014). Human and monkey striatal interneurons are derived from the medial ganglionic eminence but not from the adult subventricular zone. *Journal of Neuroscience* 34, 10906–10923. doi:10.1523/JNEUROSCI.1758-14.2014.

Wang, K. C., Kim, J. A., Sivasankaran, R., Segal, R., and He, Z. (2002). P75 interacts with the Nogo receptor as a co-receptor for Nogo, MAG and OMgp. *Nature* 420, 74–78. doi:10.1038/nature01176.

Wang, X., Mao, X., Xie, L., Sun, F., Greenberg, D. A., and Jin, K. (2012). Conditional depletion of neurogenesis inhibits long-term recovery after experimental stroke in mice. *PLoS ONE* 7, e38932. doi:10.1371/journal.pone.0038932.g005.

Wälchli, T., Pernet, V., Weinmann, O., Shiu, J.-Y., Guzik-Kornacka, A., Decrey, G., et al. (2013). Nogo-A is a negative regulator of CNS angiogenesis. *Proceedings of the National Academy of Sciences* 110, E1943–52. doi:10.1073/pnas.1216203110.

Weibel, D., Cadelli, D., and Schwab, M. E. (1994). Regeneration of lesioned rat optic nerve fibers is improved after neutralization of myelin-associated neurite growth inhibitors. *Brain Res.* 642, 259–266.

Weinmann, O., Schnell, L., Ghosh, A., Montani, L., Wiessner, C., Wannier, T., et al. (2006). Intrathecally infused antibodies against Nogo-A penetrate the CNS and downregulate the endogenous neurite growth inhibitor Nogo-A. *Mol. Cell. Neurosci.* 32, 161–173. doi:10.1016/j.mcn.2006.03.007.

Wenk, C. A., Thallmair, M., Kartje, G. L., and Schwab, M. E. (1999). Increased corticofugal plasticity after unilateral cortical lesions combined with neutralization of the IN-1 antigen in adult rats. *J. Comp. Neurol.* 410, 143–157.

West, M. J. (2013). Getting started in stereology. *Cold Spring Harbor Protocols* 2013, 287–297. doi:10.1101/pdb.top071845.

Wichterle, H., Garcia-Verdugo, J. M., and Alvarez-Buylla, A. (1997). Direct evidence for homotypic, glia-independent neuronal migration. *Neuron* 18, 779–791.

Wiessner, C., Bareyre, F. M., Allegrini, P. R., Mir, A. K., Frentzel, S., Zurini, M., et al. (2003). Anti-Nogo-A antibody infusion 24 hours after experimental stroke improved behavioral outcome and corticospinal plasticity in normotensive and spontaneously hypertensive rats. *J. Cereb. Blood Flow Metab.* 23, 154–165.

Wills, Z. P., Mandel-Brehm, C., Mardinly, A. R., McCord, A. E., Giger, R. J., and Greenberg, M. E. (2012). The Nogo Receptor Family Restricts Synapse Number in the Developing Hippocampus. *Neuron* 73, 466–481. doi:10.1016/j.neuron.2011.11.029.

Wolak, D. J., and Thorne, R. G. (2013). Diffusion of macromolecules in the brain: implications for drug delivery. *Mol. Pharm.* 10, 1492–1504. doi:10.1021/mp300495e.

Wolak, D. J., Pizzo, M. E., and Thorne, R. G. (2015). Probing the extracellular diffusion of antibodies in brain using in vivo integrative optical imaging and ex vivo fluorescence imaging. *J Control Release* 197, 78–86. doi:10.1016/j.jconrel.2014.10.034.

Wurm, F., Keiner, S., Kunze, A., Witte, O. W., and Redecker, C. (2007). Effects of skilled forelimb training on hippocampal neurogenesis and spatial learning after focal cortical infarcts in the adult rat brain. *Stroke* 38, 2833–2840. doi:10.1161/STROKEAHA.107.485524.

Xu, C.-J., Wang, J.-L., and Jin, W.-L. (2015). The Neural Stem Cell Microenvironment: Focusing on Axon Guidance Molecules and Myelin-Associated Factors. *J. Mol. Neurosci.* doi:10.1007/s12031-015-0538-1.

Yaghi, S., Eisenberger, A., and Willey, J. Z. (2014). Symptomatic intracerebral hemorrhage in acute ischemic stroke after thrombolysis with intravenous recombinant tissue plasminogen activator: a review of natural history and treatment. *JAMA Neurol* 71, 1181–1185. doi:10.1001/jamaneurol.2014.1210.

Yamashita, T., Ninomiya, M., Hernández Acosta, P., Garcia-Verdugo, J.-M., Sunabori, T., Sakaguchi, M., et al. (2006). Subventricular zone-derived neuroblasts migrate and differentiate into mature neurons in the post-stroke adult striatum. *Journal of Neuroscience* 26, 6627–6636. doi:10.1523/JNEUROSCI.0149-06.2006.

Yan, J., Zhou, X., Guo, J.-J., Mao, L., Wang, Y.-J., Sun, J., et al. (2012). Nogo-66 inhibits adhesion and migration of microglia via GTPase Rho pathway in vitro. *J. Neurochem.* 120, 721–731. doi:10.1111/j.1471-4159.2011.07619.x.

Young, S. Z., Lafourcade, C. A., Platel, J.-C., Lin, T. V., and Bordey, A. (2014). GABAergic striatal neurons project dendrites and axons into the postnatal subventricular zone leading to calcium activity. *Front Cell Neurosci* 8, 10.

doi:10.3389/fncel.2014.00010.

Yu, X. H., Moret, V., and Rouiller, E. M. (1995). Re-examination of the plasticity of the corticothalamic projection after unilateral neonatal lesion of the sensorimotor cortex in the rat: a phaseolus vulgaris-leucoagglutinin tracing study. *J Hirnforsch* 36, 123–133.

Z'Graggen, W. J., Metz, G. A., Kartje, G. L., Thallmair, M., and Schwab, M. E. (1998). Functional recovery and enhanced corticofugal plasticity after unilateral pyramidal tract lesion and blockade of myelin-associated neurite growth inhibitors in adult rats. *J. Neurosci.* 18, 4744–4757.

Zagrebelsky, M., Schweigreiter, R., Bandtlow, C. E., Schwab, M. E., and Korte, M. (2010). Nogo-A stabilizes the architecture of hippocampal neurons. *Journal of Neuroscience* 30, 13220–13234. doi:10.1523/JNEUROSCI.1044-10.2010.

Zhang, Y., and Pardridge, W. M. (2001). Mediated efflux of IgG molecules from brain to blood across the blood-brain barrier. *J. Neuroimmunol.* 114, 168–172. doi:10.1016/S0165-5728(01)00242-9.

Zhao, R.-R., Andrews, M. R., Wang, D., Warren, P., Gullo, M., Schnell, L., et al. (2013). Combination treatment with anti-Nogo-A and chondroitinase ABC is more effective than single treatments at enhancing functional recovery after spinal cord injury. *European Journal of Neuroscience*, n/a–n/a. doi:10.1111/ejn.12276.

Zhu, D.-Y., Lau, L., Liu, S. H., Wei, J. S., and Lu, Y. M. (2004). Activation of cAMP-response-element-binding protein (CREB) after focal cerebral ischemia stimulates neurogenesis in the adult dentate gyrus. *Proc. Natl. Acad. Sci. U.S.A.* 101, 9453–9457. doi:10.1073/pnas.0401063101.

Zhu, D.-Y., Liu, S. H., Sun, H. S., and Lu, Y. M. (2003). Expression of inducible nitric oxide synthase after focal cerebral ischemia stimulates neurogenesis in the adult rodent dentate gyrus. *Journal of Neuroscience* 23, 223–229.

Zörner, B., and Schwab, M. E. (2010). Anti-Nogo on the go: from animal models to a clinical trial. *Annals of the New York Academy of Sciences* 1198 Suppl 1, E22–34. doi:10.1111/j.1749-6632.2010.05566.x.

VITA

Daniel Shepherd was born in Boston, Massachusetts. He received a Bachelor of Science degree in Biochemistry from Trinity College (Hartford, CT), and worked as a research assistant at the University of Maryland School of Medicine after graduation. In 2010, he entered Loyola's MD/PhD program, and after completing two years of medical school, he joined the Neuroscience Program and laboratory of Dr. Gwendolyn Kartje. In Dr. Kartje's lab, Dan's work focused on the potential effects of neutralizing antibody treatment against the growth-inhibitory protein Nogo-A on post-stroke neurogenesis. His work in the lab was supported by a pre-doctoral fellowship from the American Heart Association awarded in July 2015.